Real-Time Monitoring and Optimization of the Oil and Gas Well Drilling Process

A thesis submitted in fulfilment

of the requirements for the award

of

Doctor of Philosophy

By

SENTHIL S

Roll No. 156107010

Under the Guidance of

Prof. Senthilmurugan Subbiah

&

Prof. Ramgopal V. S. Uppaluri

Department of Chemical Engineering

Indian Institute of Technology Guwahati

Guwahati – 781 039, Assam

November 2022

Dedicated to my beloved uncle and teacher
(Mr. V. Udaiyappan M.Sc., M.Ed., M.Phil) who had sheltered me and showed the world outside my village

Department of Chemical Engineering
Indian Institute of Technology Guwahati
Guwahati-781039
INDIA

DECLARATION

This is to certify that I have carried out the research work in this thesis entitled "**Real-time Monitoring and Optimization of the Oil and Gas Well Drilling Process**", at the Department of Chemical Engineering, Indian Institute of Technology Guwahati, under the supervision of **Prof. Senthilmurugan Subbiah and Prof. Ramgopal V. S. Uppaluri**. The results documented in this thesis are obtained by me and have not been submitted to any other university or institute for the award of any degree or diploma.

In keeping with the general practice of reporting scientific observation, due acknowledgement has been made wherever the work described is based on the findings of other investigations.

Senthil S
Regd.No.156107010
Department of Chemical Engineering
Indian Institute of Technology Guwahati
Guwahati-781039, Assam, India
November 2022

Department of Chemical Engineering
Indian Institute of Technology Guwahati
Guwahati-781039
INDIA

CERTIFICATE

This is to certify that the work contained in this thesis entitled "**Real-time Monitoring and Optimization of the Oil and Gas Well Drilling Process**", being submitted by **Senthil S** (**Regd.No.156107010**), for the award of Ph.D. degree, is a record of bona fide research carried out by him at the Department of Chemical Engineering, Indian Institute of Technology Guwahati, under our guidance and supervision. The work embodied in this thesis has not been submitted to any other University or Institute for the award of any other degree or diploma.

Prof. Senthilmurugan Subbiah
Professor
Department of Chemical Engineering
Indian Institute of Technology Guwahati
Guwahati-781039, Assam, India
November 2022

Prof. Ramgopal V.S. Uppaluri
Professor
Department of Chemical Engineering
Indian Institute of Technology Guwahati
Guwahati-781039, Assam, India
November 2022

ACKNOWLEDGEMENT

I would like to express the deepest appreciation to my Ph.D. supervisors Prof. Senthilmurugan Subbiah and Prof. Ramgopal V.S. Uppaluri who continually and convincingly conveyed a spirit of adventure in regard to research and scholarship and an excitement in regard to teaching. Without their guidance and persistent help this research work would not have been possible. They have always supported and guided me untiringly through this vast endeavour whenever I felt lost and undirected.

I would like to thank my doctoral committee members Prof. Muthukumar, Prof. Pankaj Tiwari and Prof. Senthil Kumar S who rectified my mistakes and helped me be focused so that I will be aimed through the right path towards completion of my research work. They always encouraged me through their insightful comments and fruitful discussions. I also thank Prof K. Mohanty, Head of the Department of Chemical Engineering, for providing all the facilities needed for my research work. I would like to take this opportunity to thank all the faculty and staff members of the institute for their valuable suggestions and cooperation during this Ph.D. program.

I am obliged to the Ministry of Education, Government of India (MoE) and Oil and Natural Gas Corporation Limited, India (ONGC) for providing me with fund to carry out my research work. The present work is a part of Make- in- India initiative and PAN-IIT-ONGC program. I will sincerely express my gratitude towards ONGC for their technical and financial assistance. I would like to extend my gratitude to the senior management of ONGC, Mr. Sanjay Kumar Gauba (DGM), Mr. Amol Musale (SE).

Finally, I would like to acknowledge friends who supported me during my time in IIT Guwahati. I wanted to express my gratitude to my colleagues at Prof. Senthilmurugan's and Prof. Uppaluri'S research groups, Department of Chemical Engineering for making my stay livelier and more meaningful. I want to express special gratitude to Dr.Vishwant Ramba and Mr. Bala Kumara Vignesh for their stupendous support throughout my tenure.

Abstract

Fossil fuel has been serving the world's energy needs for a century. The depletion of fossil fuels from conventional resources has forced the drilling industry to explore complex oil fields. Multiple downhole complications could arise during the drilling operation. Few of them are contagious to the life of the drilling floor workers, such as kick events, oil spills and blowouts. In addition to the above risks, techno-economical sustainability also hampers the process of exploring unconventional reservoirs.

A typical drilling plan is made based on the geotechnical survey report and historical data of the exploratory well of the same oil field. However, the uncertainties and deviations from the anticipated downhole conditions are often encountered during drilling, leading to complications in drilling. In such situations, a drilling supervisor suggests a change in process parameters to treat the undesired response of the wellbore and continue further drilling. The new process parameters suggested by the experts may not be the optimum for the newly encountered downhole condition. The sub-optimal drilling process may often result in more energy consumption and time for the completion of the well. Therefore, optimization of drilling parameters and monitoring of downhole conditions should work parallelly to achieve energy-efficient drilling of oil and gas wells. This approach is demonstrated by developing a decision support system (DSS) for oil and gas well drilling.

The developed DSS can 1) detect critical drilling problems in real-time and take preventive measures, 2) suggest the best search range of process parameters for optimal drilling operation from the historical data, and 3) do real-time optimization for the dynamic wellbore conditions

It is well known that inadequate hole-cleaning is the root cause of many downhole problems during the drilling operations. Prediction and treating the root causes of the problem in real-time could prevent many downhole complications. Therefore, the proposed DSS architecture

takes care of model calibration, prediction and monitoring and alarm generation for anomalies relevant to the hole-cleaning in real-time. The wellbore model was constructed like a process flow sheet consisting of different sections of the mudflow path. The mudflow path covers surface equipment, inside drill string, drill bit and annulus section around the drill string. Unlike previous research, the annulus section was divided into many small continuous stirred tanks (CST) connected in series (i.e., finite element, dynamic lumped model). The developed model can predict the spatial variation of cutting concentration, which was required for real-time root cause analysis. Two case studies were conducted to validate the model, and the model was able to predict drill string washout, cutting accumulation, and mud pump failures before they occurred.

The second module was developed to analyze the energy consumption of major rig activities and improve drilling rig performance and environmental impact in terms of CO_2 emission. Rig activities were identified using previously developed fuzzy-rule and random forest machine learning algorithms. In addition, a simplified methodology for energy audit was adopted for the energy consumption analysis. A two-step hierarchy was followed to determine the best possible oil well drilling parameters (step 1) and subsequent implementation in the offset wells to improve rig performance (step 2). During energy analysis, it has been observed that the energy consumption in non-productive operations was the second highest after drilling. The case studies considered in this work proved the possibility of reducing drilling time and overall energy consumption through energy analysis. Energy analysis was done in Well-A followed by its findings were applied to the offset Well-B during drilling. The above method helped in reducing drilling time by 27.1 % and energy consumption during drilling operation by 55 %. Further, formation-wise energy analysis was also conducted and inferred that depth, dogleg, and drilling process parameters but not formation lithology are the most significant parameters that affect energy consumption.

The third module focuses on real-time optimization of the drilling operation. An ML-based two-layer ROP prediction model was developed and integrated with the optimization module. The ROP prediction model takes minimal input available in a typical drilling rig and is accessible in real-time. The most influential and controllable parameters such as weight on bit (WOB), rotation per minute (RPM) and mudflow rate Q_{mud}, and a few measurable parameters such as total depth, dogleg severity and mud density were fed to the ROP prediction module. An incremental learning technique has been adopted for the ROP prediction model, where the ML model is being trained for every one hour of drilling with the last four hours of data. The training data set was chosen by the moving window technique. The prediction accuracy of ROP was satisfactory ($R^2 > 0.7$) for using the model in real-time optimization of drilling operations. An optimization problem was formulated by combining energy consumption terms and ROP to minimize the energy requirement per meter of drilling. The optimization results were found to be increasing ROP by 32%. for a well drilled in the northeast part of India.

Nomenclature

A_b	Cross-sectional area of the bit (in^2)
A_{no}	Cross-sectional area of drill bit nozzle (in^2)
C_a	Correction coefficient
C_{SC}	Coefficient of surface connection
C_d	Drill bit coefficient
C_{cut}	Cutting concentration (%)
C_{in}	Concentration at the inlet (%)
C_{out}	Concentration at the outlet (%)
C_{set}	Concentration of the settling (%)
C_{gen}	Concentration of the cutting generation (%)
C_{at}, C_{at2}	Turbulent constant of the friction factor caluclation for the annulus side
C_p	Correction coefficient at the pipe side
C_{al}	Laminar constant of the friction factor caluclation of the annulus
C_{pl}	Laminar constant of the friction factor caluclation for the pipe side
C_{pt}, C_{pt2}	Turbulent constant of the friction factor caluclation for the pipe side
$D_{no,q}$	Diameter of the 'q^{th}' nozzle (in)
D_{cut} , D_c	Cutting diameter (m)
D_{bit}	Bit diameter (m)
D_i	Inner diameter (m)
D_{noz}	Nozzle diameter (m)
D_{po}	Drill pipe outside diameter (m)
D_{pi}	Drill pipe inside diameter (m)
D_h	Hole diameter (m)
E_{drill}	Energy spent in drilling operation (kWh)
ΔE_{SPP}	The deviation of predicted STP from the actual (psi)
E_j	Energy consumed for 'j^{th}' operation
E_{tran}, E_t	Transport efficiency (%)

Fn_{obj}	Objective function
f_p	friction factor at the pipe side
f_a	friction factor of the annulus
g	Acceleration due to gravity (m/s^2)
HPP_b	Hydraulic horsepower at the bit (hp)
HL	Hookload (ton (US))
i	Activity reference number
j	Operation reference number
k	Flow consistency index
L_{drill}	Wellbore length (m)
L	Length of a section (m)
n	Flow behavior index
nn	Number of nozzles
$norm$	normalization
$\Delta P_b, \Delta P_{bit}$	Pressure drop at the drill bit (psi)
ΔP_{SC}	Pressure drop at surface equipment
ΔP_{stp}	Standpipe pressure (psi)
ΔP_a	Pressure drop per a section of annulus (psi)
ΔP_{aT}	Total pressure drop at the annulus (psi)
ΔP_p	Pressure drop per a section of drill pipe (psi)
ΔP_{pT}	Total pressure drop at the drill pipe (psi)
$PW_{b,avg,k}$	Average power at the bit for the 'k^{th}' stand (kW)
P_{form}	Formation pressure (g/cm^3)
P_{frac}	Fracture pressure (g/cm^3)
Q_{mud}	Mud discharge rate (gpm)
Q_{in}	Inlet flowrate (m^3/s)
Q_{out}	Outlet flowrate (m^3/s)
$Q_{\min}$	Minimum flowrate requirement (m^3/s)
Q_{set_out}	Settling rate of cuttings in the current section (m^3/s)
Q_{set_in}	Settling rate of cuttings in the previous section (m^3/s)

Q_{cut}	Rate of cutting generation (m^3/s)
q	Nozzle reference number
Re_a	Annulus Reynolds number
$Re_{eq,a}$	Equivalent annulus Reynolds number
$Re_{eqcr,a}$	Equivalent critical annulus Reynolds number
Re_p	Pipe side Reynolds number
Re_{cp}	Critical Reynolds number
$ROP_{avg,k}$	Average rate of penetration for the 'k^{th}' stand (m/h)
t	Time (h)
Δt	Time difference (h)
T	Torque (ft-lbs)
v_c	Critical velocity (m/s)
v_a	Annular velocity (m/s)
v_p	Mud velocity inside drill pipe (m/s)
v_{slip}	Slip velocity of cuttings (m/s)
V_{ann}	Volume of the annulus section of length L
V_{cut_ann}	Volume of cuttings in the annulus section of length L
V_{st}	Volume of cutting removed (m^3)
$W_{rot,i}$	Power consumed in rotating the drill string in the 'i^{th}' activity (kW)
$W_{mp,i}$	Power consumed by mud pump in the 'i^{th}' activity (kW)
$W_{dw,i}$	Power consumed by draw work in the 'i^{th}' activity (kW)
$W_{bhp,i}$	Hydraulic power at the bit in the 'i^{th}' activity (kW)
W_b	Power at the bit during drilling activity (kW)
W_{drill}	Power consumption during drilling operation (kW)
W_{trip}	Power consumption during tripping operation (kW)
W_{ream}	Power consumption during reaming operation (kW)
W_{circ}	Power consumption during circulation operation (kW)
W_{reci}	Power consumption during reciprocation operation (kW)
W_{NPT}	Power consumption during non-productive operations (kW)

Greek symbols

θ_3	Rheometer reading at 3 rpm
θ_{300}	Rheometer reading at 300 rpm
θ_{600}	Rheometer reading at 600 rpm
θ_{zen}	Zenith angle (rad)
θ_{Azi}	Azimuth angle (rad)
λ	Bit hydraulic factor
η_{pully}	Overall efficiency of the system of pulleys (%)
τ	Torque (kgf-m)
τ_o	Yield point (N/m^2)
μ_{ep}	Effective viscosity at pipe side
μ_{ea}	Effective viscosity at the annulus
π	pi (the ratio of a circles circumference to its diameter)
ρ_{mud}	Mud density (kg/m^3)
$\rho_{effective}$	Effective mud density (kg/m^3)
ρ_{cut}	Cutting Density (kg/m^3)
ω	Angular velocity (rpm)

Acronyms

AI	Artificial intelligence
ANN	Artificial neural network
ATT	Annular transport time
BHA	Bottom hole assembly
BD	Bit depth (m)
BH	Block height (m)
CCS	Confined compressive strength (psi)
CH	Cased hole
CST	Continues stirred tank

CSS	Cascading style sheets
DC	Drill collars
DS	Drill String
DSE	Drilling specific energy (psi)
DVs	Decision variables
DW	Draw work
ECD	Equivalent circulation density (g/cc)
EDM	Equivalent depth method
GB	Gradient Boosting
GTO	Geotechnical order
GUI	Graphical user interface
HIF	Hydraulic impact force
HB	Hand break
HHPbit	Hydraulic horse power at the bit
HHPspp	Total hydraulic horse power measured at the stand pipe
HWDP	Heavy weight drill pipe
HM	Hydraulic motor
H/UP	Held up
HTML	Hypertext markup language
HKL	Hookload
HL	Hookload (ton (US))
ITT	Interval transport time
IoT	Internet of things
KPI	Key performance index
KKR	Kernel ridge regression
LGBM	Light Gradient Boosting Machine
LPS	Liters per stroke
MD	Measured depth (m)
MIF	Mud inlet flow
ML	Machine learning
MOF	Mud outlet flow

MWD	Measuring while drilling
MWI	Mud weight at the inlet
MWO	Mud weight at the outlet
MS SQL	Micro-soft structured query language
MP	Mud pump
MSE	Mechanical specific energy (psi)
MTA	Mud tank agitator
MS-SQL	Microsoft structured query language
NPA	Non-productive activities
NPT	Non-productive time (h)
NTV	Net transport velopcity
ODBC	Open database connectivity
OH	Open hole
OPC	Open platform communications
ORM	Organic friction modifiers
PLS	Partial Least Squares regression
PV	Photo voltaic
RBF	Radial basis function kernel
RF	Random forest
RT	Rotational torque
R/I	Run in
RSS	Rotary steerable system
RES	Renewable energy sectors
RPM	Revolutions per minute (rpm)
ROP	Rate of penetration (m/h)
SCADA	Supervisory control and data acquisition
SEC	Specific energy consumption (kWh/m^3)
SS	Shale shaker
SPM	Strokes per minute
STP	Standpipe pressure
STP_{act}	Actual stand pipe pressure
STP_{pre}	Predicted stand pipe pressure

SOP	Standard operating procedure
SVR	Support vector regression
TDSE	Total drilling specific energy
TDS	Top drive system
TD	Total depth (m)
TVD	Total vertical depth (m)
TOTSPM	Total strokes per minute
TI	Temperature at the Inlet (ºC)
TO	Temperature at the Outlet (ºC)
TQ	Torque
UCS	Unconfined compressive strength (psi)
WOB	Weight on bit (ton (US))
WITS0	Wellsite information transfer standard level 0
WITSML	Wellsite information transfer standard markup language

Content

List of Figures

List of Tables

Chapter 1

Introduction and Literature Review

1. Introduction and Literature Review

1.1. Preamble

1.1.1. Introduction to Oil and Gas well drilling

The hydrocarbon reservoir is developed in two phases. In the first phase, an exploratory well is being drilled to locate reservoir with available information such as the nature of hydrocarbon and the field's geological report. In the second phase, the off-set wells are drilled to increase the hydrocarbon production rate based on the exploratory well drilling (i.e., formation property, logging data). The drilling of the exploratory and off-set wells comprises the following steps [1].

1. Well Planning
2. Installation of Drilling Rig
3. Drilling
4. Well Cementing and Casing
5. Production Casing
6. Well Completion
7. Handover of well for production

The 3rd and 4th steps will be repeated for every section of drilling.

The overall drilling process consists of multiple sub-operations that have to be carried out sequentially to complete the drilling process as per the planned well profile and schedule, such as 1). drilling, 2). tripping, 3). reaming, 4). circulation, 5). reciprocation, 6). casing/Tubing and 7). Cementing (the definition for the above operations are given in appendix A). The above operations are done with the help of many types of equipment available in a drilling rig (Figure 1.1) [2].

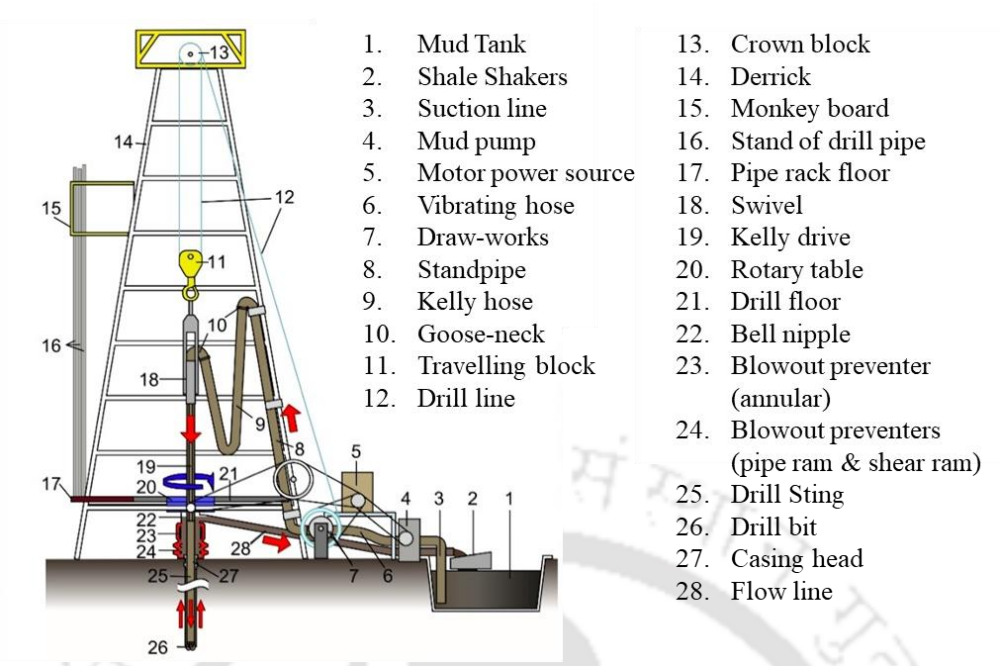

Figure 1.1. Oil well Rig

As shown in Figure 1.2, the oil and gas well can be classified based on mud type, well profile, reservoir type, and environment.

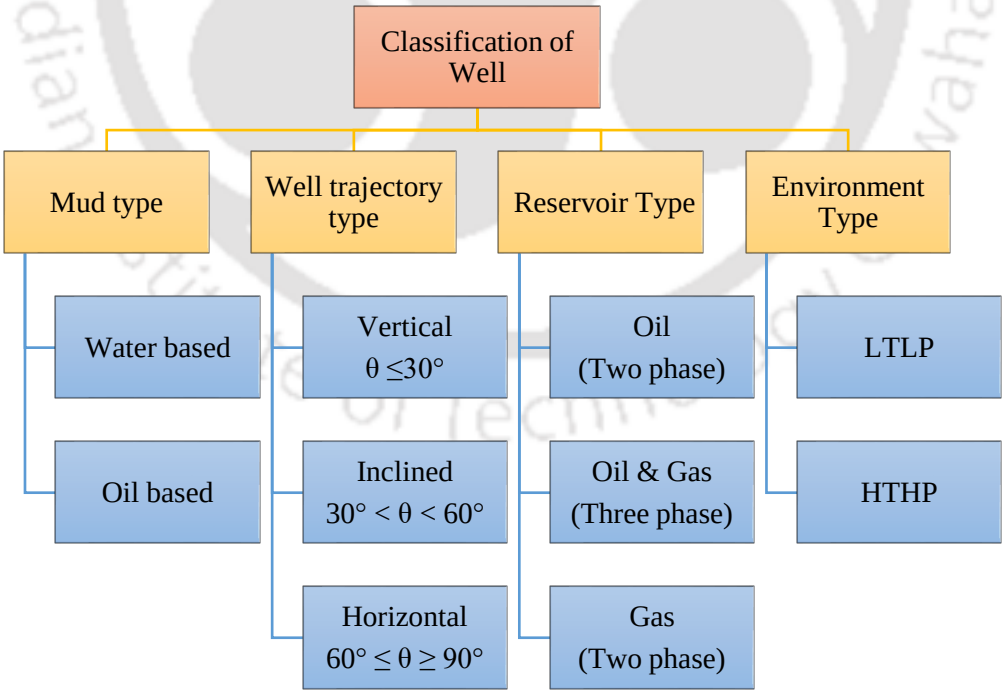

Figure 1.2. Classification of oil and gas well types

The drilling plans have been made to complete the well economically with minimum environmental impact. The hydrocarbon must not enter the wellbore during the drilling operation to ensure the safety and integrity of the wellbore. Therefore, the wellbore's equivalent circulation density (ECD) must be maintained within the pore and fracture pressure window (i.e., ECD window). Most of the drilling operations have been over-balanced (i.e., effective circulation density of mud column should be slightly greater than pore pressure) to achieve the above constraint. However, the formation properties of the offset wellbores are expected to have minor deviations. Achieving the best rig performance in a dynamic well condition is near impossible. Therefore, real-time optimization and down-hole problem prevention become essential to achieving the above objectives.

1.1.2. Importance of Drilling in Sustainability of Fossil Fuel Sector

The oil and gas industry is looking forward to optimize the hydrocarbon exploration and production cost, and that will increase profit of oil and gas industry. Drilling has been one of the major and expensive operations contributing 30-65 % of the oil and gas production cost [3]–[6]**.** Drilling and completion costs depend on several factors such as well profile, formation type, target depth, the daily rig rate, time spent in downhole problem solving, and other external factors [7]. In comparison with vertical wells, the inclined and horizontal wells have been analyzed with several critical issues [8]–[10]. Similarly, shale and highly active formations tend to generate more downhole complications [9], [11], [12] and are hence more expensive to drill.

The contribution of drilling costs can be classified under four categories as follows [13]

i. Mobilization rates (i.e., rig and equipment movement and installation)
ii. Operating rates (i.e., day rate of rig and payment for drilling crew)
iii. Reduced rates (i.e., charges for logging, maintenance, and testing)

iv. Special rates (i.e., interruption due to any unplanned reason such as surface and down-hole problems, harsh weather conditions, force majeure, and legal issues)

Completing drilling operations as quickly as possible without any significant drilling problems could reduce drilling costs by minimizing operating costs and special costs. However, achieving the above objective is possible only if extensive drilling operation planning and optimization are carried out.

Since the last decade, the technologies used for drilling have been evolving to reduce the drilling cost. It is being targeted by maximizing the drilling rate and minimizing the time spent in pipe handling, non-productive operations, and downhole problem solving [6], [14]. Advanced sensing technology, internet of things (IoT) based remote monitoring and support solutions, managed pressure drilling, drilling with the rotary steerable system (RSS), and closedloop drilling automation solutions are being developed and implemented to achieve the above goal.

Many research groups have attempted the integration of the above technologies to guide the drilling process [15]–[18]. Such an integrated system can be called a decision support system (DSS). In this method, the DSS is restricted to providing suggestions to the drilling supervisors based on the predictions. The implementation of the recommendations shall be done manually by the driller. However, fully automated closed-loop systems are also being attempted by the drilling community.

The following criteria should be satisfied by a DSS for drilling operation

- Identification of early signs of trouble (i.e., prediction)
- Identification of the problem (i.e., detection) and root cause
- Real-time simulation, monitoring, and optimization

- Mitigate and advisory (based on the optimization, history, and standard operating procedure (SOP))
- Post analysis of the results and verification of the actions taken (i.e., performance evaluation)

The main challenges in DSS is accuracy of problem identification. The accuracy can be improved by introducing sensor redundancy, frequent sensor calibrations and appropriate data pre-processing techniques.

1.1.3. Vital Problems during Drilling Process

Many problems could arise while drilling, which could be majorly classified as surface and down-hole problems. The total time lost in solving them is called rig's non-productive time (NPT). It is reported that 20 % of the total drilling time is NPT, and 80% of that has been wasted only in down-hole problem solving [19]. The major problems while drilling are given below (definitions are given in appendix A).

1. Pipe Stuck
2. Loss of Circulation
3. Hole-ballooning
4. Hole-deviation
5. Drill pipe failures
6. Kick and blowout
7. Borehole instability
8. Mud contamination

Hole-cleaning is the process of transporting drilled cuttings from the bottom to the surface with the help of drilling fluid. The state of inadequate hole-cleaning could lead to many downhole problems listed above. The cuttings generated during drilling have to be removed at the same rate at which it has been generated. Failing could lead to inadequate hole-cleaning, which could cause all the downhole complications listed in Figure 1.3.

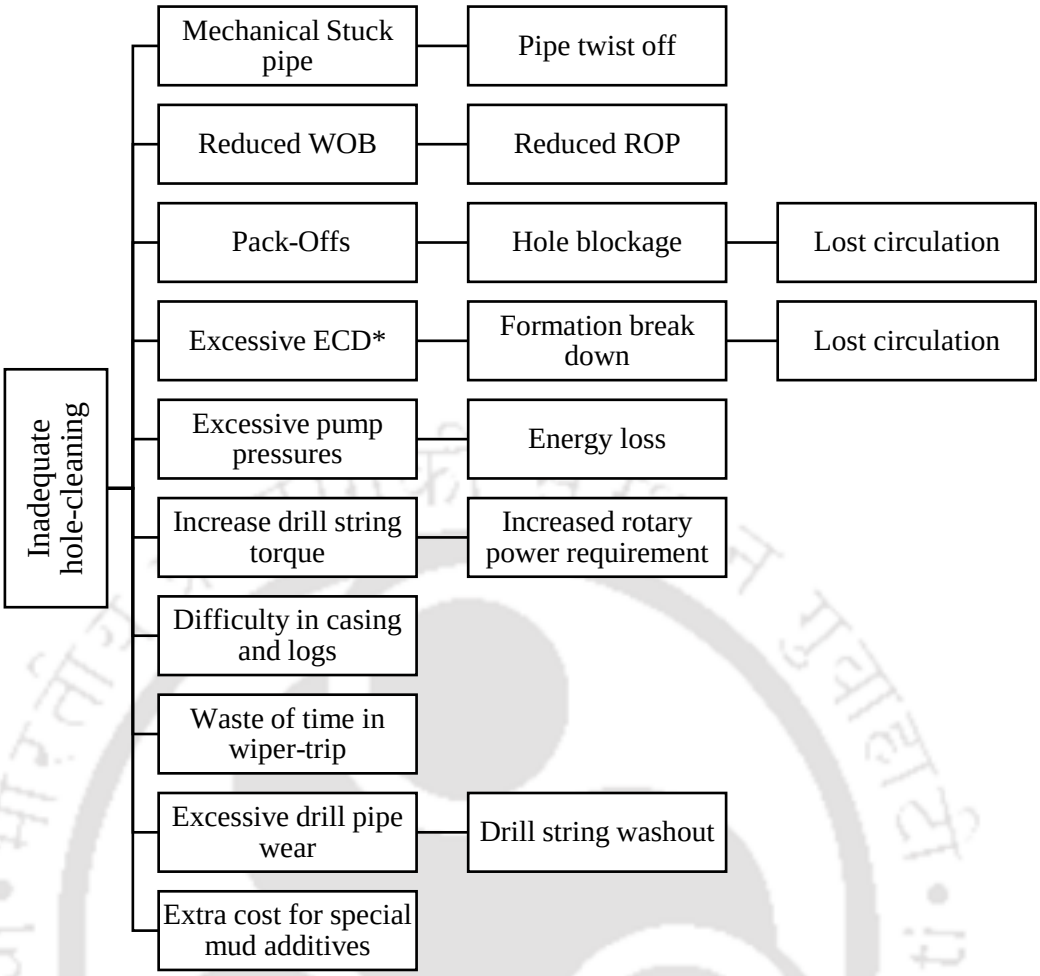

Figure 1.3.The problems associated with inadequate hole-cleaning

The cutting transport is a function of many factors [20]–[24], grouped under four major categories as shown in Table 1.1.

Table 1.1. Parameters that influence cutting transport in annulus

Sl. No.	Property of cuttings	Drilling fluid properties	Operational parameter	Wellbore configuration
1	Cutting density	Mud weight	Mudflow rate	Inclination angle
2	Cutting Size	Rheology	Drill string rotation	Wellbore size
3	Shape		Rate of penetration	Casing size
4	Annulus cutting %		Depth	Drill string size
5	Cutting bed porosity		Pipe eccentricity	Pump capacity
6	Angle of repose			

The relative controllability and sensitivity of the key variables influencing cutting transportation efficiency are depicted in Figure 1.4 [25]. The 'x' axis measures the controllability and 'y' axis measures the sensitivity of the variables.

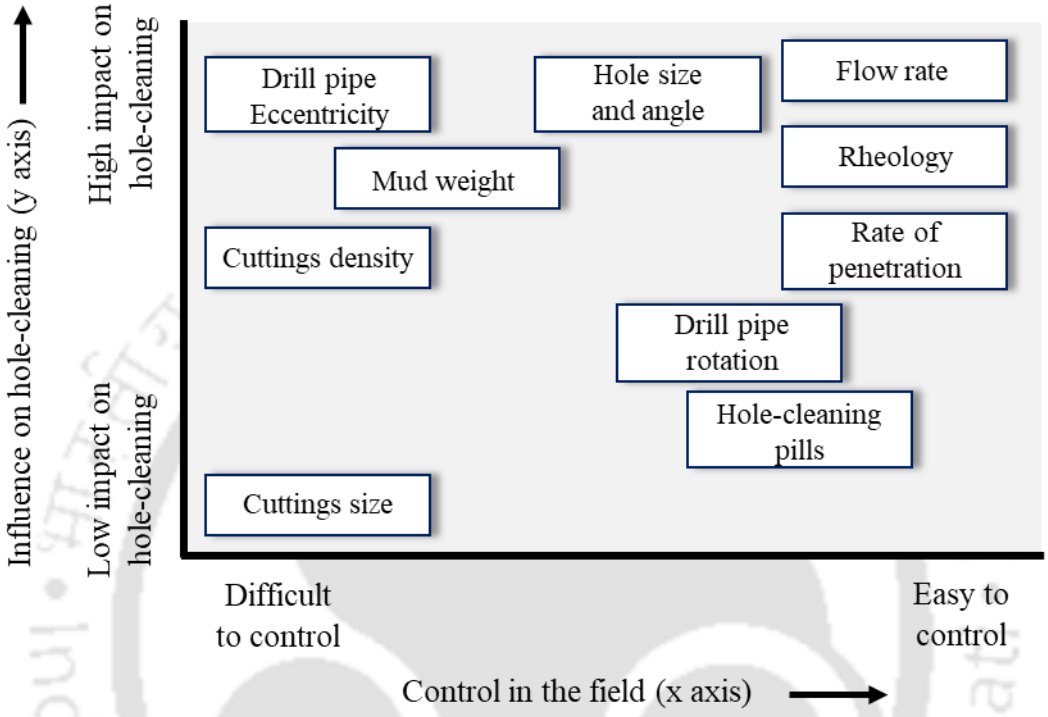

Figure 1.4. Key variables which influence cuttings transport

1.1.4. Targeted Perspective

The objective of this section is to carry out a critical assessment of the available prior-art in the field of oil well drilling for the hole-cleaning, rig performance evaluation, and optimization of the drilling operation to improve the drilling efficiency of the rig.

The existing literature work relevant to this thesis's primary objective is captured by analysing the context given below:

i. To facilitate a clear understanding of the effect of the drilling process, design and geological parameters on the hole-cleaning efficiency. Further to analyze the

drilling problems that could arise due to inadequate hole-cleaning and methods to predict and prevent those complications.

ii. To improve the drilling efficiency of the offset wells through the energy consumption and performance evaluation studies by utilizing data obtained from previous wells.

iii. To maximize the rig performance and eventually minimize the drilling cost per meter by optimizing the drilling process.

The above perspectives are anticipated to broaden the scope of concurrent research pertaining to the prediction and prevention of downhole problems related to inadequate hole cleaning. Real-time optimization for cost-effective and energy-efficient drilling operation with minimum available rig site data is also deliberated.

1.2. Prior Art

Based on the targeted perspective, the available prior art in the field of oil well drilling can be classified into the following themes:

i. Data pre-processing in prediction and automation of drilling operation
ii. Hole-cleaning and wellbore stability
iii. Performance evaluation and identification of best operating parameter range
iv. Optimization of drilling operation to reduce cost and improve rig performance
v. Developing a decision support system (DSS) for oil well drilling

The following subsections comprised a brief overview of the literature followed by the lacunae found. At the end of this chapter, the objectives of the thesis work are listed.

1.2.1. Data pre-processing in prediction and automation of drilling operation

The quality of sensor measured data that has been recorded in the drilling rig is expected to detoriate with time due to many inherent problems such as noise, connection loss during transmission, sensor calibration issues etc. The predictions made by DSS with those data are expected to have lower accuracy. Many literatures have reported the problems mentioned above, while only a few have actually tried to solve them [26]–[29].

Kyllingstad et al. (1993) have observed and reported the types of errors present in the mud logging data, which could hamper the accuracy of the monitoring and prediction for drilling advisory such as DSS [28]. The drilling mud log data errors were classified under four aspects: 1) sensor accuracy, 2) data acquisition, 3) data corrections, and 4) operations (i.e., parameter reset, testing and updating) [28]. Further, it was pointed out that sensor measured parameters such as hookload, swivel height, heave and torque have to be given frequent attention to improving data quality.

Similarly, Sawaryn et al. (2011) have explained the influence of data quality in decision-making for real-time drilling applications [29]. Frequent sensor calibration and checking of data transmission are mandatory to implement more complex and effective workflows. So that planning and automation of drilling operations can be established. It was recognized that moving average as one of the most effective techniques to reduce the noise to signal ratio of all the measured real-time sensor data.

Nybø et al. (2012) have elaborated upon the challenges in using inconsistent and inaccurate data for real-time application for prediction and decision making for calibration and prediction of standpipe pressure (STP) and ECD [26]. Further, the problem in processing the wells' history data was also described in their study.

Andrzej et al. (2022) have recently reported the importance of data quality and pre-processing for AI/ML-based drilling automation [27]. Therefore, the pre-processing of time series data becomes mandatory to deploy a predictive algorithm in real-time. They have proposed a gap coefficient parameter to identify the data gap in the historical data. In the data pre-processing step, the large interval of data gaps were dropped from the data set, and small data gaps were filled with imputation techniques such as forward/backward filling and linear interpolation.

An automated rig activity detection stands crucial to evaluate real-time rig performance in terms of energy and time spent in various rig activities. Tripathi et al. (2021) have proposed a hierarchical classifier-based method that used a fuzzy rule-based classifier and a random forest classifier in two layers to carry out the classification for real-time application.

A highly secure and reliable real-time data transfer system needs to be established for real-time simulation, prediction, monitoring, and control of the drilling operation.

1.2.2. Hole-cleaning and wellbore stability

The nonlinear interaction between process variables and wellbore conditions requires more accurate real-time monitoring and control algorithms in the field of oil well drilling [30]–[32]. The drilling operation may often be interrupted if the process parameters are not maintained within the operating window. Inadequate hole-cleaning may lead to many problems which will be expensive and time-consuming to resolve (Figure 1.3). The problem can sometimes be very severe and could make it impossible to reach the target point . Hence, efficient strategies are required to forecast and avoid downhole problems during the oil well drilling.

For example, if the critical issues, like cuttings accumulation and hydrocarbon entering the wellbore, are identified before it occurs, then the major complications such as well collapse, pipe stuck, kick, and blow out can be avoided.

The available state-of-the-art provides valuable guidelines to improve and develop a robust methodology to monitor the oil well hole-cleaning process. For a given mud and formation property, good hole-cleaning can be achieved by maintaining drilling fluid velocity above the slip velocity of the drilled cuttings [33]. Further, many researchers [21]–[23], [34], [35] studied the relationship between the slip velocity and other factors such as mud density, viscosity, yield values, cutting size, drill string eccentricity, and drill string rotation.

The experimental result of Siffreman et al. [23] reported that only 70-90% of cuttings are lifted at theoretical slipping velocity. The study concluded that the annulus fluid velocity and drilling fluid rheological properties are the major factors affecting cutting transport, and the rest are less important. The above observation agrees with another study on the relative effects of two or more drilling variables on rate of penetration (ROP) (i.e., ROP is affected by cutting accumulation) [22].

In the case of an inclined well, the cutting transport is greatly affected by inclination. Tomren et al. (1986) experimentally found the cutting build-up and downward sliding taking place in the angle range of 40 to 50º. In the same year, Slavomir et al. [35] reported that 45º to 55º angle is a challenging region to do cutting transport, and the chaotic motion of cuttings could be the reason for the incapability of cutting transportation.

The cutting bed formation and its movement are studied by Ford et al. (1990) [10]. Two distinct cutting transport mechanisms were found: rolling/sliding and suspension. Further, it was observed that the slurry follows seven flow patterns which are homogeneous and heterogeneous suspension, suspension/saltation, sand cluster, separated moving bed (dunes), continuous moving bed and stationary cutting bed.

Alfredo et al. (1999) [36] observed that the rotation speed of drill string above 125 rpm could cause some cuttings to go over the pipe from the lower velocity side of the annulus to the higher

velocity side. Transportation of smaller cuttings was comparatively easy at a high rotation speed, and the lower viscous drilling fluid was found to be better for cutting transportation at high wellbore inclination.

Adari et al. (2000) optimized the drilling fluid properties and flow rate to reduce the total circulation time requirement before tripping. A reduction in cutting bed height is assumed to follow an exponential equation [25].

As the fabrication of an experimental setup is too expensive and less likely to replicate actual field conditions, many researchers [37]–[44] have done mathematical modelling and simulation studies for the drilling process and tried to optimize the process parameters to enhance the hole-cleaning efficiency. All these mathematical simulation studies have improved our understanding of cutting transport behaviour.

Kenny et al. (1996) [37] developed a model for hole-cleaning. They analyzed the effect of the flow behaviour index ("n") of the Herschel-Bulkley rheological model for a drilling fluid over cutting transport. It was reported that higher values of fluid factor "n" enhance hole-cleaning for highly inclined well at pipe-eccentric conditions.

Saasen (1998) [45] analyzed the effect of the pumping rate of drilling fluid and the rheology on cutting transport in deviated well drilling. He reported that the annular frictional pressure drop and the consolidation of the cuttings bed (i.e. the formation of gel structures within and including the cuttings bed) are the two major factors controlling the hole cleaning properties.

Bilgesu et al. (2007) [46] did a computational fluid dynamics (CFD) study to find the effect of major fluid and drilling parameters on cuttings transport. He reported that hole-cleaning is better for bigger particles for a given drilling fluid flow rate. However, an increase in velocity (i.e. increasing flow rate) of drilling fluid helps to improve smaller cutting transport for highly

inclined wells. He also found that drill string rotation is more pronounced for the transport of smaller cuttings.

Hopkin's method is the most used model to determine the minimum required pumping rate required for a given diameter wellbore, cutting density and depth of drilling. In 2003, Bizanti et al. [47] developed a mathematical model to predict the minimum required flow rate and found that the model worked well for high angle drilling > 45º.

To improve the prediction accuracy for the inclination range of 0º to 90º, Mohammadsalehi et al. (2011) [48] combined Larsen's correlation (55º to 90º) with Moore's correlation of cutting transport to form a mechanical model. The resultant model was used to optimize the flow rate of cutting transportation and compare it with the actual flow rate. The latter was selected if the actual flow rate was lesser than the optimized one. Otherwise, the fluid property would be changed until the optimum flow rate becomes greater than the cutting removal flow rate.

Dosunmu et al. (2015) [32] developed a model to predict and monitor cutting volume in real-time and integrated it with the existing hole-cleaning models. The output of the theoretical cutting transport model was compared with the actual cutting volume in the outlet. Finally, The cutting volume was interpreted with torque and drag data to correlate with the drilling problem in real-time.

From all the reported studies discussed above, it can be concluded that prediction of the slipping velocity of the cutting is very important to decide the required flow rate to achieve adequate hole-cleaning. Numerous mathematical and artificial neural network (ANN) based models were used by researchers to represent the drilling fluid behaviour and their capability of cutting transport [49], [50], [51]–[54], which involve moderate to severe computational effects. The most commonly used models in the field are the Power law and Bingham plastic models (i.e. two-parameter models). However, the analytical and empirical models such as

Hershel-Buckley and Chein models are also available to predict fluid hydraulics and cutting transport respectively [55], [56].

The hydrocarbons/formation fluids are in the compressed state. Therefore, the hydraulic pressure exerted by the formation fluid is called pore/formation pressure. To maintain the wellbore stability, the entry of formation fluids into wellbore annulus must be prevented. Therefore, the hydrostatic and hydraulic resultant pressure (i.e., ECD) exerted by the mud column on the formation should be in between the pore pressure (i.e., formation pressure and fracture pressure window.

The real-time prediction of pore pressure and fracture pressure window using semi-empirical models such as the 'D' exponent method and equivalent depth method (EDM) was also established in the literature [31], [57]–[59].

1.2.3. Energy consumption studies and rig performance evaluation

The benchmarking of energy and time consumed for each rig operation could aid in improving the future performance of the drilling rig. The improved rig performance is expected to reduce the loss associated with the low oil price regime and enhance the profit during the high oil price regime [60]–[63]. Beyond commercial benefits, the improved energy efficiency can also reduce the carbon footprint of the drilling process.

The concept of mechanical specific energy (MSE) in the drilling domain was first introduced by Teale (1965) to evaluate drilling operation efficiency [64]. The MSE was defined as the amount of mechanical energy (i.e., thrust and torsional) spent in the braking unit volume of the formation rock. Dupriest and Koederitz (2005) indicated that the actual MSE consumed was much higher than the minimum energy required to break the rocks (i.e., unconfined compressive strength (UCS)) [65]. It was attributed to the energy loss in the drill bit due to bit balling, bit masking, and regrinding of cutting beneath the bit.

The mud jet's hydraulic impact force (HIF) aids in excavating the cuttings from beneath the bit. As a result, the formation could be drilled at a lesser MSE closer to its confined compressive strength (CCS). Further, Armenta (2008) defined a term called drilling specific energy (DSE) to incorporate the effect of HIF in MSE. DSE is the amount of energy required to destroy and remove a unit volume of rock beneath the bit [66]. Armenta modified Teale's equation with a third negative term (i.e., hydraulic component). Ramba et al. (2021) recently utilized DSE's concept to optimize drilling parameters by adapting a play-back methodology [67]. Thereby have achieved a significant reduction in DSE by maximizing the ROP during drilling.

Agreeing with Armenta's expression, Mohan et al. (2009) and Hammoutene (2012) had assumed that the hydraulic force could also take part in rock breaking along with mechanical energy [68], [69]. However, this model might not suit for hard formation and low-pressure drilling scenarios. In those cases, the bit hydraulic force can only aid in excavating the cuttings from beneath the drill bit [70].

Drilling at maximum ROP is expected to reduce the well completion time. In this regard, it can be noted that, as of 2010, the reported rig daily rate was around 100,000 $/day for onshore and 600,000 to 800,000 $/day for the deep-water offshore well of Mexico [71]. Therefore, the overall profit generation due to the rig rental and energy consumption reduction may decide the best strategy to drill a well.

Early attempts to maximize ROP were targeted by Graham and Muench (1959) [72]. The authors analytically assessed the weight on bit and rotary speed combinations and thereby extracted statistical expressions for bit life expectancy and drilling rate as a function of drill bit diameter, rotational speed, and weight on bit (WOB).

Galle and Woods (1963) discussed the importance of calculating the drill bit balling rate and identifying the right time for the bit change [73]. It was concluded that the drilling cost for the

last meter drilling could be as high as twenty times that of the first-meter drilling for the case involving no replacement of the worn-out bit. Legarth and Saadat (2005) carried out a 'site-specific' analysis of energy consumption for a geothermal well to evaluate the parametric influence on the ROP [74].

1.2.4. Optimization of drilling operation through ROP maximization and energy minimization

The drilling rate is a function of many variables such as process parameters, formation properties (i.e., hardness and reactive nature of formation with drilling mud), bit wear rate and other downhole conditions. Among these variables, only few process parameters can be measured and controlled in real-time. Other variables may vary inherently with respect to downhole conditions. In conventional drilling practice, the process parameters for development wells are set based on the exploratory well's drilling data, which may not be optimum.

The effective prediction and optimization of ROP become crucial to optimize the efficacy of the drilling process. The prediction of ROP as a function of the drilling variable is vital. It paves the way for the objective function formulation to maximize ROP and minimize specific energy. The optimum drilling operation is expected to reduce the overall drilling cost significantly.

The accuracy of ROP prediction model is crucial while using it for optimization of drilling operation. However, it is not easy to directly model the ROP as a mathematical function of some critical parameters due to its highly non-linear behaviour [75]. Apart from this issue, the inherent noise in the sensor data restricts the accurate model prediction and ROP optimization benefits.

Several methods have been developed to predict the ROP for drilling optimization, and significant results were published after the mid-20th century. ROP prediction models can be classified mainly into first principle and data-driven models [76]. The first principle based ROP

models try to establish the mathematical expression between the primary variables such as ROP, WOB, and rotations per minute (RPM), usually these models are developed based on many assumptions to simplify the complexity of the model equation and its solving procedure.

Maurer (1962) [77] proposed an equation to predict the roller-cone bits' ROP for the rock cratering process based on the rock strength, WOB, RPM, and drill bit size. Galle and Woods (1963) [73] established an analytical equation to estimate ROP as a function of WOB, RPM, formation type, and bit tooth wear.

Simplified ROP analytical model as a function of WOB and RPM was proposed by Bingham (1965) [78]. The author included the effect of rock strength in the proportionality constant. Neither Maurer's nor Bingham's models consider the impact of formation compaction, differential pressure, bit hydraulics, and bit wear on ROP change, which significantly lowers the predictability accuracy of ROP using these correlations.

Later, Bourgoyne and Young (1973) [79] developed a well-known mathematical model for ROP prediction and drilling optimization using multiple regression analysis. In this model, the authors considered the effects of drilling parameters such as formation depth, formation compaction, WOB, RPM, pressure differential across the bottom hole, bit diameter, bit wear, and hydraulics on ROP. The inclusion of these parameters increased the accuracy of the models considerably. Osgouei (2007) [80] modified Bourgoyne and Young's model to enable ROP estimation for the directional and inclined boreholes using a linear regression model.

Similarly, several research works have been done to compare the result of ROP prediction using artificial intelligence (AI) techniques with traditional ROP models [76], [81], [82]. They concluded that ROP prediction could achieve higher accuracy using artificial intelligence techniques when good amount of historical data is available. Also very difficult to capture all the downhole phenomenon in the first principle based ROP model.

One of the first applications of machine learning (ML) in drilling parameters prediction was made by Arehart (1990) [83], who used an artificial neural network (ANN) to predict the grade of the drill bit (i.e., state of bit wear) while drilling. Later, Bilgesu et al. (1997) [84] predicted ROP using ANN, and it was further improved by Mantha (2016) [85] by integrating statistical regression and ANNs.

Ahmed et al. (2018) [86] used support vector regression (SVR) to predict ROP by taking both drilling variables (i.e., WOB, RPM, mudflow rate (Q_{mud}) STP and torque (TQ)) and mud properties (i.e., mud weight, funnel viscosity, plastic viscosity, yield point and solid %) as input. It was claimed that SVR was able to predict ROP with high accuracy ($R^2 > 0.997$ and absolute percentage error < 2.828%)

Hegde (2018) [87] presented a hybrid model to estimate ROP where the ANN was combined with traditional models and developed a unique predictor. The ANN model integration helped to improve the R^2 from 0.12 to 0.84 for ROP prediction. It was reported that unconfined compressive strength (UCS) had a maximum correlation with ROP compared to all other drilling parameters. However, the UCS value used for ROP prediction cannot be measured in real-time, limiting the proposed method for the applicability of real-time ROP prediction and optimization [88].

Elkatatny (2021) has developed an ANN model to predict the change in ROP with drilling of a complex lithology [89]. The model was fed with all the drilling variables and mud properties, similar to the model validated by Ahmed et al. (2018). In addition, gamma-ray logging data also was given, which carries the information about the type of formation.

1.2.5. Develop a decision support system (DSS) for oil well drilling

The DSS for drilling can be defined as a programmed computer system that takes well-site information and real-time sensor data to analyze and produce predictions, root cause analysis of problem and guidance to the driller in real-time.

The analytical modules of DSS can be powered by first principal, AI/ML, expert knowledge, case-based reasoning (CBR) or an ensembled engine of all the above models. One of the noticeable DSS for drilling was developed by skallel et al. (2004) [15]. The expert knowledge-based reasoning (KBR) tool (TrollCreek) was developed to predict drilling problems based on similar events experienced in history and recommended the same decision taken to reduce the rig downtime.

Similarly, Verdande Technologies also developed a DSS (DrillEdge) for drilling operations [16]. The DrillEdge used the CBR approach to predict drilling problems of the current well being drilled by comparing it with a similar 'case' built by the drilling experts. The DrillEdge aimed to overcome the drawbacks of the real-time operation centre (RTOC), which requires 24 × 7 monitoring of the critical process variables in 12 h shift by the drilling experts. The solution suffered greatly because the cases have to be built manually based on the history.

The DSS developed by Sergey et al. (2019) [90] focused on supporting geo-steering through real-time well trajectory optimization. The pre-drill reservoir's geological data were updated with readings from measuring while drilling (MWD) tool. Consequently, the new optimum trajectory angle was found to maximize production capacity and reduce drilling and production costs.

Shokouhi et al. (2009) developed knowledge-intensive case-based reasoning (KiCBR) and compared with plain CBR and KBR. KiCBR is a combined approach of CBR and KBR with root cause analysis as a new feature. The prediction performance on hole-cleaning related

problems was tested. [18]. It was reported that KiCBR was more efficient and reliable in predicting problems and reducing the rig downtime.

1.3. Possible scope for further research

1.3.1. Data pre-processing in prediction and automation of drilling operation

Researchers have reported the drawbacks of using bad quality drilling data [26]–[29] and pointed out the most critical parameters and respective sensors that have to be calibrated frequently [28]. However, it is still a dream to perform data acquisition and transformation without error, noise, or loss [29].

Therefore, pre-processing of drilling data before any predictions and analysis become mandatory. Many pre-processing techniques available in the prior art have proved their effectiveness in multiple domains, and few have also been tried in the drilling domain [27], [29]. From the literature review, it can be inferred that there are multiple kinds of errors present in drilling data such as noise, outlier, missing data and repeated entry. Thus, a solution for the pre-processing requirement is not possible by adapting to a single technique.

There are multiple techniques available in each category to carry out the pre-processing. However, all of them have their pros and cons. For example, the moving average is one of the most used techniques to reduce noise to signal ratio. Nonetheless, the time delay introduced to the data is unavoidable in the above technique [29]. Researchers have suggested data smoothing, outlier removal [91], and data reconciliation [92] methodologies to address the issue but not exclusively applied to drilling data for real-time applications.

A combination of multiple and robust sets of error, outlier and noise removal and data reconciliation techniques have to be configured to perform predictions. The activity-specific

analytics can be implemented in real-time if the rig activity identification programs are integrated with other pre-processing methods.

1.3.2. Hole-cleaning and wellbore stability

The existing methodology for evaluating the hole-cleaning efficiency and prediction of downhole problems involves indirect methods that may not be feasible for real-time application, such as monitoring torque and drag trends during drilling and tripping operations. The expert knowledge-based system adopted by the oil industry enables the identification of problems but not in a real-time and quantitative format.

Among the available models, the Hershel-Bulkley model (i.e., yield power-law model) has been proven to be more reliable than the two-parameter models for drilling fluid hydraulics [49], [53] and Chein model [93] empirical model for slip velocity prediction, However, the empirical constants recommended in the literature are specific to the lithological property of the well, mud property, and the rig or the experimental setup which had been used for the studies. Therefore, there is a huge difference between the STP predicted and measured data. Hence, the approach is not robust enough to monitor the drilling operation in real-time due to the dynamic nature of wellbore parameters. In this regard, the potential for real-time use of dynamic models is encouraging to improve modelling efforts [94]. As the wellbore conditions are dynamic in nature, the model parameters also have to be calibrated in a frequent interval.

1.3.3. Energy consumption studies and rig performance evaluation

Many researchers have reported the importance of the net energy recovered from a well on the sustainability of oil well drilling [95]–[97]. However, most of them have only focused on the ROP improvement, and very few attempts have been made to reduce the energy consumption of other rig operations [98]. The efficiency of the drilling operation and other energy-

consuming rig operations such as tripping, reciprocation, reaming, circulation, and non-productive operations also need to be addressed to improve the overall rig performance.

The following benefits can be expected from an energy analysis:

- Reduction of drilling duration through ROP improvisation
- Identification of harder formation through energy consumption pattern
- Benchmarking and tracking of tripping speed facilitating the evaluation of tripping efficiency
- Benchmarking of the rig performance for the similar well to assure possible scope of comparable rig production scenarios
- Reduction of non-productive time and associated energy consumption
- Utilization of previous well drilling data to make strategies towards the saving of energy and time in the future off-set wells

1.3.4. Optimization of drilling operation through ROP maximization and energy minimization

The ROP is a function of many interactive parameters that makes it challenging to develop an analytical model for its prediction. The models available in the prior-art suffer due to the above fact. Soares et al. (2016) [99] have exposed the limitations of such models, including the conventional model of Bourgoyne and Young (1974) [79]. The predictive data-driven models overcame the shortcomings of such models. Contrary to the traditional models, predictive data-driven modelling involves searching through the data to identify complex relationships and patterns. The self-learning ability of AI algorithms and handling complex data patterns without prior assumptions has gained much popularity over the last few years in petroleum engineering [100], [101].

ML algorithms are quite flexible and can overcome the shortcomings of the analytical models. Hyper-parameters specific to each model controls the model architecture. ANNs, Random Forest (RF) and Support Vector Machine (SVM) are the most popular drilling parameter prediction algorithms.

The formation properties have been one of the primary parameters affecting the ROP. Unfortunately, most drilling rigs do not have a real-time sensor to find the formation properties. In a typical drilling rig, the formation type can be classified using gamma ray logs and the uniaxial compressive strength (UCS) can be found through sonic logs. However, the logging processes could not be done during drilling (MWD). Therefore, the effect of formation properties has to be isolated from predicting the ROP in real-time.

The manipulating valuables (i.e., decision variables) should also be controllable in real-time to carry out real-time optimization. The secondary variables of the model should be measurable in real-time to simulate the dynamic nature of the wellbore system.

1.3.5. Developing a decision support system (DSS) for oil well drilling

The DSS reported in the prior art are working on the concept of learning from past events such as CBR, KBR and KiCBR [18]. These methods have proved a significant advantage in the early prediction and rectification of problems. However, the above solutions suffer greatly in case building and updating with new experiences of drilling problems [18]. The drilling expert's intervention requirements in the above tasks make it vulnerable to human errors. Therefore, analytical and AI-based self-learning hybrid DSS needs to be developed to avoid human intervention in learning and predicting problematic events. The developed DSS should be capable of learning, predicting, detecting, analyzing root cause, and guiding the driller in real-time. Consequently, the DSS should be integrated into acquisition system and drillers display console.

1.4. Objectives of the thesis

1) To develop a Hershel-Bulkley fluid mathematical model for the prediction of the total pressure drop of the rig (STP) and integrate it with cutting transport model (cutting concentration and ECD calculation) of the annulus. The developed model will be used for identification of downhole complications.

2) To develop a module for evaluating the energy consumption and carbon footprint of all the rig operations. Thereby minimizing the energy consumption of the drilling process and NPT

3) Comparison study of energy consumption of drilling process across various operations, phases and formation lithology to enable benchmarking of energy consumption values

4) Developing a real-time optimization module for the minimization of energy consumption in drilling operations and thereby achieving maximum ROP (i.e., predicted by ML model) and adequate cutting transport

5) Integration of monitoring and optimization module with the DSS and validation with the field data

1.5. Organization of the thesis

Chapter 1. Introduction and Literature Review

This chapter provides general information regarding the drilling technologies and drilling complications, followed by a literature survey is presented in detail for the following aspects:

- A study on cutting transport and wellbore stability models and its applications

- Review on hole-cleaning and associated downhole complications
- Exploring the utilization of specific energy concepts and operation wise energy distribution across different phases and formation
- Studies on various drilling optimization techniques to achieve better drilling rates at low energy consumption

Based on the pertinent lacuna of the methodologies being followed in the relevant prior art, the objectives of the current thesis have been framed.

Chapter 2. Methodology and Overall System

The overall system architecture of the decision support system (DSS) is presented in this chapter, where the individual modules were integrated to form a real-time support system. The hole-cleaning, energy audit and drilling optimization modules are also explained with a detailed flowchart.

Chapter 3. Downhole Problem Prevention by Enhanced Cutting Transport

This research work proposes a method that was successfully tested in the oil field to predict drilling fluid hydraulics and its effect on cutting the transport capacity of the system in real-time. Improper hole-cleaning can lead to many downhole problems in the oil well drilling field. A new system architecture is presented to ensure hole-cleaning and wellbore stability based on the dynamic well conditions. The module also takes care of model calibration, monitoring, and alarm generation at the time of anomaly related to the hole-cleaning and wellbore stability. The model development and implementation in Dymola are described. The sensitivity analysis and the case study with model predictions were presented.

Chapter 4. Improving Oil Well Drilling Rig Performance through Energy Consumption Studies

This chapter focuses on computing energy consumption at the different types of rig activities carried out during drilling an oil and gas well. The operation wise energy consumptions were analyzed, and benchmarking was established for each operation. The possibility of improving drilling rig performance through energy analysis was delineated through case studies.

Chapter 5. Real-Time Optimization Using Artificial Intelligence

A real-time drilling process optimization module has been developed as part of this chapter. The developed module was integrated with DSS. The module takes care of real-time AI/ML model training and prediction for STP, TQ, and ROP. The sensitivity analysis model and prediction results of the developed model are presented. Further, the developed model was used to optimize the drilling operation for real-time application.

Chapter 6. Conclusion and Future Work

This chapter summarises the findings and implementation of the DSS for real-time application. After that, the chapter also presents a brief overview of the direction for future research and development in downhole problem prevention and optimization for decision making.

Chapter 2

System Architecture and Methodology

2. System Architecture and Methodology

2.1 Overall system architecture

A decision support system for oil and gas well drilling is developed with the four modules namely 1. Data pre-processing, 2. Hole cleaning, 3. Energy audit, and 4. Real-time optimization (Figure 2.1).

The data collected during drilling operations can be classified into two types as follows

1. The real-time sensor measured time-series data from the supervisory control and data acquisition (SCADA) system. The collected data from SCADA will be a raw data without any pre-processing. All the SCADA data are real-time data unless until the well was already drilled
2. Offline being further classified as:
    a. Manual data (directional survey such as inclination, dogleg severity, pump selection, BHA configuration, drill bit specifications, and drill pipe)
    b. Laboratory data such as mud and cutting properties (i.e., density and size) measured or estimated from experimental or geological survey
    c. Geotechnical order data (GTO) (formation details such as porosity, fracture pressure and density based on geological survey, well-planning details)
    d. Historical data of previously drilled nearby wells (formation properties, SCADA data)

The raw data from SCADA contains both measured and derived parameters (Table 2.1). All the above data were collected and stored in Microsoft's structured query language-based database (MS SQL). The required data are fetched from the database to MATLAB software using open database connectivity (ODBC), an application programming interface (API).

Table 2.1. Commonly available SCADA parameters in drilling rig

S.N.	SCADA parameter	Unit
1	Hookload (HL)	ton (US)
2	Weight on bit (WOB)	ton (US)
3	SPM#1 (Mud pump #1's piston speed)	spm
4	SPM#2 (Mud pump #2's piston speed)	spm
5	TOTSPM	spm
6	Stand pipe pressure (STP)	kgf/cm^2
7	Rotation speed (RPM)	rpm
8	Rate of penetration (ROP)	m/h
9	Discharge rate (Q_{mud})	gpm
10	Density of inlet mud	g/cc
11	Density of outlet mud out	g/cc
12	Flow out relative %	%
13	Total depth (TD)	m
14	Bit depth (BD)	m
15	Block height (BH)	m
16	Torque (TQ)	kgf-cm
17	Ton Mile	m

As shown in Figure 2.1, the DSS consists of the following four modules

- Data pre-processing module
- Hole-cleaning monitoring and prediction module to ensure adequate cutting transport and wellbore stability during the drilling operation
- Energy analysis module that performs energy evaluation and establishes benchmarking to improve rig performance

- A real-time optimization module to find the optimal process parameter to achieve incremental performance compared to the previous drilling operation

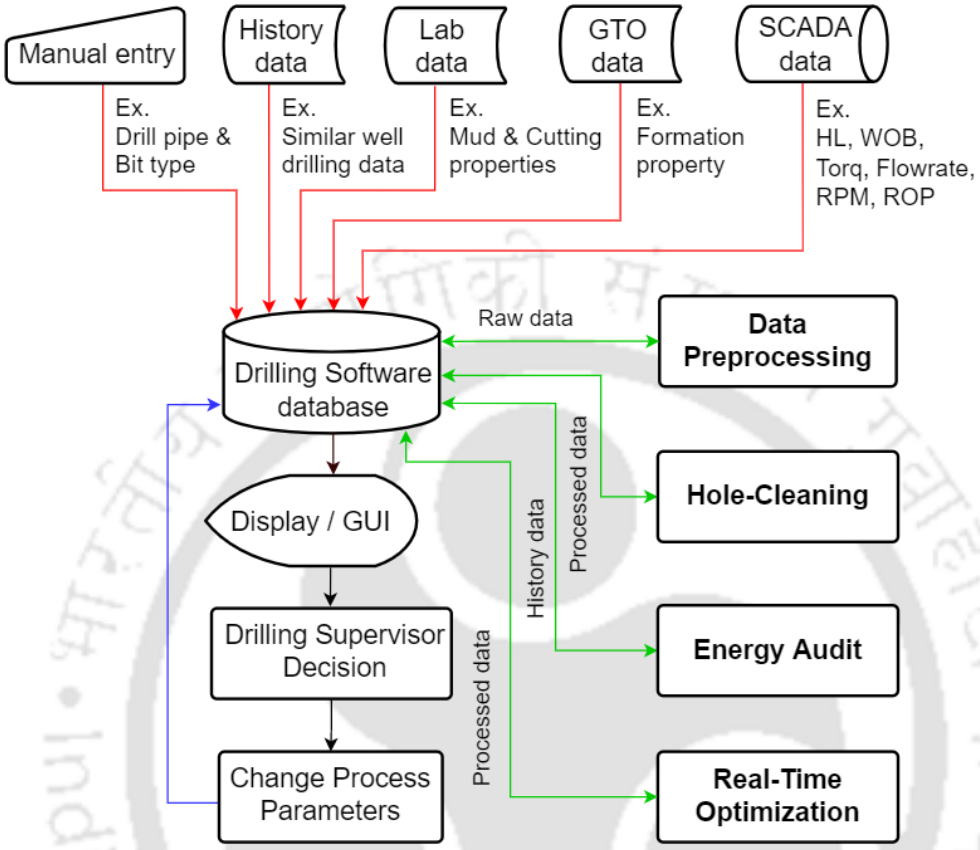

Figure 2.1. Architecture of drilling support system for monitoring and optimization for oil well drilling

The operating steps of the developed DSS are as follows

Step 1: Both time series and static data from different sources were stored in a database (MS SQL)

Step 2: Pre-processing module developed in MATLAB takes the time series data from the database and stores the processed data with an activity tag in the database again

Step 3: Hole-cleaning computation, energy analysis and drilling process optimization are performed in their respective modules parallelly

Step 4: The Python software will access the values of module outputs and alarm flags. The alarm notifications and critical output values will be displayed using a web application (i.e., HTML, CSS) to the driller

Further detailed architectures of the DSS modules are described in the below section.

2.2 The architecture of individual modules

2.2.1 Pre-processing and activity detection module

A highly secure and reliable data transfer system needs to be established for the real-time simulation, prediction, monitoring and control of the drilling operation. Data quality can also be improved by calibrating the primary sensors at frequent intervals. However, most of the current drilling rigs lag in the above tasks. Therefore, pre-processing becomes inevitable for drilling data. The data pre-processing steps are depicted in Figure 2.2.

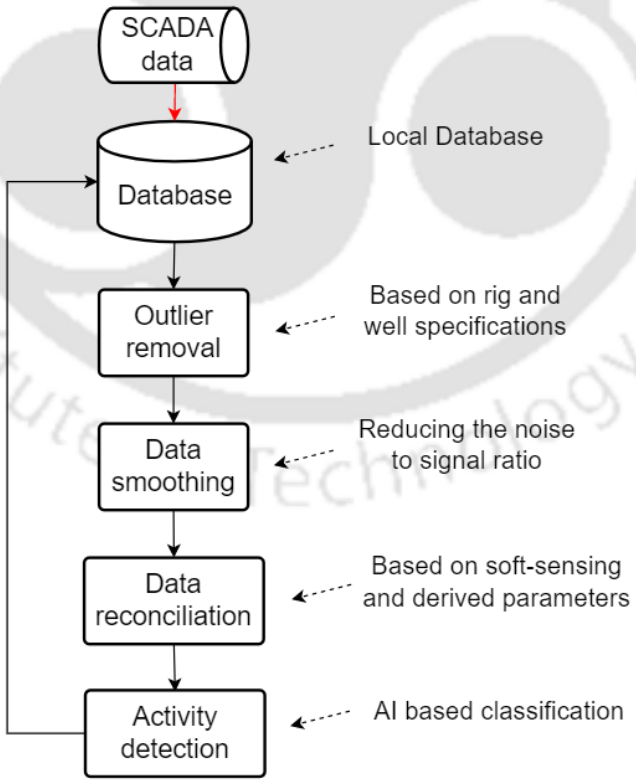

Figure 2.2. Process flow of data pre-processing module

2.2.1.1 Types of errors in SCADA data

The raw SCADA data stored in the MS-SQL could not be directly used for the computation. A typical SCADA data set of drilling operations have the following issues, which have to be filtered, removed, or reconciled before using them:

(i) For some instances of data collection or transfer, the values can exceed outside the possible range of the parameters. For example, the ROP could vary in the order of a few hundred to a thousand meters per hour.

(ii) Sudden jump or drop in total depth (TD) value in a time series data. For example, change in total depth by ten meters in a few seconds

(iii) The bit depth (BD) may be higher than the total depth. The BD and TD values should be equal during drilling as the drill bit is at the bottom of the wellbore while drilling. In contrast, it was observed that in the real-time data, the difference between BD and TD is from a few meters to a few hundred meters. This is due to sensor errors.

(iv) WOB refers to the partial load exerted by the drill string and bottom hole assembly (BHA) on the bit. The hookload has been adjusted so that part of the buoyed weight can be transferred to the drill bit. The WOB can either be a positive value or zero. At times, drilling data can show negative WOB values. This happens due to poor calibration of the hookload sensor or negligence in resetting the WOB value to zero before resuming.

(v) The wellsite information transfer standard markup language (WITSML) has been implemented in most oil well rigs. Still, the data transfer in few rigs are being carried out through old standards such as wellsite information transfer standard level zero (WITS0). Due to the usage of superannuated standards or data mapping errors, the units of parameters at times were misrepresented.

(vi) In case of data transfer interruption, there can be a possibility for duplicate entry of the last data received or some default error code that signified the loss of network connection until the connection got restored.

The data was first fed to a pre-processing module for noise and outlier removal and data reconciliation to rectify the issues described above.

2.2.1.2 Outlier removal

The outlier data points can be removed by applying bounds in the form of a logical filter to the data set. The bounds for outlier removal were decided by taking expert opinion, well plan, and rig specification. The bounds used in this work are given in Table 2.2.

Table 2.2. Pre-processing conditions for outlier removal from raw drilling data

S. N.	SCADA parameter	Lower bound *	Upper bound *	Units
1	HL	> 0	150	ton (US)
2	WOB	0	20	ton (US)
3	TOTSPM	0	200	spm
4	STP	0	150	kgf/cm^2
5	RPM	0	120	rpm
6	ROP	0	100	m/h
7	Flow out relative %	0	100	%
8	TD - BD	0	> 0	m
9	BH	0	30	m
10	TQ	0	690	kgf-cm

* The values may vary with respect to the drilling rig, well profile, and equipment used

2.2.1.3 Data smoothing (noise removal)

The time-series data generated during drilling must be free from the noise before using them for predictions [26], [102]. The time-series data of the Well-AV of Assam asset, ONGC, India,

was used to validate different types of smoothing techniques. Different smoothing techniques were applied to identify the best one for real-time application Figure 2.3.

The data shown in Figure 2.3 belongs to a situation where the flow rate was raised from zero and tried to maintain around 700 gpm. The local regression technique was not performing well when the parameter was changed in a step from low to higher value (marked by (1)). Both Savitzky-Golay and local regression methods were found to be not effective compared to moving average and median techniques in reducing the fluctuations (marked by (2) and (4)). As the moving average gives equal weight to both past and present data, it always predicts with lesser fluctuation than actual data. However, a time delay was observed in the moving average data. The median technique was able to remove noise without time delay and robust in removing fluctuations (marked by (3)). The median technique was selected for data pre-processing by comparing all those pre-processing techniques.

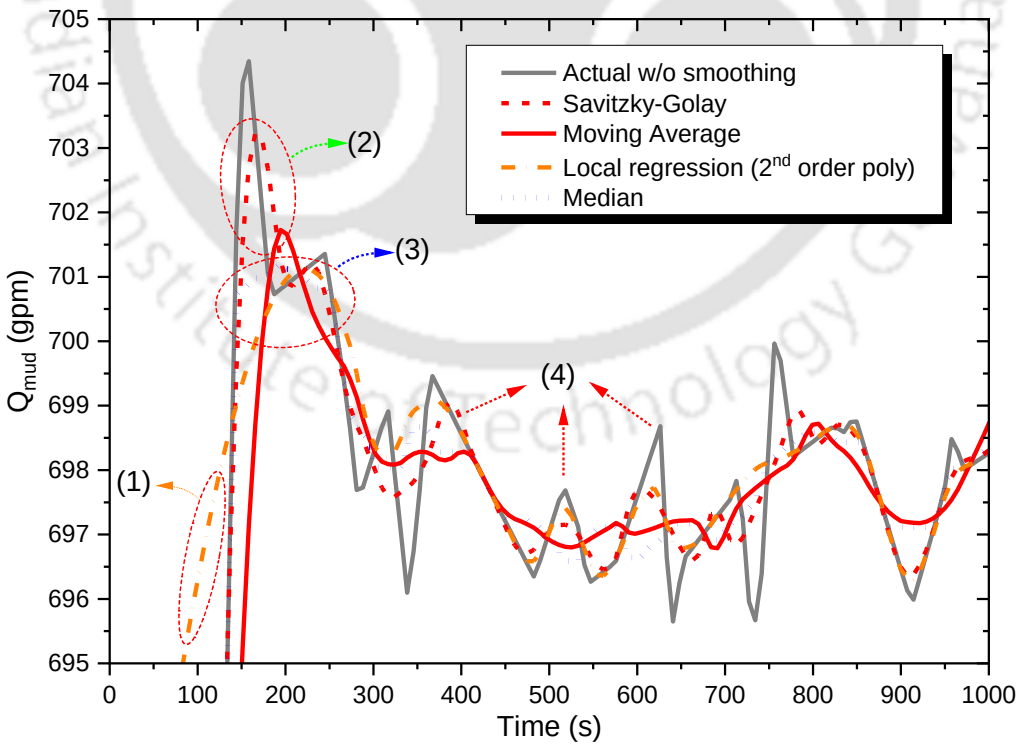

Figure 2.3. Performance of different data smoothing techniques

For the computation of hole-cleaning and energy analysis modules, only the median technique was used for data smoothing. In addition, Hampel and Z-score filter were also used for training of ROP predictions model (i.e., AI model) as it would be used for ROP optimization.

2.2.1.4 Data reconciliation and correction

The abrupt change in SCADA parameters mentioned in section 2.2.1.1 was corrected by applying logical control on the rate of change in total depth. The difference between TD and BD was admitted for the tolerance of ±1 meter for drilling activity.

Auto resetting the value of WOB to zero after every pipe connection before the bit touching the bottom was done. The data set of one complete stand of drilling was adjusted with its initial error value to rectify. The data mapping and unit conversion errors were addressed by re-mapping and conversion factors, respectively, before using the data for computation.

2.2.1.5 Activity detection

The raw SCADA data does not provide information regarding the type of rig activities associated with the time-series data. The type of activity is often documented manually in the driller's shift report (international association of drilling contractors (IADC) report). Such reports have minimal information concerning the duration of various activities without a time-stamp. The rig activities can be identified by drilling experts or by executing activity detection algorithms for such situations. For the high-resolution real-time data, manual tagging is a tedious process to be deployed in real-time. In this article, the activity identification algorithm developed by Tirupathi et al. (2021) was integrated and utilized for energy evaluation and optimization modules [103]. The activity detection module was executed as a two-step process:

Step 1: Firstly, after pre-processing, the real-time sensor data was classified into one of the four predetermined classes/categories such as drilling (with and w/o rotation), tripping in/out (with and w/o rotation), circulation (on/off bottom), and reciprocation using a pre-trained fuzzy

rule-based classifier. The fuzzy classifier deployed the Takagi-Sugeno-Kang (TSK) model for rules being designed as per expert suggestions [104]. The weighted sum aggregation of the rules did provide the classification labels.

Step 2: Next, along with certain features being determined from the sensor data, the label from step-1 was given as an input to a pre-trained random forest classifier. The activity detection module also identifies the data that belongs to (i) rig disengaged from all the operations enlisted Table 2.3, (ii) incorrect data due to sensor problems, and (iii) data loss due to communication problems and will be classified under no operation conditions. The pre-processed SCADA data was expected to be free from outliers and sensor error. Hence, an additional activity tag label for each activity will be added to the processed SCADA data as shown in Table 2.3. Further, similar and complementing activities were grouped under six major operations Table 2.4.

Table 2.3. A summary of tag label and types of oil rig activities.

Tag label	Activity name	RPM	Tag label	Activity name	RPM
1	Drilling with rotation	> 0	2	Drilling without rotation	= 0
3	Tripping out (back reaming)	> 0	4	Tripping out	= 0
5	Tripping in (reaming)	> 0	6	Tripping in	= 0
7	Circulation (rotation on bottom)	> 0	8	Circulation	= 0
9	Circulation (rotation off bottom)	> 0	11	Non-productive Operations	≥ 0
10	Reciprocation	> 0			

The pre-processed data with activity tag will be stored in the MS SQL database for subsequent use.

Table 2.4. Major rig operations and associated grouping of tag labels

S.N.	Operation name	Tag label
1	Drilling	1 + 2
2	Tripping	4 + 6
3	Reaming	3 + 5
4	Circulation	7 + 8 + 9
5	Reciprocation	10
6	Non-productive Operations	11

2.2.2 Hole-cleaning module

Hole-cleaning is a process of transporting cuttings from the bottom hole to the surface. The hole-cleaning monitoring module is divided into 1) hydraulic management and 2) ECD management (Figure 2.4).

The hydraulic management part calculates the mudflow requirements for the drilling fluid to achieve enough cutting transport. The main inputs to the hydraulic management part's computation are the cutting and mud properties, discharge rate, ROP, and directional data. It evaluates the minimum mud discharge rate required, net transport velocity (NTV), transport efficiency, cutting concentration, annular transport time (ATT) and effective density in the annulus, and pressure drop across the wellbore sections.

Along with the effective density and the annulus hydraulic pressure evaluated in the hydraulic management part, the formation and mud properties were also fed as input to the ECD management part's computation. The ECD management part evaluates the critical velocity and ECD at multiple wellbore depths.

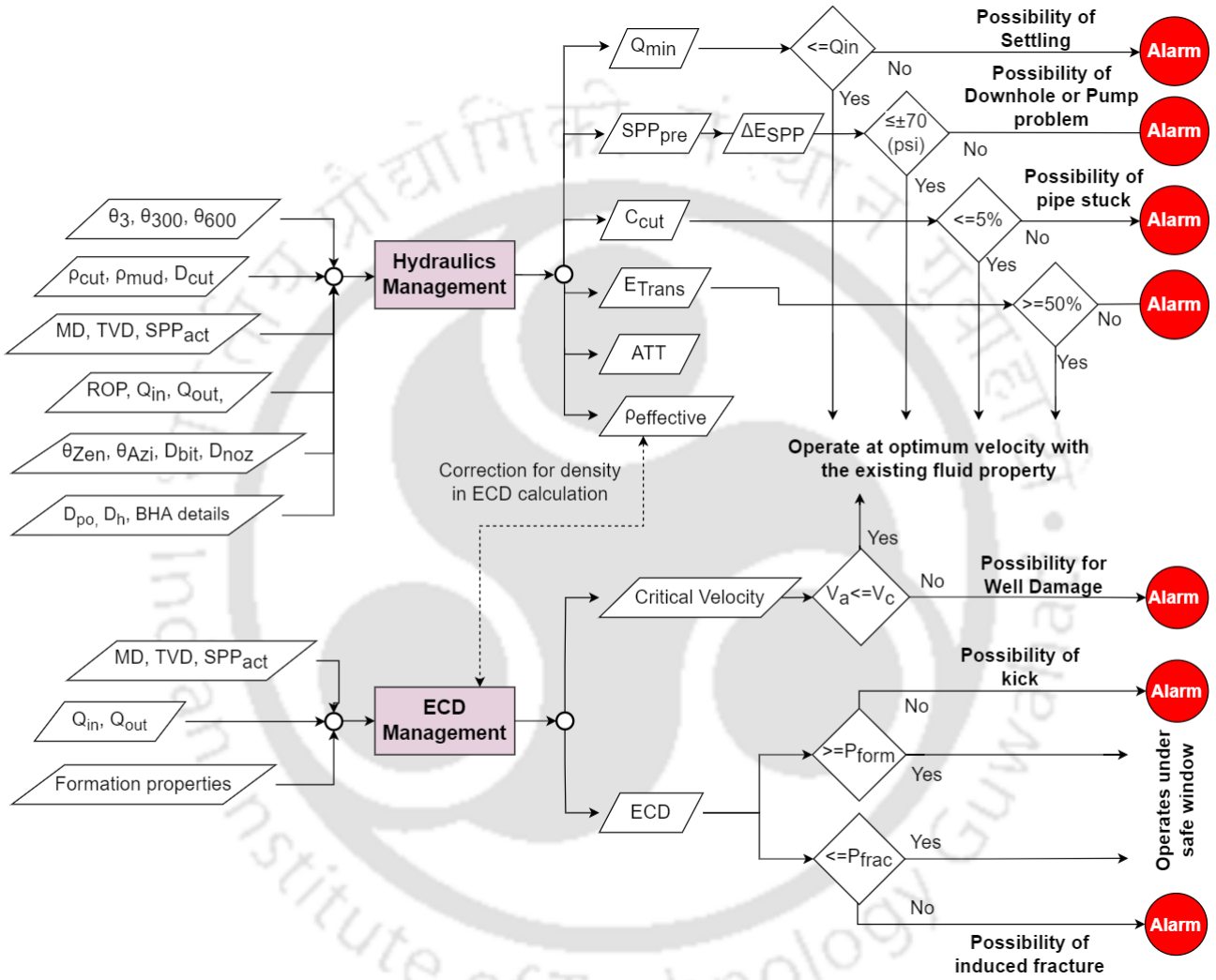

Figure 2.4. Process flow of hole-cleaning monitoring and well bore stability module

The hydraulic management division warns the driller to make corrective actions for the following criteria violation

- Whenever the overall annulus cutting concentration increases more than 5%
- The transport efficiency decreases below the benchmarking value of 50% [21]
- The deviation between measured and predicted STP is more than 70 psi

Similarly, ECD management plays a crucial role in maintaining wellbore stability. This division will compute the ECD profile from the bottom to the surface of the wellbore. The ECD profile will be compared with the formation and fracture pressure gradient (i.e., ECD window) and generates an alarm to the supervisor whenever the open hole ECD approaches either side of the permissible window (i.e., 10 % offset as an acceptable window for ECD).

When the ECD is approaching formation pressure, the alarm for kick will be raised. Similarly, a warning for induced fracture (i.e., the possibility of mud loss and well collapse) will be raised when the ECD comes close to fracture pressure.

Critical velocity is the velocity above which the flow regime of drilling fluid changes from laminar to turbulent. The laminar flow is recommended over turbulent flow in the open-hole section for better cutting transport and wellbore stability. The minimum fluid velocity (i.e., to transport the cutting) and the critical velocity are the lower and upper limits of the mud velocity in the annulus. Therefore, the alarm will be raised whenever the annulus velocity violates the limit.

2.2.3 Energy audit module

For the case of offset development wells, the historical data of the exploratory and previous wells were also collected and stored in the Microsoft structured query language (MS-SQL) database.

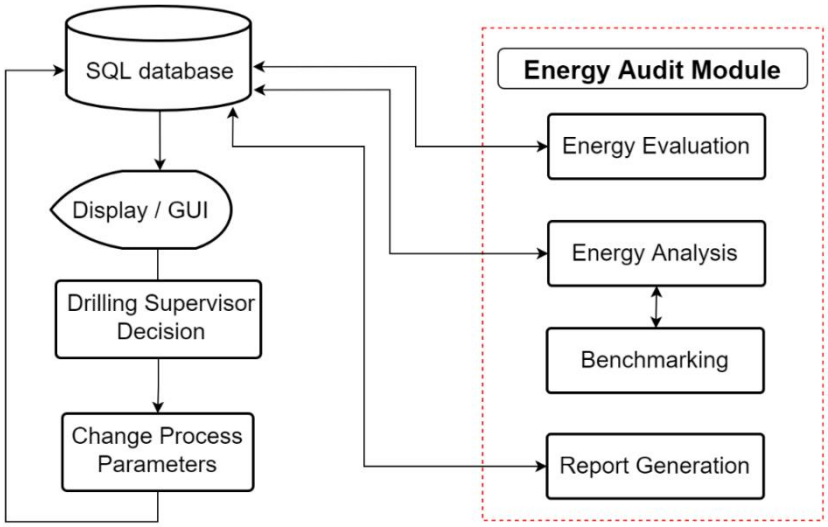

Figure 2.5. Process flow of energy analysis module

As shown in Figure 2.5, the pre-processed and activity tagged data that was stored in the database is supplied to the energy audit module along with additional information such as the phase of drilling, drill bit details, mud properties, and mud pump specifications (i.e., model number, liner size, volumetric efficiency, mechanical efficiency). In the first step, the module evaluates the power consumed by each piece of equipment individually. In the second step, the energy consumption for each piece of equipment has been estimated by integrating the power. However, the tripping-in operation was powered by gravity and was controlled by a hand brake.

From the fuel consumption data of the drilling site, it was recognized that the brake's power consumption is negligible compared to the energy consumption of other major equipment. Therefore, the energy consumption during tripping-in was only attributed to mud pumps if circulation was enabled. The calculated energy consumption details were stored in the database

and updated for real-time monitoring in the drilling supervisor's display. The energy evaluation outputs were further analyzed to improve the real-time rig performance of the well or any offset development wells in the future.

2.2.4 Real-time optimization module

The real-time optimization module is depicted as a standalone system architecture in Figure 2.6.

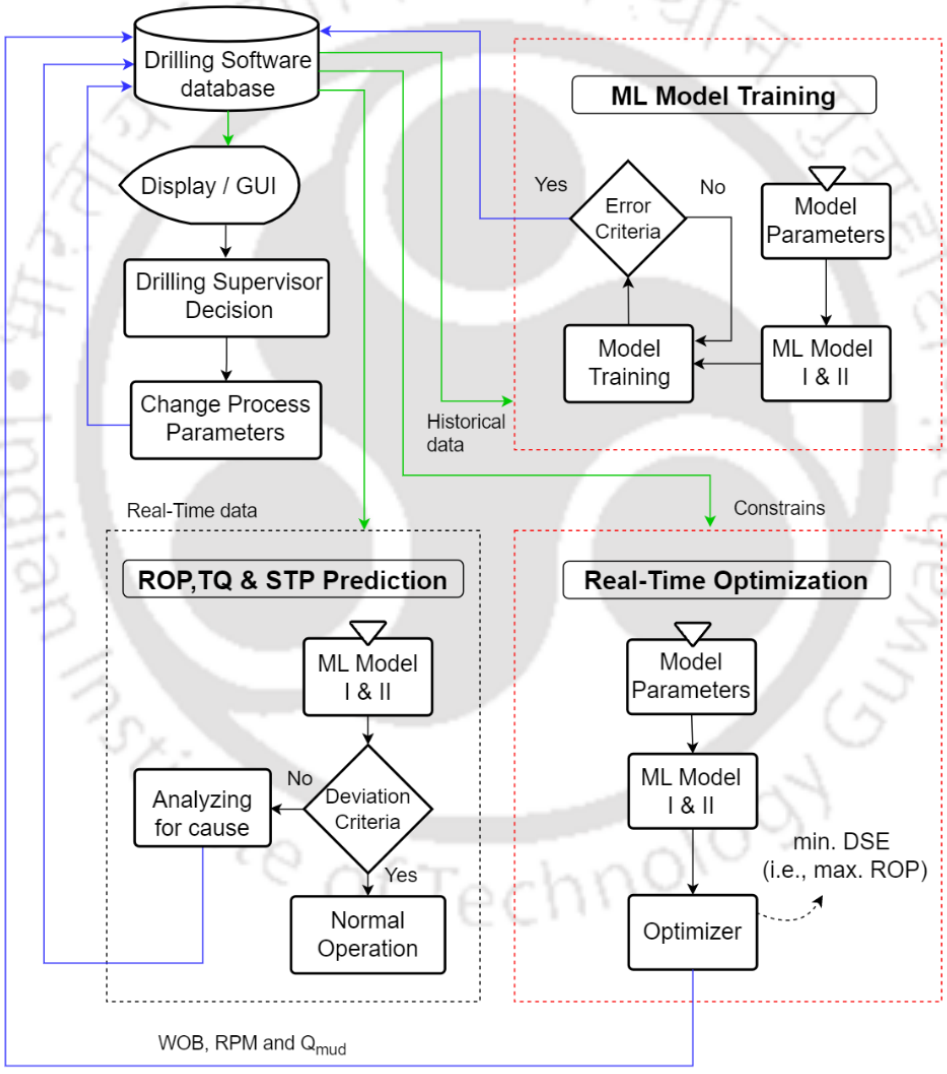

Figure 2.6. Process flow of real-time optimization module

As described before, the pre-processed data stored in the local database (MS SQL) was utilized by this module also. The pre-processed data of the last four hours were used to train the AI

models I and II. Consequently, the trained model was employed in the real-time prediction of STP, TQ and ROP until the next training cycle. The duration of the model validity period has been fixed as an hour (i.e., the model prediction horizon).

The real-time optimization of drilling was performed in the optimization sub-module. The objective of the sub-module was to maximize ROP for lower energy consumption. The optimizer was given the constraint to maintain the mudflow rate above the minimum required rate to achieve better hole-cleaning. The prediction output and optimization results will be stored in the database and displayed through a web-based graphical user interface (GUI). As the proposed system is open-loop, the driller will decide the implementation of the optimization result.

The detailed model development and implementation of hole-cleaning monitoring, energy analysis and optimization modules are given in chapter-3, chapter-4 and chapter-5, respectively.

Chapter 3

Downhole Problem Prevention by Enhanced Cutting Transport and Wellbore Stability

3. Downhole Problem Prevention by Enhanced Cutting Transport and Wellbore Stability

3.1 Problem statement

It is well known that inadequate hole-cleaning can lead to many downhole problems. Prediction and treating the root causes of the problem in real-time could prevent drilling operation from major complications. There comes a need for development of a system to predict critical wellbore parameters and monitor the drilling process in real-time. The proposed system in this thesis work is expected to predict wellbore hydraulics and cutting transport mechanisms in real-time. The wellbore consists of surface equipment, drill string, drill bit, and annulus as the mud flowing path. All these sections are modelled using an object-oriented programming language 'Modelica' to perform the above task

3.2 Mathematical model development

The hole-cleaning module described in this chapter has been integrated with the DSS illustrated in Figure 2.1 of chapter 2. The hole-cleaning module has two sub-modules such as hydraulic and ECD management. The following assumptions are considered to develop the mathematical model for hydraulic and ECD management.

1. Mud loss through pores/fractured formation wall is negligible; it will be true when the drilling fluid's solid content is adequate for pore bloacking and cake formation.
2. Openhole diameter is assumed to be constant.
3. The well is considered to be vertical; as the data used was belong to wells having inclinationn between 0º to 30º.
4. The surge and swab effects are negligible during drilling and mud circulation.

5. The annulus mudflow does not consists of formation fluid and gas; for the condition of overbalanced drilling.

The nonlinear mathematical model used in hydraulic and ECD management divisions should be solved in real-time. They include unsteady-state material and momentum balance equations for different wellbore sections such as surface equipment, drill string, drill bit and annulus. Table B.1 [2] shows that the mud rheological properties such as flow behaviour index, flow consistency index, and yield point were calculated using shear stress measured at different shear rates such as 3, 300 and 600 rpm. The model equations for the drill bit and surface equipment are given in Table B.2 [56], [105]. The model equation for the drill string and annulus sections are shown in Table B.3 and Table B.4, respectively [1], [49], [56].

The drilling fluid is filtered and the cutting are removed in shale shaker. As there is no cutting generation inside the drilling string, the mud present in it does not carry any cuttings. Therefore, the inlet flow rate becomes equal to the outlet flow rate. The model equations presented in Table B.3 consider mudflow rate, rheological properties, and drill string dimensions such as inside diameter and length for each section as inputs to calculate the frictional pressure drop inside the drill string section (equations (B.6) to (B.16)). As shown in Table B.4, equations (B.31) to (B.42) are used to calculate the pressure drop in annulus section.

The empirical constants (C_{at}, C_{at2}, C_{al}, C_{pl}, C_{pt} and C_{pt2}) in these pressure drop equations vary with respect to formation roughness and temperature, and mud cake growth rate. Therefore these parameters can be tuned to predict the actual pressure drop. The subscripts; ‘a’, ‘p’, ‘l’ and ‘t’ denote the annulus side, inside drill pipe, laminar flow regime and turbulent flow regime.

In addition to the above pressure drop calculations, the unsteady state mass balance equation for the cutting transport is solved to predict the cutting concentration in the annulus section.

Figure 3.1 shows the pictorial representation of volume balance for a single annulus section. The volume balance and cutting transportation are written in mathematical form in equations (B.17) and (B.30) assuming mud is incompressible fluid and hence the density is constant in downhole. The cutting generation term will appear on the bottom section. Similarly, the topmost section does not have an incoming settling term, and the bottom most section will not have an outgoing settling term.

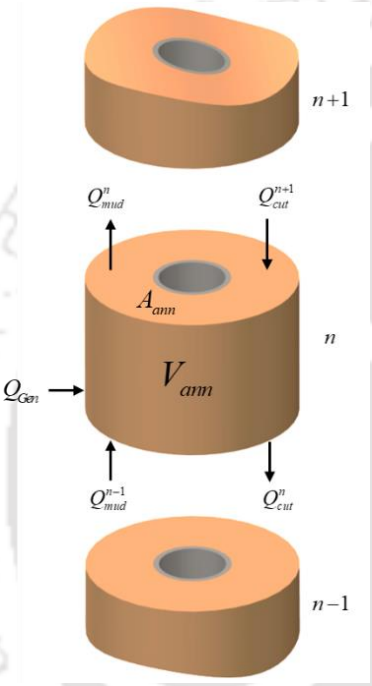

Incoming settling of the top section is zero ($Q^{top+1}_{cut} = 0$)

Outgoing settling of the top section is zero ($Q^{Bottom}_{cut} = 0$)

Cutting generation in all the section except bottom section will always be zero

Figure 3.1. Pictorial representation of volume balance in annulus section

3.3 Model implementation in Dymola

The model for surface equipment, drill string, drill bit, and annulus section was implemented in an object-oriented programming language, 'Modelica', using the 'Dymola' programming tool. The individual models were used to create a flowsheet model as shown in Figure 3.2. The blue and red dotted lines denote mud flow and cutting settling, respectively. The dimensions of different sections are fixed based on the wellbore configuration sheet given in Table 3.1. The phase of the drilling defines the wellbore sections of different casing diameter. As the

drilling progress, the diameter of the open hole (i.e., drill bit size) will be reduced after every casing to enable further drilling.

Table 3.1. Wellbore configuration for Well-AV

Variable name	Abbreviation (Unit)	Phase I	Phase II	Phase III
Casing Length	CL (m)	297	2547.8	4001.5
Casing Diameter	OD (in)	20	13.375	9.625
	ID (in)	19.124	12.715	8.755
Drill Pipe	OD (in)	5	5	5
	ID (in)	4.7767	4.276	4.276
	Unit Wt (lb/ft)	19.5	19.5	19.5
Drill bit Diameter	D_{bit} (in)	26	17.5	12.25

The challenge arises while predicting the effective frictional pressure drop in the annulus and inside the drill string. The friction factor between mud and the formation wall will vary with respect to depth due to changes in the formation properties. A one-dimensional unsteady-state model was developed in Dymola to incorporate those variations along with the depth. Further, the annulus section was split into multiple sub-sections to improve the prediction accuracy.

The drilling string consisted of ten segments to incorporate the variation in drill string diameters. The annulus was split based on the variations in the diameter of the open hole, cased hole, and drill string sections. The open and cased-hole portions were divided into three sub-sections to improve the accuracy of slip velocity and cutting concentration computation. The integrated flowsheet model was solved using the 'Lsodar' solver available in the Dymola tool.

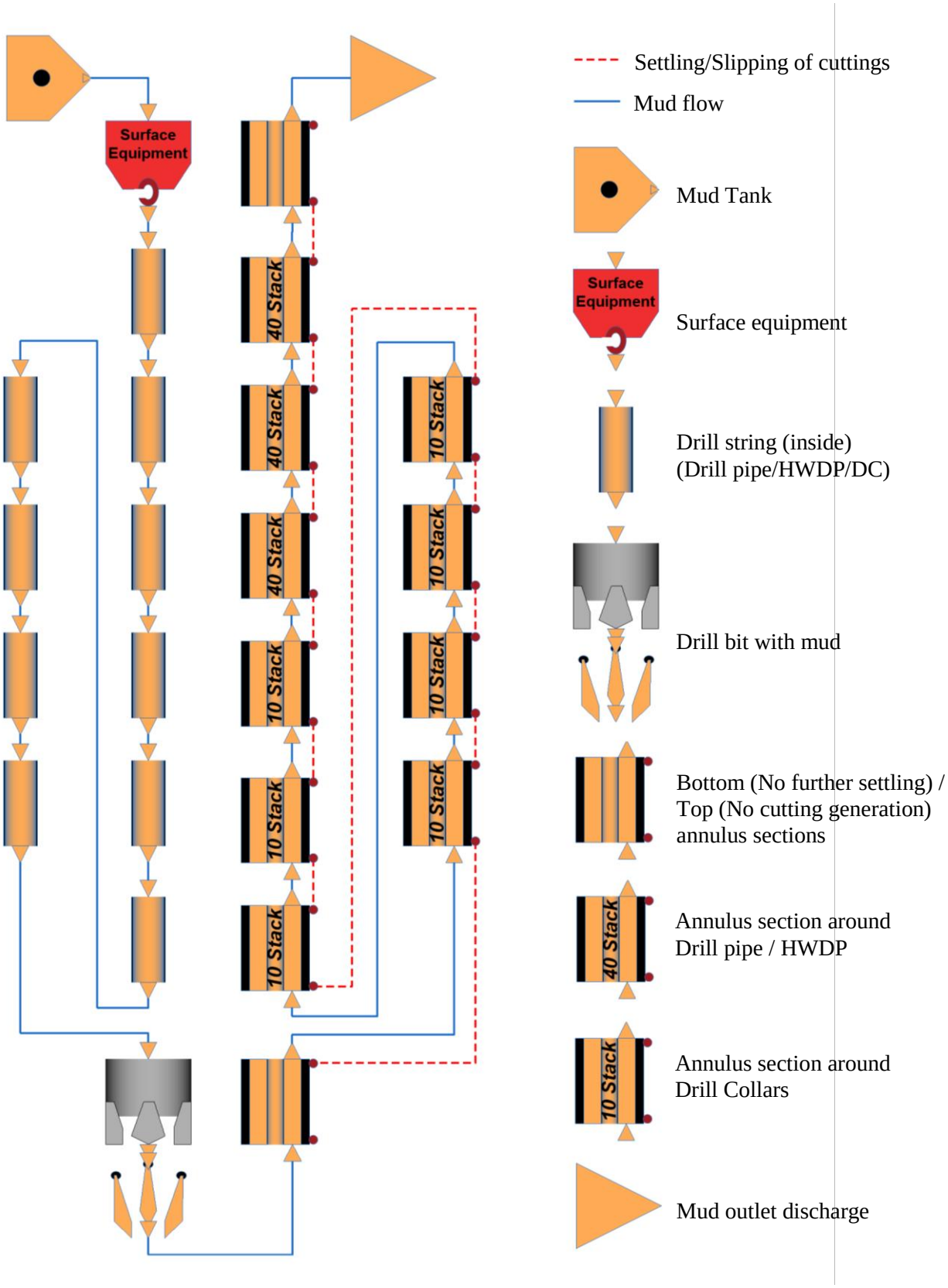

Figure 3.2. Architechture of the flow sheet model for mudflow by using Dymola

The input required for the hole-cleaning module and its output are listed in Table 3.2.

Table 3.2. The critical input and output variables for the flowsheet model

S. No.	Variable Name	Type	Default Values
1	Q_{mud} (m^3/s)	Input	0.05 (792gpm)
2	Mud weight (g/cm^3)	Input	1.145
3	ROP (m/h)	Input	15
4	Cutting Size (in)	Input	0.3
5	Cutting density (g/cm^3)	Input	2.4
6	Depth (m)	Input	3.0
7	Initial cutting concentration (vol %)	Input	1
8	θ_3	Input	7
9	θ_{300}	Input	28
10	θ_{600}	Input	35
11	STP (psig)	Output	NA
12	Annular Transport Time (s)	Output	NA
13	Transport Efficiency (%)	Output	NA
14	Minimum mud flowrate (m^3/s)	Output	NA
15	Cutting concentration (%)	Output	NA
16	Effective mud density (g/cm^3)	Output	NA
17	ECD (g/cm^3)	Output	NA
18	Critical Velocity (m/s)	Output	NA
19	Slip velocity	Output	NA

3.4 Simulation studies

3.4.1 Sensitivity analysis

3.4.1.1. Effect of critical model parameters on STP

A sensitivity analysis was done on the Modelica flowsheet model to finalise the parameters to be tuned. As shown in Table 3.2, the model was developed to provide more than one output. However, experimentally the STP alone was measured in real-time.

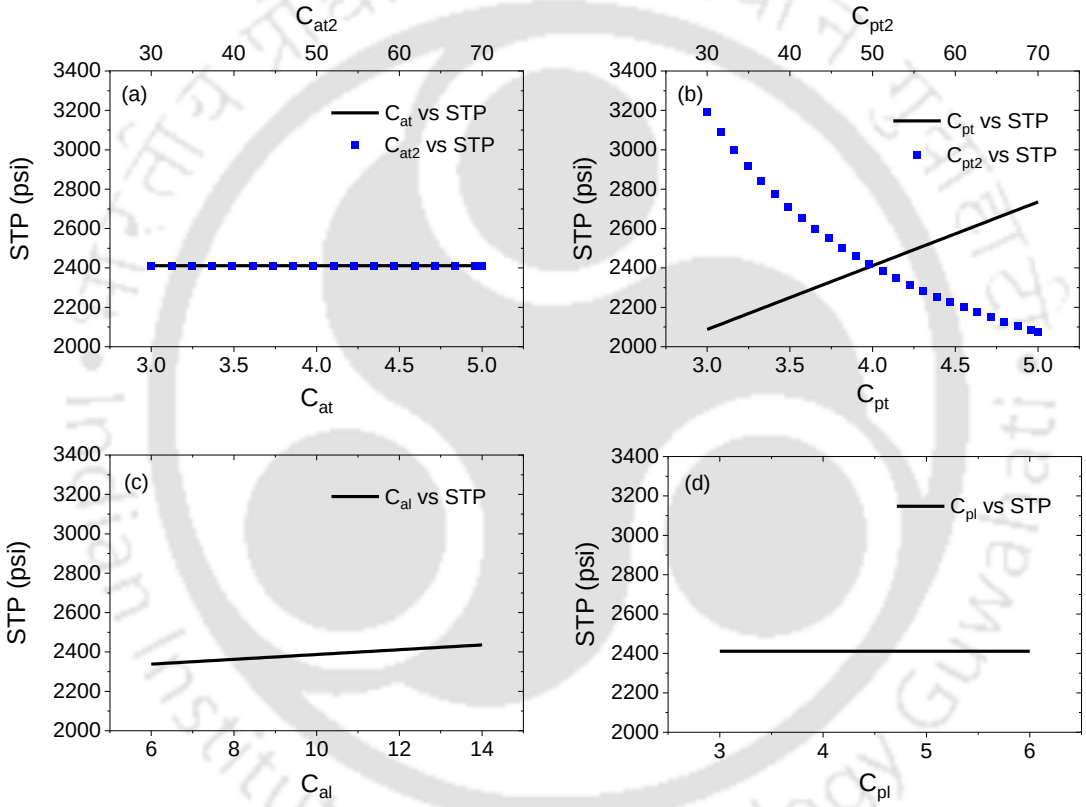

Figure 3.3. (a) Effect of model parameters C_{at}, C_{at2} on STP. (a) Effect of model parameters C_{pt}, C_{pt2} on STP. (a) Effect of model parameters C_{al}, C_{pl} on STP
(Electronic version is recommended to differentiate colour)

As described in section 3.2, the empirical constants, C_{al}, C_{pl}, C_{at}, C_{at2}, C_{pt} and C_{pt2} may need to be re-estimated at different intervals for a given well. Therefore, the variation in STP with respect to model parameters were simulated as shown in Figure 3.3.

The flow regime around the drill string (i.e., the annulus side) is expected to be laminar (i.e., except around BHA). Therefore, the effect of constant C_{at} on the STP was insignificant (Figure 3.3(a)). The STP maintains a linear relationship with C_{pt} changing from 3 to 5 (Figure 3.3 (b)). Whereas the STP exponentially decreased for variation in C_{pt2} is changed from 30 to 70. As the STP was sensitive to C_{pt} and C_{pt2}, they were chosen as the tuning parameters for the turbulent regime (i.e., turbulent flow dominates inside the drill string).

Similar to C_{pt}, the parameter C_{al} (i.e., simulation range 6 to 14) was also found to have a linear relationship with STP. However, the gain in STP was lesser compared to C_{pt} (Figure 3.3(c)). The flow inside the drill string was dominated by turbulent flow. Therefore, the laminar flow's empirical constant (C_{pl}) does not have any impact on the STP (Figure 3.3(d)). From the above analysis, the model parameters C_{pt}, C_{pt2} and C_{pl} were chosen for model tuning to predict STP.

3.4.1.2. Effect of mud flowrate and density on the critical variables

The mudflow rate (Q_{mud}) and density are critical process variables that have been controlled to maintain the required value of STP, NTV, transport efficiency (E_{tran}), slip velocity, effective mud density, and ECD to achieve optimal hole-cleaning, ROP and wellbore stability. The effect of mud flowrate and mud density on hydraulic and cutting transport variables are depicted in Figure 3.4.

As shown in Figure 3.4(a) and Figure 3.4(b), annular velocity (V_a) and net transport velocity (NTV) maintained a linear correlation with mudflow rate. The transport efficiency increased non-linearly and approached an asymptotic value for a linear increase in mud flowrate. The slip velocity is almost constant for a fixed mud density and viscosity. Hence, a further rise in mudflow rate did not help to increase transport efficiency. ECD is a function of annulus frictional pressure drop, a non-linearly function of mudflow rate. Therefore, The ECD increased non-linearly with a linear increase in mudflow rate for a given mud property.

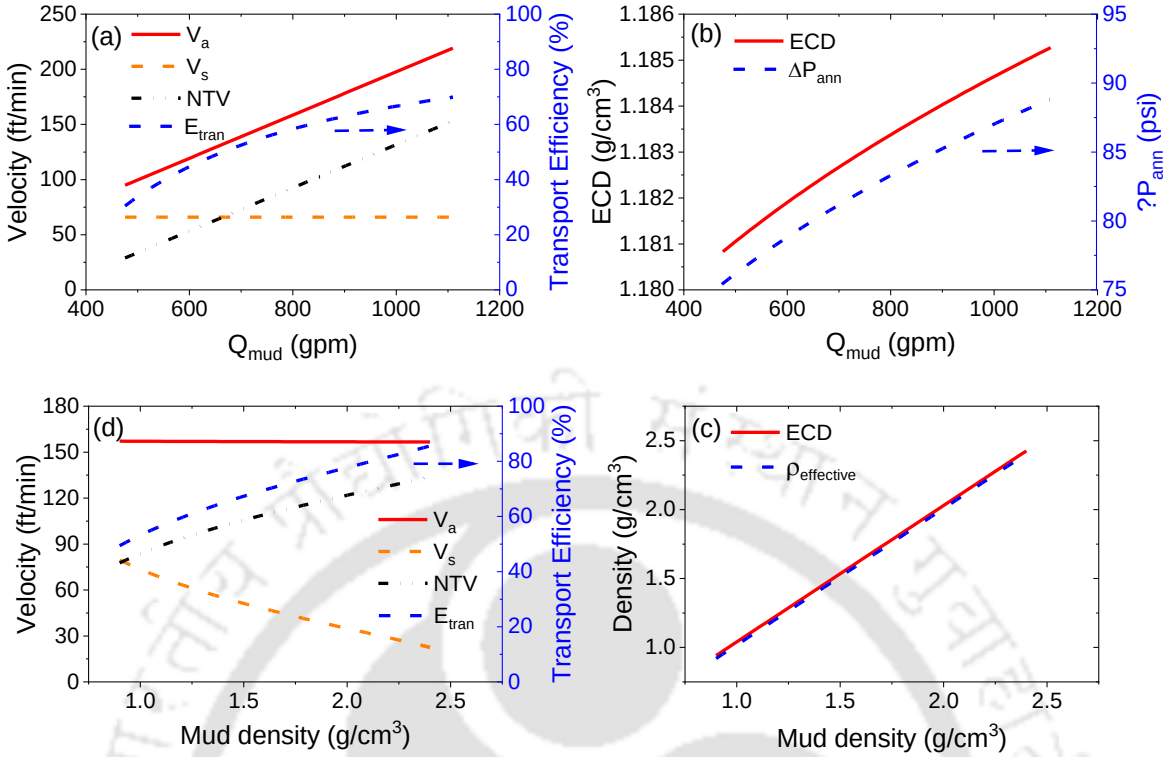

Figure 3.4 (a) Effect of mud flowrate on V_S, V_a, NTV and E_{tran}. (b) Effect of mud flowrate on ECD and ΔP_{ann}. (c) Effect of mud density on V_S, V_a, NTV and E_{tran}. (c) Effect of mud density on ECD and ΔP_{ann} (Electronic version is recommended to differentiate colour)

The dependency of NTV and transport efficiency on the annulus velocity was vivid for a flow rate variation from 0.03 to 0.07 m^3/s (476 to 1110 gpm). The mud velocity in the annulus changed linearly with the mudflow rate, also reflected in NTV. For a given mud property, the minimum flowrate required was affected by ROP (i.e., rate of cutting generated) and wellbore hole size.

The density of typical drilling fluid will vary from 0.9 – 2.4 g/cm^3. In general, low-density mud was used for subnormal formation pressure applications. High-density mud will be required for deep and highly active wells to avoid kick events. The effective mud density of the wellbore maintained the linear relationship with inlet mud density. The ECD increased linearly due to increasing mud density and STP (Figure 3.4 (d)). The slipping velocity of cuttings reduces for an increase in mud density. The simulation study concludes that the transport efficiency can be

improved by 133 % and 70 % by manipulating the mudflow rate from 0.03 to 0.07m^3/s and mud density from 0.9 to 2.4 g/cm^3 (Figure 3.4 (c)), respectively**.**

3.4.1.3. Effect of mudflow rate on unsteady-state behaviour of cutting concentration

The dynamic behaviour of cutting concentration for a fixed mud flowrate, mud density and ROP is illustrated in Figure 3.5. The variation in cutting concentration with respect to time for both ideal condition (i.e., ROP = 0 m/h, Q_{mud} = 0 gpm) and drilling operation (i.e., ROP = 15 m/h, $Q_{mud} \neq 0$ gpm) were simulated.

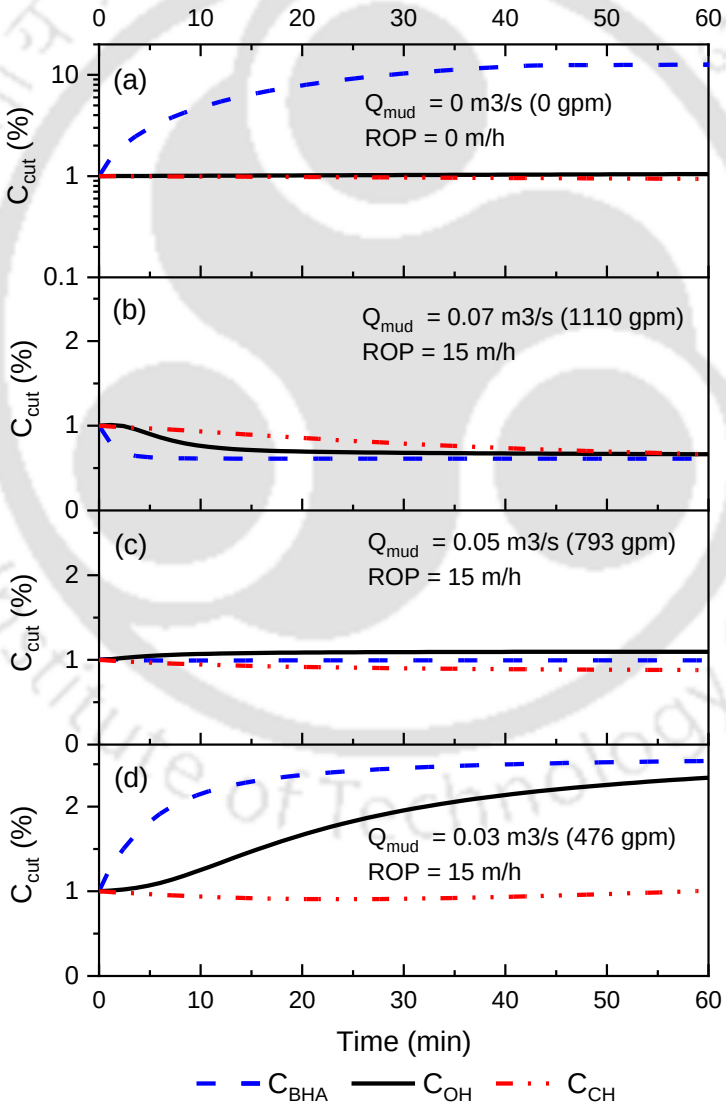

Figure 3.5 Effect of time on cutting concentration of wellbore annulus for the cases of (a) no circulation and no drilling. (b) high circulation rate and drilling (c) medium circulation rate and drilling. (d) low circulation rate and drilling

The initial cutting concentration of the annulus was assumed to be 1 % (vol/vol). The average cutting concentration around BHA, open hole (OH) and cased hole (CH) are plotted with respect to time. In the case of no drilling and no circulation, the cutting concentration in the upper section (i.e., CH) was depleting as the cuttings were transported to the bottom section due to settling. The OH section around the drill pipe (i.e., the section above BHA and below CH) has maintained the cutting concentration between section BHA and CH (Figure 3.5 (a)).

The effect of high, medium and low mud flowrate was simulated for a constant ROP (15 m/h) and shown in Figure 3.5 (b), Figure 3.5 (c) and Figure 3.5 (d), respectively. As the annular mud velocity was maintained higher than the slip velocity of cuttings, the cutting concentration decreased for the higher flow rate (Figure 3.5 (b)). In contrast, the cutting concentration increased for the lower flow rate (Figure 3.5 (d)). However, in the case of medium flow rate, the cutting concentration reached a steady-state (≈10 min) as the cutting transport from one section to another was equal to the cutting generation rate (i.e., ROP), and the same can be observed in Figure 3.5 (c).

3.5 Model validation with field data

In a typical model calibration and validation process, a portion of historical data will be used for calibration and the remaining for validation. Accordingly, the first 30 min drilling data was used to tune the model parameters to fit the current physical condition of the wellbore. The tuned model was expected to predict the STP during the typical drilling process and mud circulation. However, the actual STP is likely to deviate from model prediction during anomaly conditions: abnormal wellbore conditions, sudden change of formation properties (i.e., cutting density, pore pressure), mud property, hole size, mud pump failure, drill string washout, well collapse, kick and loss, etc.

A vertical well (Well-AV) drilling data from Galeky field, Assam asset, India, were collected to validate the model. The data range of the normal drilling and problematic drilling were classified with the help of expert knowledge and the daily progress report. The developed mathematical model was used to predict STP for a normal drilling operation using literature reported model parameters [49]. Though the trend of the predicted STP was similar to the actual, the predicted STP was much lesser than the actual STP (Figure 3.6 (a)).

After the model was calibrated with the first 30 min data, the model prediction was matched with measured STP. The model validation was done with the following 1.5 h data. The STP prediction error was reduced drastically after calibration. The relative error between model and measured STP was lower than 3% for the tuned model parameter and greater than 30% for the literature reported parameter. The drillers were requested to take action if the deviation exceeded 70 psi during the drilling operation.

3.5.1 Case studies of drilling problem prediction

3.5.1.1 Case 1: Mud pump problem and drill string washout

The mud pump failure events were observed more frequently while analysing the actual drilling data. After 5 hours of normal drilling, a frequent deviation between model predicted STP and measured STP was observed. The deviation amplitude increased with respect to time and reached a maximum deviation of 1500 psig at the 14th hour of the drilling operation.

Later, it was found that the pressure shoot up was due to an uncleaned discharge strainer of the mud pump. The debris such as valve rubber and broken pieces of the piston choked the mud pump discharge strainer. For such a case, attempting to increase the mudflow rate (i.e., strokes per minute (SPM)) shall result in enhanced pressure at the mud pump, which will not be shown in the pressure gauges beyond the strainer [106].

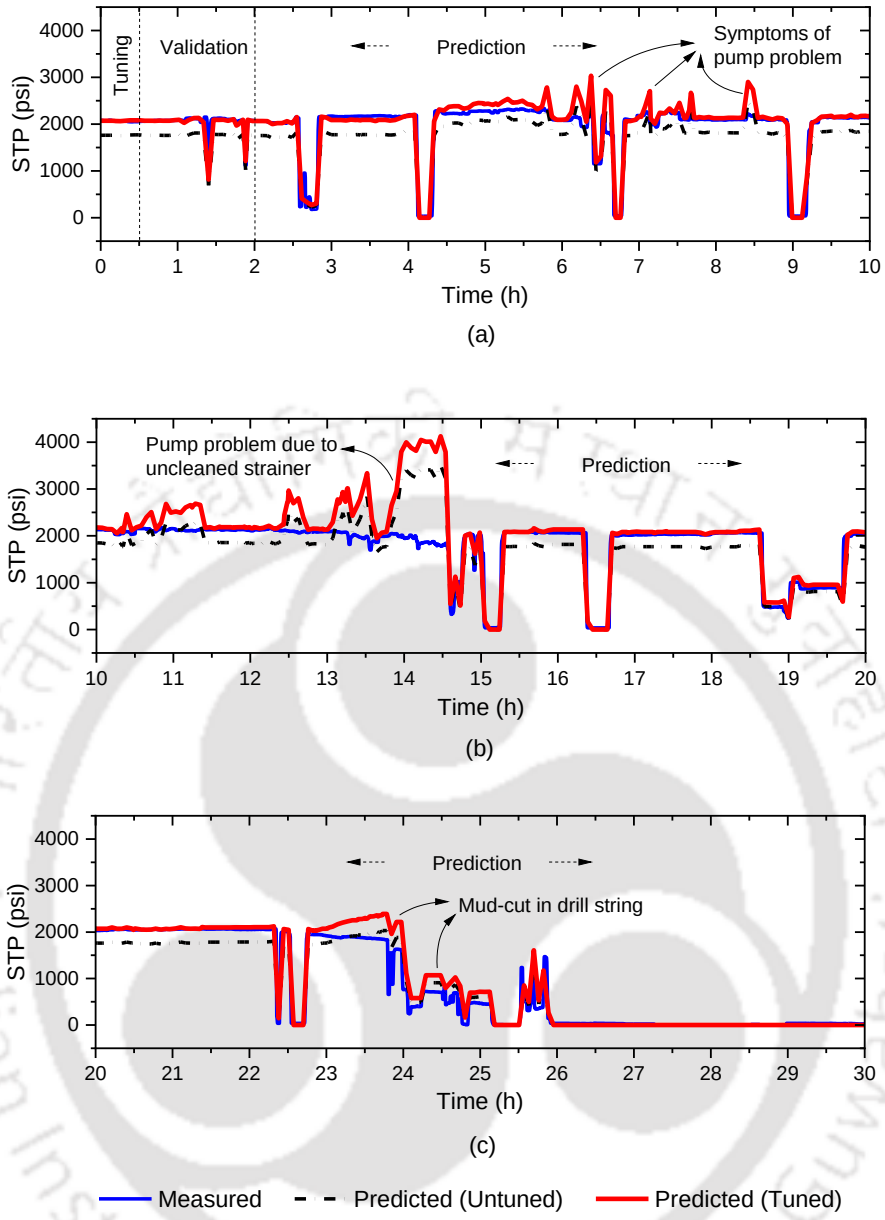

Figure 3.6. Hole cleaning model: calibration, validation and prediction of STP (case 1) (Electronic version is recommended to differentiate colour)

The STP has been measured at the standpipe located after the mud pump. The pressure fluctuations of the mud pump may not get reflected in the STP, Therefore, the fluctuations observed in the predicted STP was not observed in the measured values during the mud pump problem. The deviation between the measured and the predicted indicates the anomaly.

Therefore, the fluctuations observed in the predicted STP was not observed in the measured values during the mud pump problem. After cleaning the discharge strainer, the drilling was resumed without any problem. The strainer has to be cleaned frequently to avoid the above scenario. Though the standard practice is to clean the strainer after completing every 100 m drilling, sometimes the driller may be busy dealing with some other issues and ignore cleaning the strainer. As a result, the performance of the mud pump may deteriorate over time Figure 3.6 (b).

When the drill bit crossed the depth of 3464 m at the 22nd hour, 285 psig (20 kgf/cm^2) of pressure loss in measured STP was noticed. The driller first ensured no issue with the mud pump and surface connections. However, the measured STP decreased with time even when the flow rate was increased. It was anticipated that the pressure drop was likely due to mud cut (i.e. there was no loss in hookload as in the case of complete drill string washout), and pull out was started. Drill string mud-cut followed by washout is one of the most anticipated downhole problems. Due to the abrasion and fatigue damage to the drill string during continuous rotation of the drill string, the pin-box connection can get damaged, and drilling mud may start leaking from drill string to the annulus. The pressure difference between the drilling string mud stream and the annulus is huge. Minor damage may propagate and cause the complete drill string part to go off. The mud leakage and corresponding pressure drop will reflect in STP. The hookload readings can indicate whether there is just a mud-cut or washout.

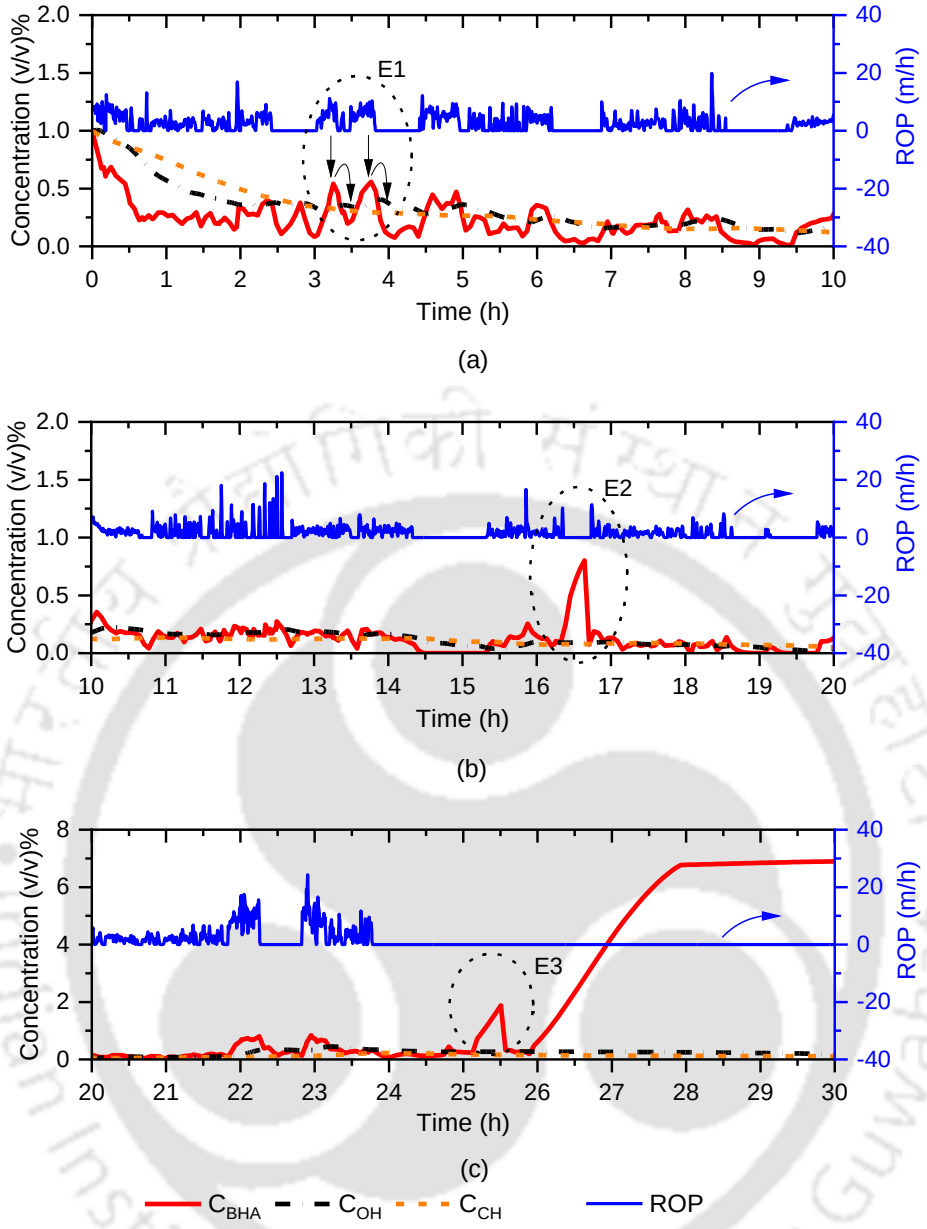

Figure 3.7. Dynamic cutting concentration prediction by hole-cleaning model (Case 1)
(Electronic version is recommended to differentiate colour)

Detecting the mud-cut early could avoid drill string washout. Once the washout happens, it will take days to weeks to engaged the broken part and retrieve the well from settled cuttings. Figure 3.7 shows the change in cutting concentration in the annulus around BHA, open hole (OH) and cased hole (CH) for Well-AV. As the cuttings are generated from the bottom of the bore well, the BHA is the first receiver of the generated cuttings. Therefore the cutting concentration

around the BHA will be very sensitive to the rate of penetration (ROP) followed by the open hole annulus section but with some time delay, as indicated by E1 in Figure 3.7 (a).

The cutting concentration in the cased hole section did not respond to the quick fluctuations in the ROP. As long as enough mudflow is maintained, the cutting concentration around the BHA will be low. After stopping the drilling activity (i.e., ROP =0 m/h), the mud circulation is necessary to ensure the complete removal of cuttings from the wellbore. If it is not followed, the cutting concentration in the BHA section will rapidly increase due to the settling in a stagnant mud condition (Figure 3.7 (b) E2 and Figure 3.7 (c) E3). However, restoration of mud flowrate can enable the cutting transport from BHA to the open hole.

3.5.1.2 Case 2: Mud pump failure and cutting accumulation

This case explains how a simple mud pump problem could get exaggerated when there is no mathematical model-based real-time monitoring system is employed. The sensor values of mud pump discharge went through sudden peaks during the drilling of Well-AV2. The drilling was continued for a few hours without noticing the fluctuations in the mud pump as the actual STP reading was not affected much (Figure 3.8(a)). After a few hours, mud pump 1 (MP#1) fails to function due to a problem associated with the chain guard at the power end. The technical team tried to repair MP#1. Meanwhile, the driller circulated the mud with MP#2 without further drilling.

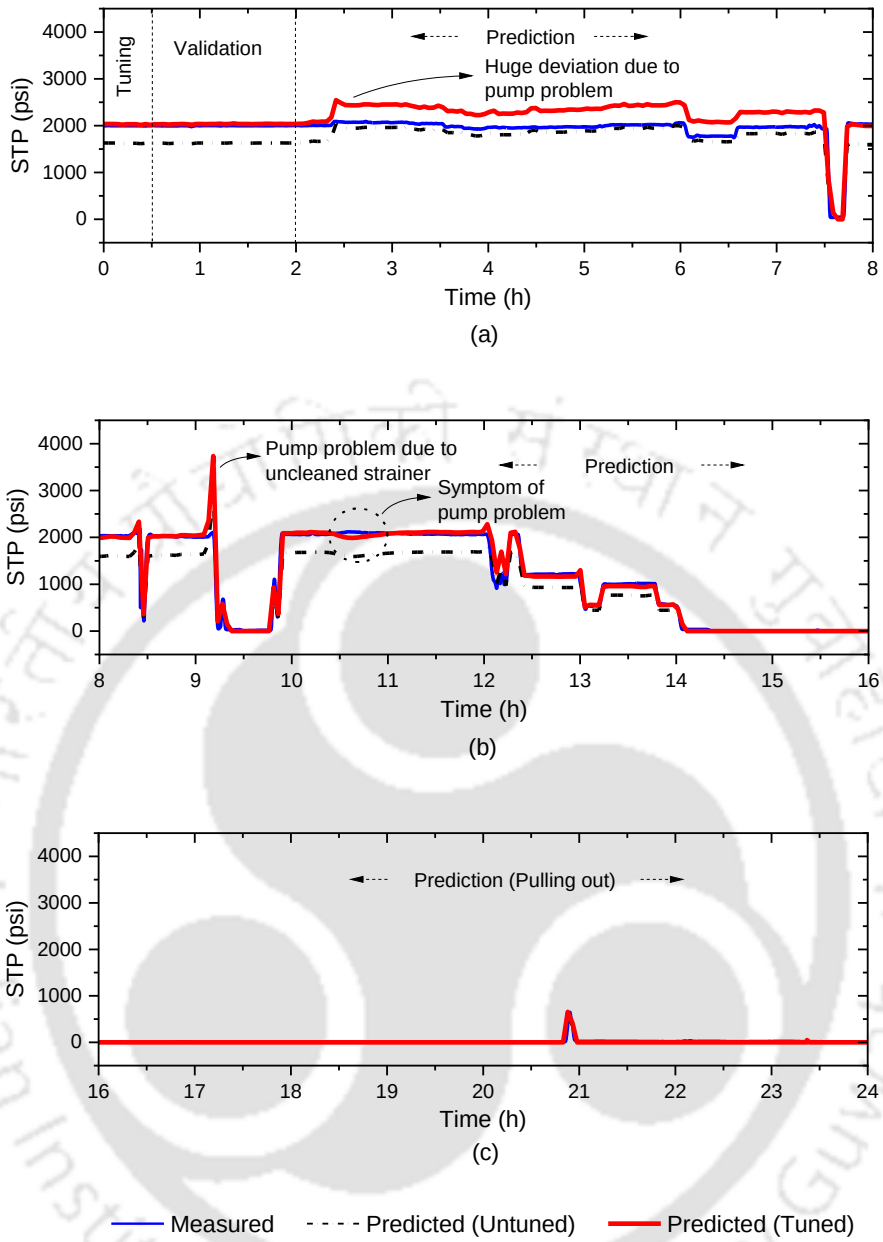

Figure 3.8. Hole cleaning model: calibration, validation and prediction of STP (case 2)
(Electronic version is recommended to differentiate colour)

Within an hour of mud circulation, MP#2 also failed to discharge mud due to valve problems. The mudflow was stopped entirely, and the annulus was left with cuttings. As per the standard operating procedure, an attempt was made to pull out the drill string to avoid the drill string stuck due to cutting accumulation. While partial pull out of the drill string, it has slipped and fell inside the wellbore. It took two days to rescue the drill string from the wellbore. During

fishing, the cuttings accumulated at the bottom and created held up (H/Up) while running in (R/I), which delayed the process of resuming the drilling operation by one more day.

The data recorded during the above case was fed to the developed mathematical model and successfully detected the mud pump problem at 2^{nd}, 9^{th} and 10^{th} hours. Later, the pump went out of order on 12^{th} hour. Based on the post-analysis, if the pump repairing/maintenance were carried out by stopping further drilling and continuing mud circulation, it might have avoided the necessity for pulling out. The driller could have managed only with drill string rotation during pump repair if the wellbore was made free of cuttings. As shown in Figure 3.9(c), the model predicted the settling of cuttings at the bottom of the wellbore, which explains the reason behind the held up while R/I.

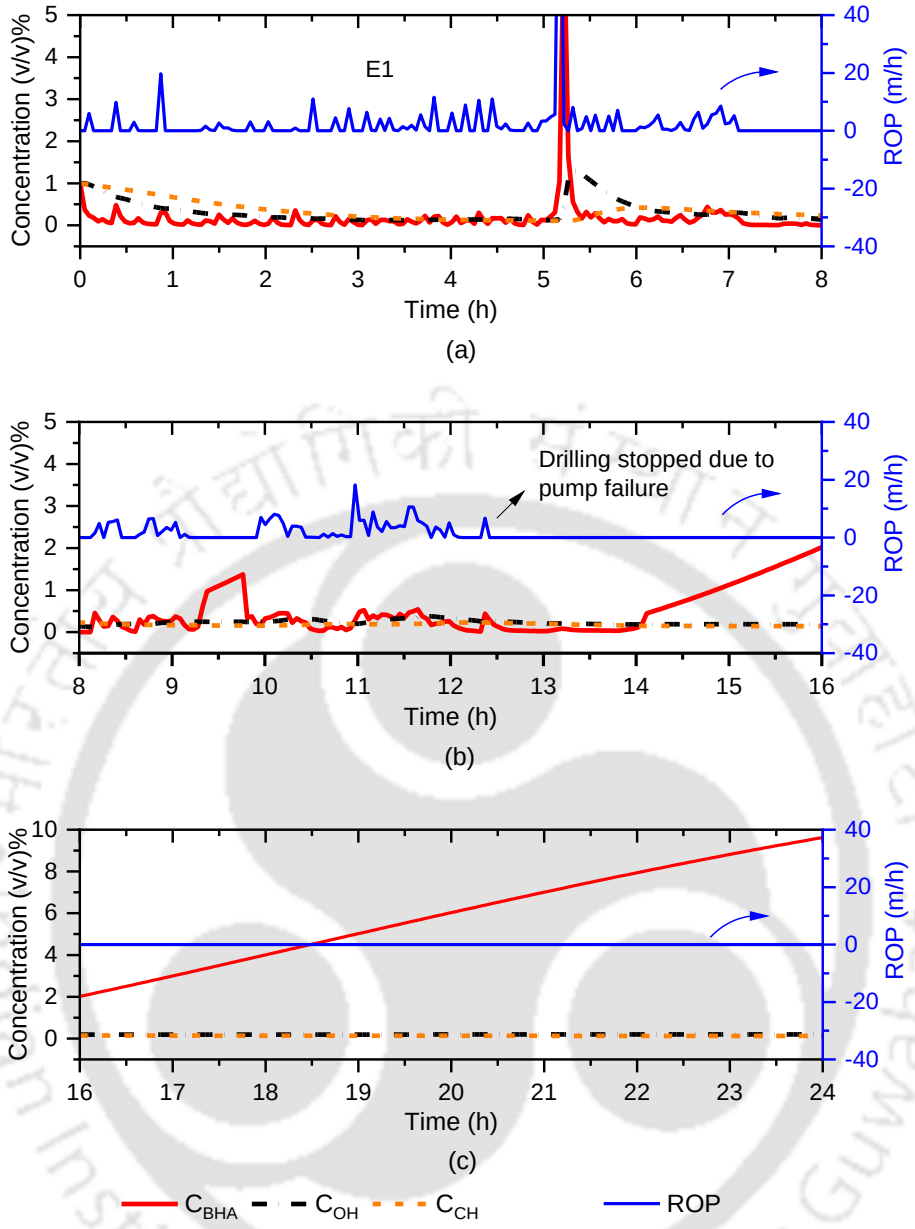

Figure 3.9. Dynamic cutting concentration prediction by hole-cleaning model (Case 2)
(Electronic version is recommended to differentiate colour)

Table 3.3. Hole-cleaning monitoring comparison with literature

S.N	Method followed	Advantages	Drawbacks	Improvement	Reference
1	Hole-cleaning monitoring by correlating cutting generated and removed from wellbore	1. Straight forward to ensure the wellbore is clean	1. Measuring actual volume of cutting removed in real-time is not available in most of the drilling rig 2. Not taking care of dynamic nature of the wellbore	1. Reduced NPT due to close monitoring of hole-cleaning	Dosunmu et al. 2015 [32]
2	Combined two models to predict cutting transport for 0-90º angle	1. Can be used for vertical well and horizontal wells	1. Wellbore stability was not considered during hole-cleaning 2. Not taking care of dynamic nature of the wellbore 3. Entire annulus is considered as a single lumped system	1. Real-time cutting volume measurement is not required	Mohammadsalehi et al. 2011 [48]
3	Finite volume approach to improve accuracy of cutting transport prediction	1. Could be implemented for real-time hole-cleaning monitoring 2. Both wellbore stability and cutting transport are monitored parallelly 3. Herschel-Buckley model was used to predict fluid hydraulics 4. The pressure drop across different sections of the wellbore is measured in real-time	1. Applicable till inclination of 45º. However, the model architecture has been designed to adapt for model updation for higher degrees	1. The annulus section was divided into multiple finite volumes 2. Implemented in the oil field and predicted cutting accumulation and pump related problems much before they occurred 3. The cutting concentration profile was created along the length of annulus in real-time	This work

3.6 Summary

In this chapter, the dynamic model development for the prediction of cutting transport along with wellbore stability model (ECD management) were presented. The implementation of the above models in an object-oriented language 'Modelica' using 'Dymola' software was explained in detail. Unless other lumped system models available in literature and drilling hand books, the mudflow path have been divided into multiple small sections to improve the accuracy of prediction results. The hydraulic and ECD management parts are synchronized and simultaneously solved for real-time updation of dynamic effective density, hydraulic and static pressure of the mud stream. The developed model was validated for real-time prediction of downhole problems related to cutting transport and surface problems related to mud pump. The field case studies were also presented as part of this chapter.

Chapter 4

Improving Drilling Rig Performance through Energy Consumption Studies

4. Improving Drilling Rig Performance through Energy Consumption Studies

4.1. Problem statement

The energy-intensive rig activities such as drilling, tripping, reaming, circulation and reciprocation are performed to complete a well drilling. The detailed analysis of energy consumption with respect to the above-mentioned rig activities and benchmarking could help in improving the rig performance. Moreover, drilling cost reduction is also possible by minimizing energy consumption and NPT. The typical energy consumed during different kinds of rig activities has not been captured in literature. In this chapter, energy audit and analysis are performed.

4.2. Mathematical model development

The energy audit module being delineated in this chapter has been integrated with the DSS (illustrated in Figure 2.1 of chapter 2). As discussed in the previous chapters, the drilling is a complex process of multiple sub-operations, and these sub-operations have to be carried out sequentially as per the planned well profile and schedule. The energy consumption will vary based on the type of operation/activity. Major operations that accompany an oil well drilling process include (i) drilling, (ii) tripping, (iii) reaming, (iv) circulation, (v) reciprocation, (vi) casing/tubing, and (vii) cementing.

Out of seven operations, the last two operations will be performed at the end of each phase (i.e., to maintain wellbore integrity) of drilling. However, they were not considered in this article due to energy consumption evaluation. Also, based on the drill string (DS) rotation/RPM and drill bit position, the other five operations were further sub-divided and listed in Table 4.1.

During the drilling process, seven major pieces of equipment are often used extensively such as (i) draw work (DW), (ii) mud pump (MP), (iii) top drive system (TDS), (iv) mud tank agitator (MTA), (v) shale shaker (SS), (vi) hand break (HB) and (vii) hydraulic motor (HM). However, all this equipment may not be employed simultaneously. Instead, they are engaged with respect to the type of operation. The first three pieces of equipment have been considered the primary energy-consuming components of the drilling process [107]. The primary equipment engaged in each operation is listed in Table 4.1. The power consumed in the data acquisition, transmission, and rig lighting facility were assumed to be constant and negligible compared to overall energy consumption. Hence, they are not included in the energy evaluation procedures.

Table 4.1. A list of oil rig activities and associated primary equipment

S.N.	Name of the activity	Draw work	Mud pump	Top drive
1	Drilling (with rotation)	✓	✓	✓
2	Drilling (without rotation)	✓	✓	×
3	Tripping out (with rotation)/back reaming	✓	✓	✓
4	Tripping out (without rotation)	✓	✓	×
5	Tripping in (with rotation - reaming)	✓	✓	✓
6	Tripping in (without rotation)	×	✓	×
7	Circulation (rotation on bottom)	×	✓	✓
8	Circulation (on bottom, without rotation)	×	✓	×
9	Circulation (rotation off bottom)	×	✓	✓
10	Reciprocation	✓	✓	✓
11	Non-productive	✓	✓	✓

The mud pump discharge rate can be evaluated from the below equation:

$$Q_{mud} = SPM_{MP1} \times LPS_{MP1} + SPM_{MP2} \times LPS_{MP2} \tag{4.1}$$

Power consumption in mud pump:

$$W_{mp,i} = 163.444 \times 10^{-5} \times \Delta P_{stp} \; Q_{mud} \tag{4.2}$$

where '*i*' is the activity reference number as given in Table 2.1

Power consumption in top drive rotary system:

$$W_{rot,i} = \frac{(\omega\tau)g}{9549} \tag{4.3}$$

Power consumption in draw works hoisting system:

$$W_{dw,i} = \frac{|BH_t - BH_{t+\Delta t}|}{\Delta t}(HL \times g) \times \eta_{pulley} \tag{4.4}$$

where 'η_{pully}' is the overall efficiency of the system of pulleys (0.782 for six sheave hoisting systems [1]).

The power utilization for each operation can be evaluated through the addition of power utilized in each deployed equipment (Table 4.1) as shown below:

Drilling:

$$W_{drill} = W_{mp,1} + W_{dw,1} + W_{rot,1} + W_{mp,2} + W_{dw,2} \tag{4.5}$$

Tripping:

$$W_{trip} = W_{mp,4} + W_{dw,4} + W_{mp,6} \tag{4.6}$$

Reaming:

$$W_{ream} = W_{mp,3} + W_{dw,3} + W_{rot,3} + W_{mp,5} + W_{dw,5} + W_{rot,5} \tag{4.7}$$

Circulation:

$$W_{circ} = W_{mp,7} + W_{rot,7} + W_{mp,8} + W_{mp,9} + W_{rot,9} \tag{4.8}$$

Reciprocation:

$$W_{reci} = W_{mp,10} + W_{dw,10} + W_{rot,10} \tag{4.9}$$

Non-productive:

$$W_{NPT} = W_{mp,11} + W_{dw,11} + W_{rot,11} \tag{4.10}$$

The actual power utilized at the drill bit during drilling is calculated by summing up hydraulic and torsional power applied at the bit:

$$W_b = W_{bhp,1} + W_{rot,1} + W_{bhp,2} \tag{4.11}$$

where '$W_{bhp,i}$' is hydraulic power at the bit during 'i^{th}' activity (kW)

The hydraulic power at the bit:

$$W_{bhp,i} = HHP_{b,i} \times 0.7457 \tag{4.12}$$

where,

$$HHP_{b,i} = \frac{\Delta P_{b,i}\, Q_{mud,i}}{1714} \tag{4.13}$$

$$\Delta P_{b,i} = \frac{Q_{mud,i}^2\, \rho_{mud}}{12032 \times C_d^2 A_{no}^2} \tag{4.14}$$

$$A_{no} = \frac{\pi}{4} \sum_{q=1}^{q=nn} D_{no,q}^2 \tag{4.15}$$

The constant 0.7457 in equation (4.12) is a factor associated with horsepower conversion to kW. The value of 'C_d' was taken from the drill bit data sheet (i.e., 0.96), and the same has been reported in the literature [108].

The power consumption will vary with time due to load fluctuation of the energy-consuming equipment. Therefore, the net energy consumed for each operation was evaluated by integrating power with respect to time. This can be implemented by using appropriate numerical integration techniques such as the trapezoidal method, newton method, etc. This work used the trapezoidal method by adapting the 'trapz' in-built function available in MATLAB 2018a.

The energy consumed for 'j^{th}' operation (Table 2.4) was evaluated as:

$$E_j = \int_{t_{j1}}^{t_{j2}} W_j \, dt \tag{4.16}$$

where 't_{j1}' and 't_{j2}' are the start and end time of 'j^{th}' operation

The energy spent to remove the unit volume of rock can be defined as the specific energy consumption (SEC_{drill}) and can be evaluated as shown in equation (4.17):

$$SEC_{drill} = \frac{E_{drill}}{V_{st}} \tag{4.17}$$

$$V_{st} = A_b \times L_{drill} \tag{4.18}$$

MSE, as described by Teale (1965) refers to the expression:

$$MSE = \frac{WOB}{A_b} + \frac{120 \times \pi \times RPM \times T}{A_b \times ROP} \tag{4.19}$$

$$A_b = \frac{\pi}{4} D_b^2 \tag{4.20}$$

Determination of the optimum parameters

The optimum operating parameters being determined from the energy analysis of the exploratory well can be deployed to minimize drilling costs for future offset wells. Further, to identify the best drilling operating parameters, the following objective function was used in this work:

$$\min\ (Fn_{obj}) = \left(PW_{b,avg,k}\right)_{norm} - \left(ROP_{avg,k}\right)_{norm} \tag{4.21}$$

The above function combines both the objectives: (i) minimizing power consumption and (ii) maximizing ROP. The average powers and average ROPs have been normalized using the min-max normalization function. The algorithm was programmed to provide WOB, RPM, and Q_{mud} for the optimum value of 'Fn_{obj}'. All the above equations were programmed in MATLAB software (version 2018a) and integrated with the DSS.

4.3. Energy evaluation and analysis

The energy consumption analysis of drilling can be a benchmark for the rig's performance, properties of the formation, and the effectiveness of the drilling operational parameters. Few researchers targeted the energy consumption associated with drilling and its influence on the drilling cost, return on oil exploration, and production investment [71], [109]. Three case studies on energy consumption were conducted. These have been delineated in respective sub-sections and as follows.

4.3.1 Energy analysis of Well-A and Well-B

In this study, two offset wells drilled with similar well profiles were chosen for the energy consumption study from an oil field, Assam asset, ONGC, India. The exploratory well (i.e., already drilled) and the offset well (i.e., real-time study) were denoted as Well-A and Well-B, respectively. Figure 4.1 shows the well casing configuration and its lithology information against the measured depth of the wells. The drilling data of phase IV were collected for the depth range from 3559 to 3829 m (270 m interval) of Well-A and the findings were implemented on Well-B during drilling. The time taken for drilling Well-A and Well-B was 160 h and 56.2 h, respectively. The duration mentioned above includes all operations required to complete the 270 m depth in phase IV. These include drilling, tripping, reaming, circulation, reciprocation, and non-productive operations. The non-productive operations include pump repairing, unplanned maintenance, mud preparation, debris fishing, and standby mud circulation during problem rectification.

As delineated in the activity identification section, the time series data were tagged with the activity reference number (Table 2.3). The energy consumed for each operation was evaluated as the summation of the energy consumed by all deployed equipment (Table 4.1). The energy consumption for all listed operations (Table 2.4) was evaluated individually for every 30 m

well depth (i.e., approximately equal to the length of one drill pipe stand) and stored in the database. Totally nine stands were used to drill 270 m of length.

Lithology	Well-A		Well-B	
	TVD (m)	Casing Plan	TVD (m)	Casing Plan
Unconsolidated coarse sand with clay	104-1139	400	100-1090	400
Loose sand and clay alternations.	1139-1654		1090-1605	
Dominantly Sandstone with Clay alterations.	1654-2114		1605-2105	
Dominantly clay & claystone with minor sandstone & silt at the bottom.	2114-2549		2105-2520	2500m
Dominantly sandstone with silt and clay intercalations.	2549-3429	2570m	2520-3370	
Coarse grained sand with alteration of coal and shale	3429-3449		3405-3455	3460m
Shale interbedded with coal and minor claystone with sand and siltstone	3449-3574	3500m	3455-3515	
Sandstone with shale inter-bedded with coal and minor claystone with Siltstone	3574-3950	3930m (MD)	3515-3840	3839m (MD)

Figure 4.1 Well configuration and lithology data of oil Well-A and Well-B

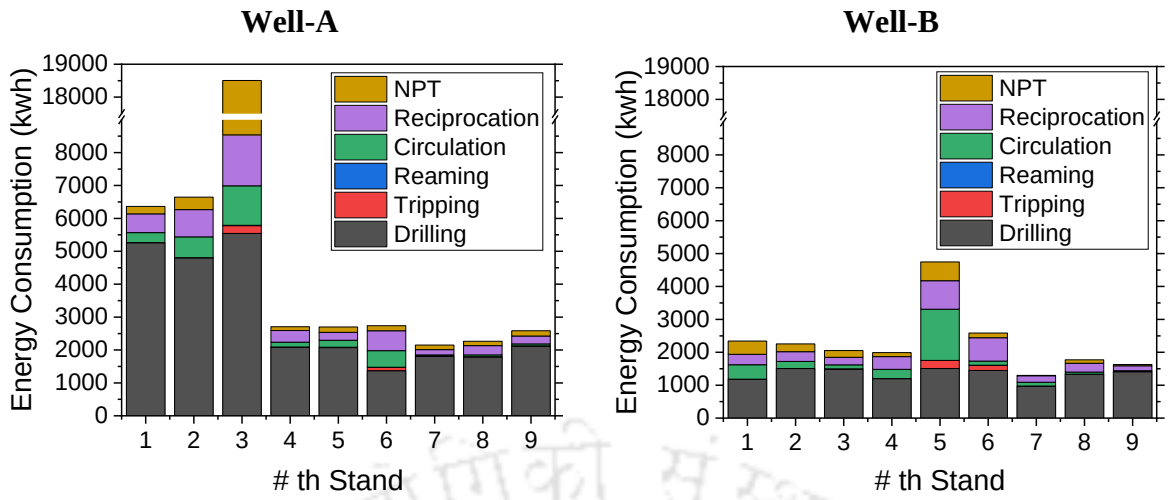

Figure 4.2 Energy consumption of oil wells for every 30 m (Phase IV, 3559-3829 m) - (a) Well-A (b) Well-B (Electronic version is recommended to differentiate colour)

The energy distribution among different operations per stand has been depicted in Figure 4.2. The Well-A consumed 26.86 MWh of energy only in drilling operation, corresponding to 57.6 % of the total energy consumed in phase IV. The activities carried out during the non-productive time (NPT) consumed 11.43 MWh (i.e., 24.5 % of the total energy). The NPT has been estimated to be 45.8 % of the total drilling duration. This is much higher than those corresponding to major operations such as drilling (30.8 %), tripping (6.8 %), circulation (9.8 %), and reciprocation (6.5 %).

A major portion of NPT has been observed during drilling of the third stand Figure 4.2. A sudden pressure drop was observed at the standpipe pressure due to choking of the strainer in one of the mud pumps (at depth 3648 m). The drill string cannot be kept idle or stopped while the issue of the mud-pump strainer is rectified. Therefore, as per the standard operating procedure (SOP), the mud was circulated with the help of a standby mud pump by maintaining a constant drill string rotation for 14 h.

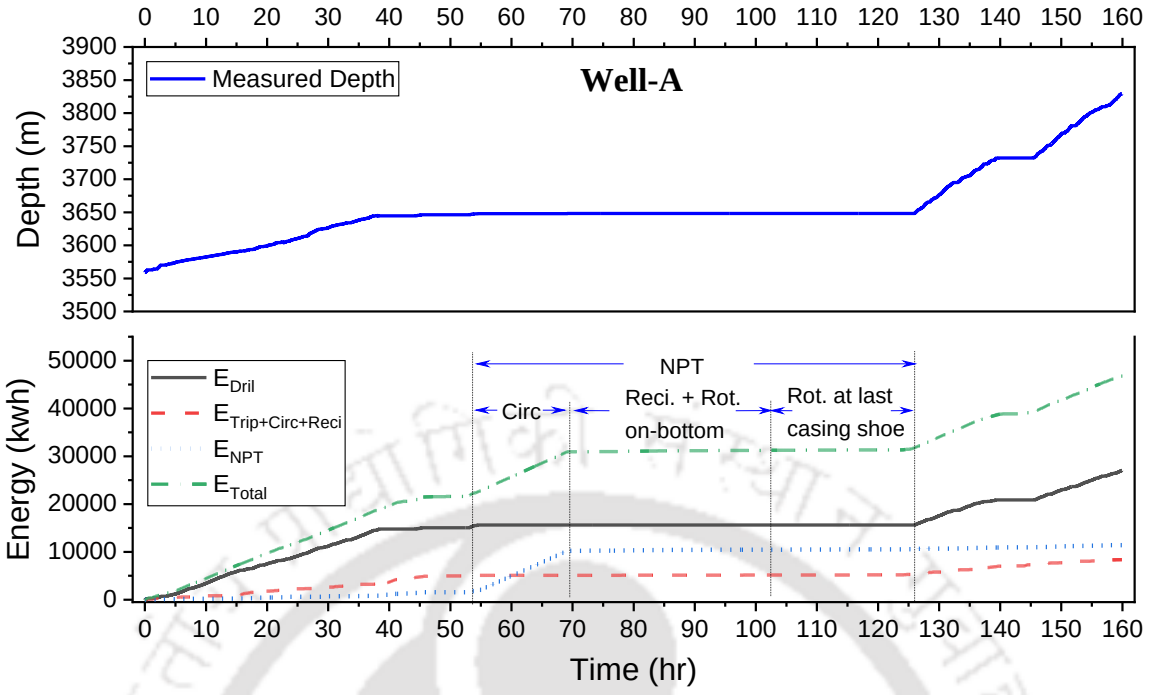

(a)

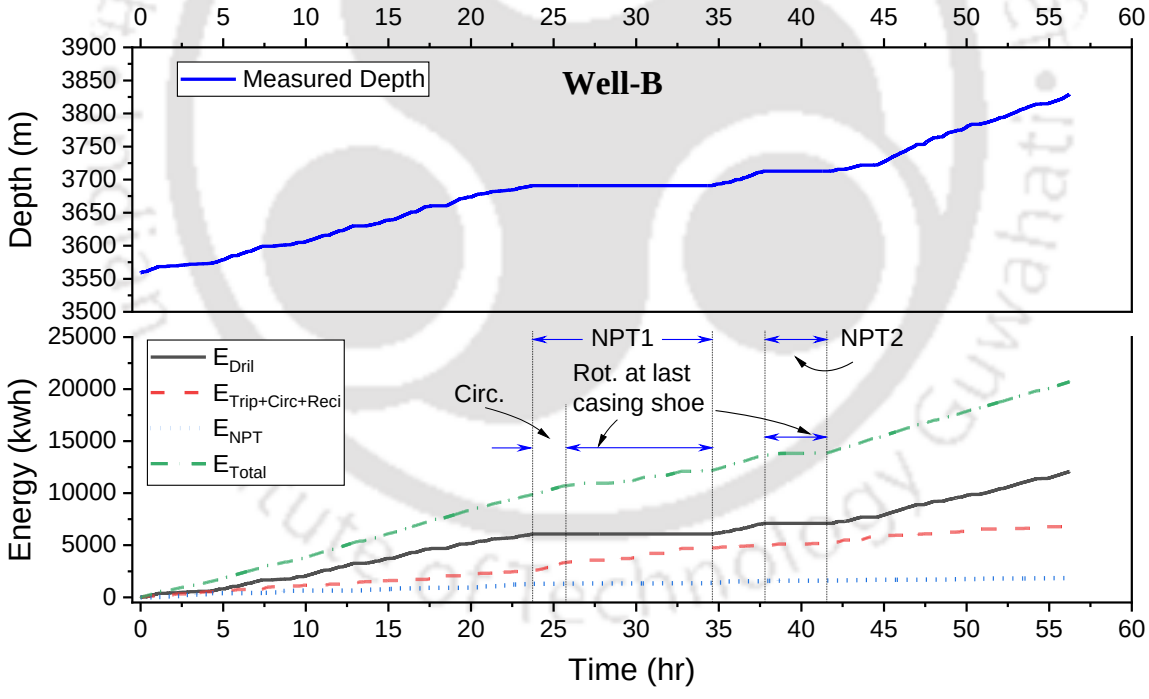

(b)

Figure 4.3 Energy consumption and total depth trends with respect to time (270 m) - (a) Well-A (b) Well-B (Electronic version is recommended to differentiate colour)

The energy consumed in the above operation was as high as 572.7 kWh per hour and was considered a non-productive operation. Meanwhile, a sensor problem was found in the draw works. Hence, as per the SOP, the DS was reciprocated frequently to ensure that it was free from mechanical and differential stuck. During the above period, the energy consumption for reciprocation was close to 17 kWh per hour. As the sensor problem resolution took longer, it was decided to pull out the DS until the last casing shoe (i.e., 3500 m depth). At this state, the DS was rotated at frequent intervals at lower rpm. For this, the energy consumption was evaluated as 6.6 kWh per hour. Overall, no drilling operation was carried out for 71.5 h, which can be observed through the constant total depth, and zero increments in drilling energy consumption in the time duration of 54.5 to 126 h Figure 4.3.

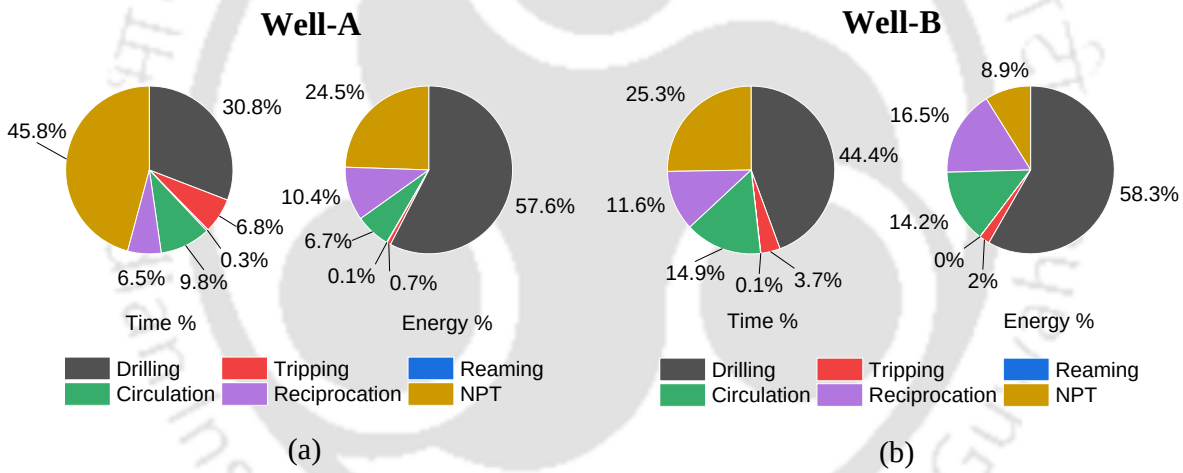

Figure 4.4 Energy and time distribution of various drilling operations (Phase IV, 3559-3829m): (a) Well-A (b) Well-B (Electronic version is recommended to differentiate colour)

The unexpected equipment and sensor failures resulted in 24.5 % energy and 45.8 % of the time in non-productive activities (NPA) Figure 4.4. The driller may predict the duration required for the mud pump and sensor repair from the previous maintenance data. Such a strategy enables energy analysis for various scenarios being available for the optimization of the drilling operation. The following two scenarios were explored to optimize the drilling energy for the chosen case.

(i) If the repair duration was very high, the driller could decide to pull out the complete DS until the last casing after removing cuttings from the borehole.

(ii) If the time required to rectify the problem was shorter than the circulation and tripping time, it would be better to maintain DS in the wellbore with the required circulation through a standby pump.

During drilling and mud circulation, it has always been recommended to choose the mud properties and flowrate such that the cutting transport efficiency (T_{eff}) is always greater than 50% (i.e., maintaining the value of annulus mud velocity (V_{ann}) equal to or more than twice of the slip velocity of the cutting (V_s)) [110]:

$$T_{eff} = \frac{V_{ann} - V_s}{V_{ann}} \times 100\ \% \tag{4.22}$$

Given that the transport efficiency was above 50 %, the maximum duration required to clean the wellbore was 3.3 hr for the Well-A at a depth of 3648 m. For the above case, excess mud circulation was done for 11.7 h to ensure that the wellbore was free from cuttings and avoid DS getting stuck. If the DS was pulled out till the last casing immediately after the circulation for 3.3 h, the energy-saving could be 6623 kWh (i.e., 11.7 h × (572.7 - 6.6) kW)

Similar to Well-A, Well-B encountered two non-productive rig down periods due to mud pump suction problem and hosepipe burst. These respectively took 11 h and 4 h for corrective actions. During the first period, the DS was pulled out above the last casing shoe after 2 h of mud circulation and later rotated in a frequent interval (also explored during the Well-A study). During the second NPT, the circulation was not possible due to the hosepipe failure. Hence, no circulation was done, and the DS was pulled out immediately until the last casing shoe. Since the drill string was pulled above the last casing shoe with an optimal circulation period, the energy consumption during the rig down periods was found to be much lower for Well-B case

(i.e., 7.3 kWh and 9.8 kWh per hour of NPT Figure 4.3 in comparison with those being evaluated for the Well-A case.

For a drilling process, it is well known that RPM, WOB, and Q_{mud} must be manipulated to control the drilling rate (ROP). Thus, these three parameter values must be optimally chosen for minimal energy consumption. Figure 4.5 depicts a bar chart with several important terms illustrating each drilling stand's energy efficiency. These refer to

(i) Specific energy consumption of the drilling operation (SEC_{drill} (kWh/m^3))

(ii) Average power input to the rig that includes the power to the rotary system, draw works, and mud pump (W_{drill} (kW))

(iii) The average power utilized at the drill bit includes torque applied at the bit and hydraulic pressure drop at the bit (W_b (kW))

(iv) Average MSE (psi)

(v) Average rotary speed (rpm)

(vi) Average WOB (ton (US))

(vii) Average ROP achieved (m/h)

From Figure 4.5 (a), it can be observed that the average SEC_{drill} values for the first three stands were close to 4800 kWh/m^3. This value was 2.8 times the average SEC_{drill} value consumed for the rest of the stands (≈1708 kWh/m^3). This is mainly due to very low ROP (< 4 m/h) with high WOB (> 8 ton (US)) for the first three stands, for which high-energy consumption was observed in comparison with other stands. From another perspective, the high WOB could not improve the ROP owing to the low rotation speed (< 35 rpm).

Among the nine stands, the sixth stand was drilled with minimum SEC_{drill} (1250 kWh/m^3) and minimum drilling time (2.4 h). This is due to the maximum ROP (11 m/h) achieved at WOB = 3.2 ton (US), RPM = 79 rpm, and Q_{mud} = 530 gpm. The stand that was drilled at optimum

parameters has been marked in green colour Figure 4.5 (a). The optimum conditions established in this energy analysis of the exploratory well can be used to improve the performance of the future development wells. For example, in this study, the optimal range (i.e., 3 sigma range from the normal distribution curve of the best stand) conditions of Well-A (i.e., WOB = 2-4 ton (US), RPM = 75-85 rpm, and Q_{mud} = 530 gpm) were implemented in the offset well (Well-B). The rig's performance in terms of energy consumption was found to be better for Well-B than those being evaluated for the Well-A. Consequently, a high ROP value (i.e., > 9 m/h) was achieved for phase IV Figure 4.5 (b)).

The Well-B consumed 12.05 MWh of energy in drilling activity to complete 270 m of drilling. This is 55% lesser in comparison to the values obtained for Well-A. The best performance was recorded for the drilling of the seventh stand (Figure 4.5 (b)). A ROP of 15.4 m/h was achieved with minimum SEC_{drill} (888 kWh/m^3). This was about 29 % lower than the lowest recorded value of Well-A (1250 kWh/m^3). This performance was achieved with 2.1 ton (US) of WOB and 85 rpm of DS rotation speed for Well-B in comparison with 3.2 ton (US) and 79 rpm of Well-A, respectively. As a result, the total time spent in drilling operation, excluding all other operations, was 49.24 h for Well-A and 35.9 h for Well-B. Thus, the delineated methodology was able to reduce the drilling time by 27.1% from Well-A to Well-B (Figure 4.4).

The typical energy generation from diesel fuel is 3 kWh/L, and CO_2 emission varies from 1 to 5 kg per litre of diesel burned [111].

Assuming 2.5 kg CO_2/L, CO_2 emission reduction in drilling alone:

$$CO_{2,drill} = \frac{2.5}{3} \times (26800 - 12050)$$
$$= 12291 kg$$

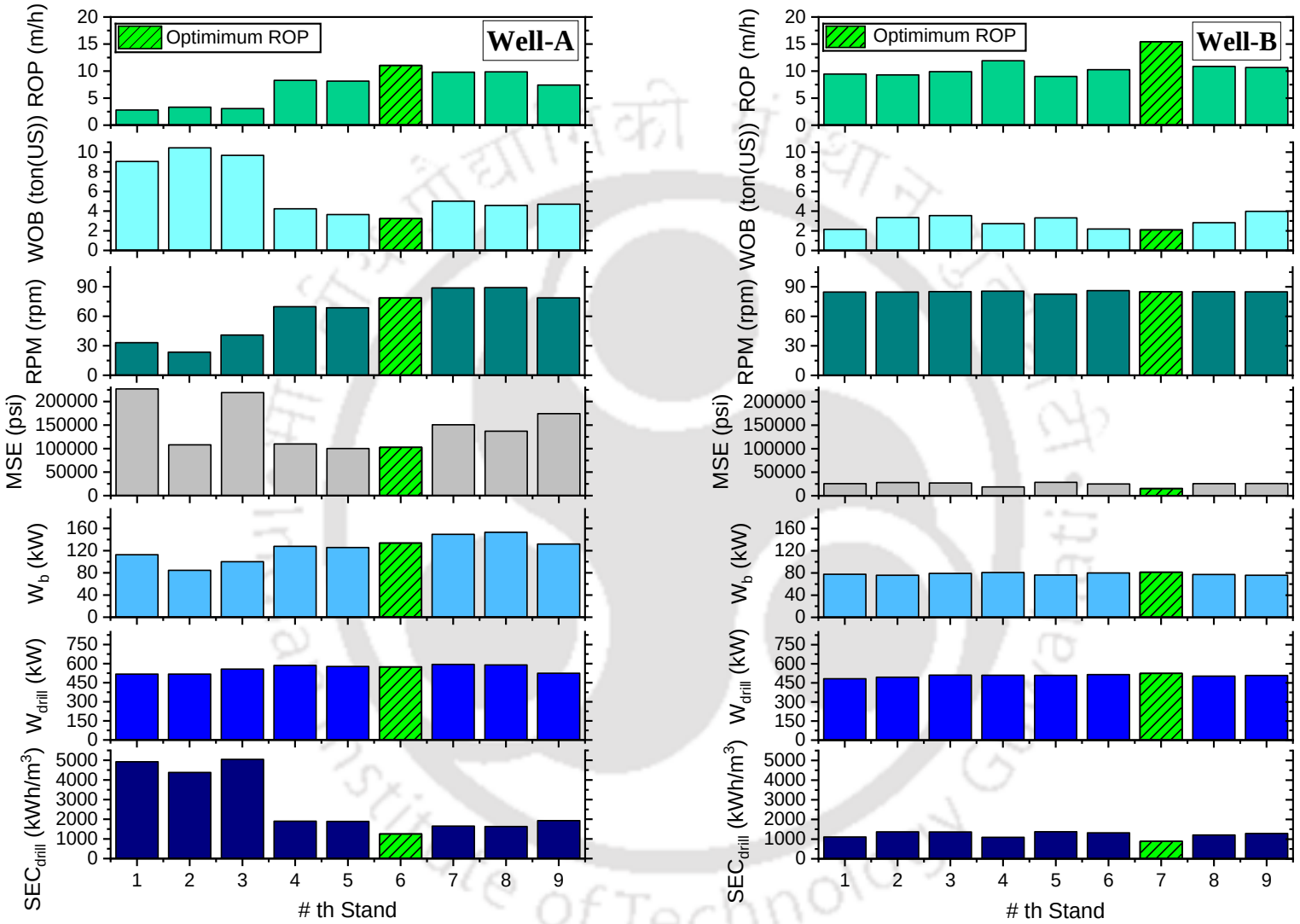

Figure 4.5 Energy consumption and drilling process parameters profile for drilling of 270 m: (a) Well-A (b) Well-B
(Electronic version is recommended to differentiate colour)

The overall energy saving in Well-B in comparison to Well-A was 55.7 % (i.e., 46.7 MWh to 20.7 MWh)

CO_2 emission reduction overall:

$$CO_{2,overall} = \frac{2.5}{3} \times (46700 - 20700)$$
$$= 21666\, kg$$

Thus, drilling at lower WOB (2-4 ton (US)) and high ROP (> 9 m/h) resulted in much lower SEC_{drill} in Well-B in comparison with the corresponding values being obtained for Well-A.

4.3.2 Energy analysis on the effect of depth

For the case study involving the analysis of energy consumption with respect to depth, Well-C was processed such that only drilling operation was considered for energy evaluation. The energy consumption per meter of drilling was evaluated and plotted to investigate the impact of depth on energy consumption (Figure 4.6). From the plot, it can be observed that the actual energy consumption increases linearly with respect to depth for each phase, given that dogleg severity is low.

The first stand of phase II consumed 16.03 kWh/m of energy (at 206 m depth), and eventually increased to 198.2 kWh/m for the drilling of the last stand. This corresponds to a 12-fold increase in an 1100 m depth interval. This might be due to the increase in frictional losses and bit balling reported by Galle and Woods (1963).

The energy consumption for phase III's first stand (121 kWh/m) was lower (> 39 % reduction) than the corresponding value obtained for phase II's last stand (198.2 kWh/m). However, the energy consumption for phase III also increased with respect to depth, as observed for phase II. The reduction in energy between phases was possibly due to the following events in the wellbore:

(i) The reduced frictional force between DS and casing wall (i.e., until casing shoe of phase II)

(ii) Reduction in the drill bit size for every next phase

(iii) Reduced requirement of mud discharge rate to maintain the cutting velocity in smaller hole size

Due to the above reasons, the energy consumption for the first few stands of phase III reduced significantly from 198.2 kWh/m of phase II to 121 kWh/m (> 39 % reduction). The same was observed when drilling was continued from phase III to phase IV. For this sub-case, the energy consumption was reduced from 178 kWh/m to 93.8 kWh/m (> 47 % reduction).

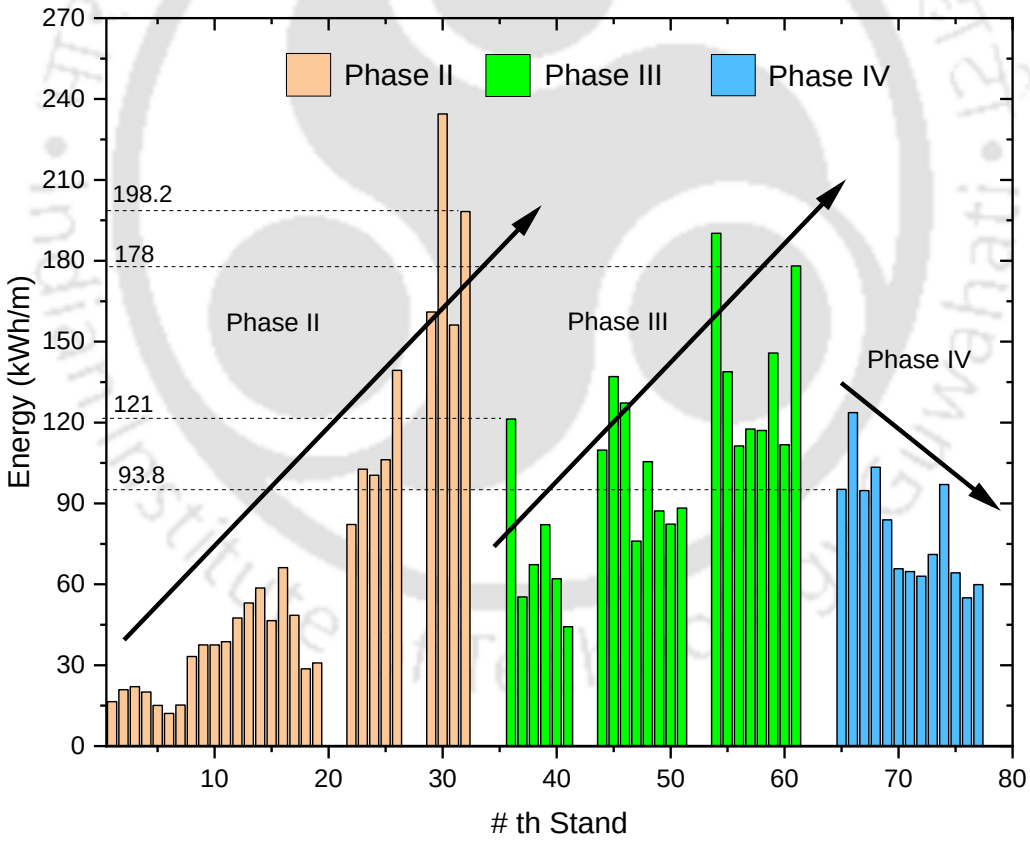

Figure 4.6. Energy consumption of Well-C with respect to depth
(Electronic version is recommended to differentiate colour)

The energy consumption for the first stand of phase IV was lower than that of phase III. However, the energy consumption gets reduced with respect to depth in contrast to the observation being made in the previous phases. This was mainly due to the abnormal dogleg severity at the start of phase IV. Later torque requirement was reduced due to the BHA moving away from the high dogleg spot (Figure 4.6).

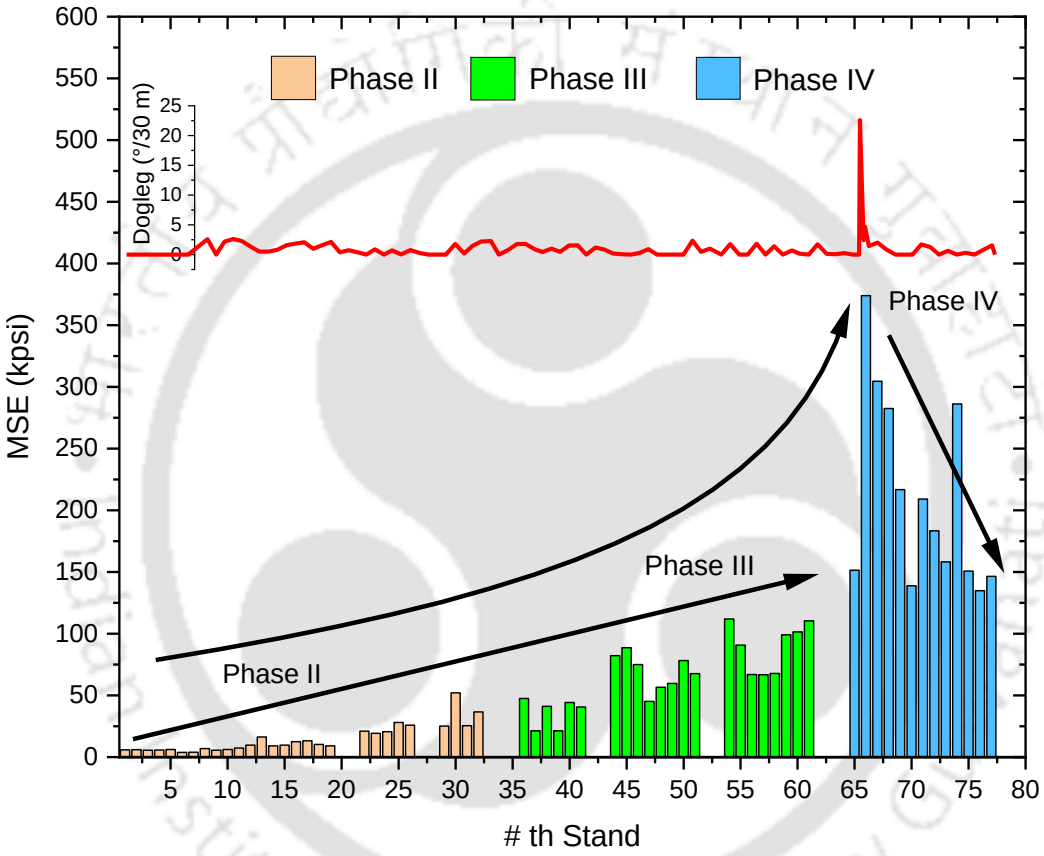

Figure 4.7 MSE profile of Well-C with respect to the depth
(Electronic version is recommended to differentiate colour)

Figure 4.7 illustrates the average MSE evaluated from equation (4.19) for each stand. As elucidated in the theory section, the MSE does not consider the hydraulic energy required to overcome the frictional pressure drop. Thus, it includes energy consumed by WOB and torque components only. As a result, the MSE increased for all phases and increased non-linearly from phase III to phase IV (i.e., reduction in energy consumption from the previous phase to the next

phase was not observed). The sudden peak in MSE can be attributed to the abnormal dogleg severity during the drilling of the 66th stand.

4.3.3 Energy analysis with respect to formations

Both Well-C and Well-D have been compared to study the effect of lithology on energy consumption during drilling. As described in the introduction, the availability of noise-free data for all parameters for the complete well has been challenging due to sensor error and data communication system failure. For both Well-C and Well-D, noisy data were observed, and corresponding depth ranges were marked with black backgrounds in Table C.1 and Table C.2 and were not considered for energy evaluation. Well-C and Well-D were drilled in 4 and 5 phases, respectively. The borewell/drill bit's diameters and casings have been provided in Table C.1 and Table C.2. The above wells were drilled in different geographical zones of northeast India. Comparatively, Well-C constitutes several types of lithology than Well-D. The formation-wise energy consumptions for both Well-C and Well-D have been depicted in Figure 4.8 and Figure 4.9, respectively. The energy consumption values for Well-C correspond to the 50-250 kWh/m range, whereas for Well-D, these varied from 5 kWh/m to 530 kWh/m.

The following analysis could be conducted from the apparent trends in Figure 4.8 and Figure 4.9:

(i) For the same formation lithography, the energy consumption was linearly increasing with respect to well depth within a phase except for the shale formation.

(ii) It can be observed that shale behaved marginally different due to shale sloughing and swelling. For 600 m of phase II stretch, the energy consumption was observed to in the narrow range of 100-120 kWh/m, excluding the seventh bar (Figure 4.8 (h)).

(iii) The energy consumption for two different wells were found to be different at the same depth range of similar lithology. For example, in the case of claystone at 1200 m, the energy consumption was 175 kWh/m for Well-C and 30 kWh/m for Well-D, which is about six times lesser than that being obtained for the Well-C. Thus, energy consumption patterns differed for both wells belonging to the same formation type and depth. These variations could be due to the heterogeneous nature of formation properties (i.e., hardness, porosity, pore-pressure), rig efficiency, and drilling parameters.

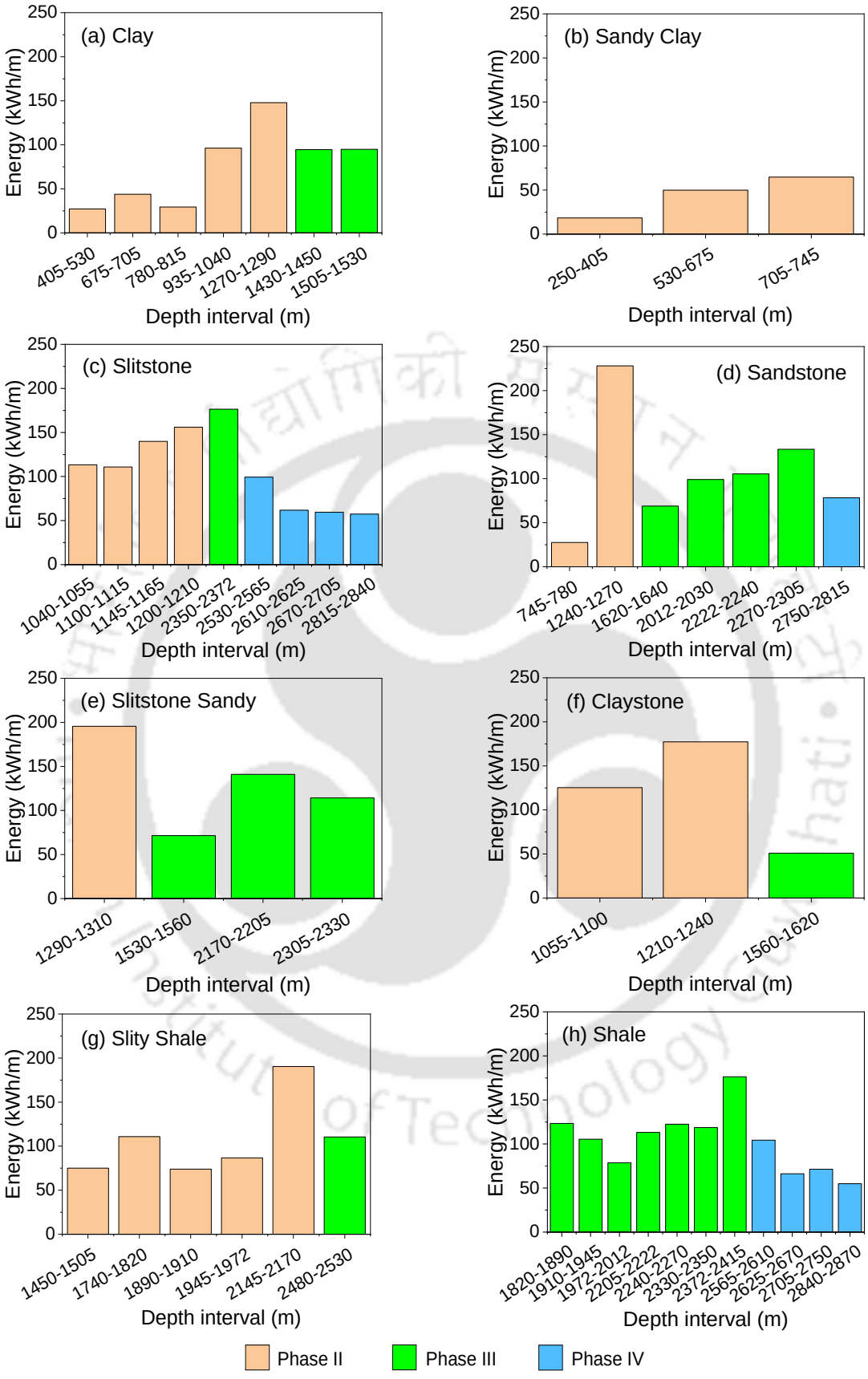

Figure 4.8 Formation-wise energy consumption patterns for oil Well-C
(Electronic version is recommended to differentiate colour)

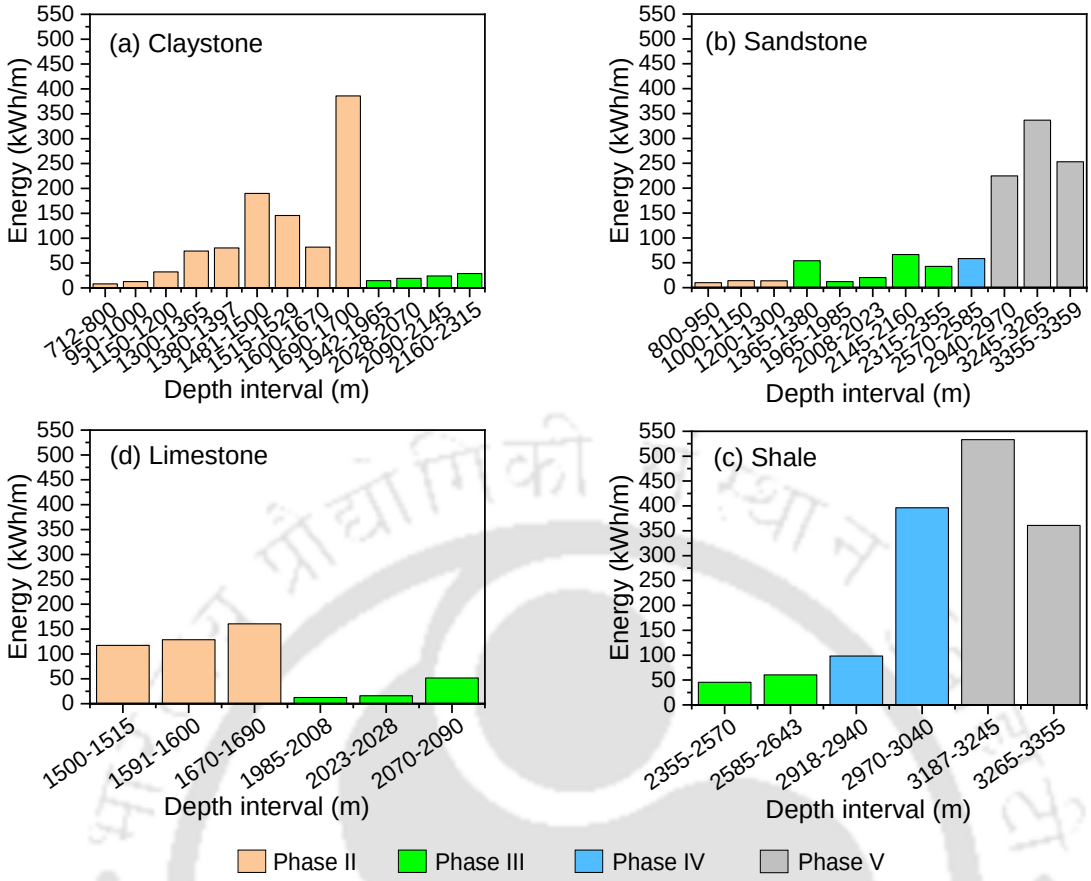

Figure 4.9. Formation-wise energy consumption patterns for oil Well-D
(Electronic version is recommended to differentiate colour)

Table 4.2. Energy consumption range with respect to the formation

S.N.	Formation lithology	Phase wise energy consumption (kWh)						
		Well-C			Well-D			
		II	III	IV	II	III	IV	V
1	Clay	25-150	95	-	-	-	-	-
2	Sandy Clay	20-70	-	-	-	-	-	-
3	Slitstone	60-160	175	50-100	-	-	-	-
4	Sandstone	25-225	70-130	75	10-20	20-70	60	225-235
5	Slitstone Sandy	195	75-135	-	-	-	-	-
6	Claystone	125-175	50		10-375	20-30	-	-
7	Slitshale	75-185	120	-	-	-	-	-
8	Shale	-	75-175	60-100	-	50-60	100-400	350-525
9	Limestone	-	-	-	115-160	20-50	-	-

Figure 4.8 and Figure 4.9, and Table 4.2 confirm that the lithology profoundly influenced energy consumption during the drilling operation. However, the lithology has been inferred to be less critical than other factors such as depth, dogleg severity, WOB, RPM, and Q_{mud} for a given well and drilling rig.

Table 4.3. Comparison of the energy audit method with literature

S.N	Method followed	Advantages	Drawbacks	Improvement	Reference
1	Evaluation of mechanical specific energy (MSE) consumption	1. Benchmarking of MSE for a formation	1. MSE needs downhole sensor readings for WOB and TQ to produce a comparative analysis at different depths and wells 2. Not a real-time method to rig performance, improving	1. A method to compare actual energy consumption with the minimum energy required to break the rock (UCS)	Teale 1965 [3]
2	Identification of inefficient drilling condition using DSE	1. Considers hydraulic energy spent at the bit while energy evaluation	1. The hydraulic energy contribution in breaking the rock is applicable only for soft formation 2. Not a real-time method to rig performance improving	1. Reduces overall mechanical energy requirements	Armenta 2008 [2]
3	Improving drilling rig performance through actual energy consumption	1. All the major drilling rig operations are considered for energy evaluation 2. Major energy consuming operation and equipment can be identified 3. Best operating parameters can be identified by analysing the history data	1. Not a real-time method to rig performance improving	1. Energy consumption can be calculated in the unit of kWh which can be easily related to fuel saving and CO_2 emission 2. Performance evaluation and benchmarking was able to reduce energy consumption of drilling by 55% and time taken to drill 270m by 27.1%	This work

4.4. Summary

In the competitive energy market, the sustainability of the fossil fuel sector has been challenged by other emerging technologies. Therefore, the drilling industry has been forced to look for better technologies and methods to reduce the overall exploration cost of fossil fuel. In this chapter, the above objective was targeted by lowering the energy requirement of drilling operations through benchmarking and improving rig performance. The energy consumption distribution across different types of rig activities showed that the non-productive operations were the second most energy-consuming component after the drilling operation. The case study performed in two similar and offset wells proved that energy analysis could find the best process parameters range from the historical data and help improve the rig performance and reduce NPT in the subsequent offset wells. The formation lithology-based energy consumption analysis also observed that formation lithology has less influence over the energy consumption per unit length of drilling compared to wellbore configuration and drilling process parameters.

As an exploratory well for the new field, the Well-A had minimal field information and process parameters were chosen as per the initial plan. Since no benchmark data exist for process parameters, non-productive time (NPT) and energy consumption have been available during the drilling phase of well-A, the NPT and energy consumption were very high. However, the new benchmarking values obtained through the DSS for the Well-A were implemented in Well-B. This resulted in the substantial reduction of NPT and energy consumption.

Also, due to the alteration in formation properties, well profile, drill bit type, process parameters and downhole uncertainties, the energy consumption will vary across wells. Such variations can be reduced by choosing an offset well with similar well profile and drill bit. In the case study targeting performance improvement, Well-A and Well-B were chosen with the above criteria for a comparative assessment of the findings and inferences. Also, to converge

upon a comparable well is extremely difficult due to several variables being involved in the drilling process. However, the methodology and findings can be implemented in multiple wells and can illustrate similar improvement in the rig performance.

Chapter 5

Real-Time Optimization Using Artificial Intelligence Model

5. Real-Time Optimization Using Artificial Intelligence Model

5.1. Problem statement

The mathematical model that can predict ROP for a given input such as the available influencing variables and parameters is essential to optimize drilling operation. The most influencing parameters on ROP that can be controlled in real-time are WOB, RPM and Q_{mud} [84], [87], [112]. In addition, the measurable influencing factors such as mud properties, wellbore inclinination and depth sensor readings also can be passed as input to improve the accuracy of prediction and optimization of ROP. However, the changes in the formation properties are also found to be influencing ROP to an extent. As the formation properties are not accessible in real-time in most of the drilling rigs due to the sophisticated sensors and equipment required, there is a need for a methodology to isolate the effect of formation properties on ROP. This chapter proposes a method that can be implemented for real-time drilling process optimization.

5.2. Model development

The hole-cleaning module takes into account cutting transport and wellbore stability. The energy audit module sets benchmark and determines the range of drilling process parameters for the betterment drilling performance based on historical data of similar wells. However, the real-time optimization module focuses on the determination of the optimal parameter values within the range prescribed by the energy audit module. In addition, the real-time optimization module has been constrained by the hole-cleaning module for trouble free drilling.

5.2.1. Data description

The statistical analysis of drilling data is very important to develop AI/ML model for ROP prediction. As shown in Figure 5.1, the distribution pattern of the critical variables for four hour sample data of Well-E is plotted. The volume of the data points is plotted (y-axis) against the actual values of the parameter (x-axis).

The mean value of ROP is 12.38 m/h for the distribution range of 8.19 m/h to 16.86 m/h (Table 5.1). Therefore, it can be understood that some duration of the drilling was done at a sub-optimal condition, and hence there was a possibility to maximize the ROP.

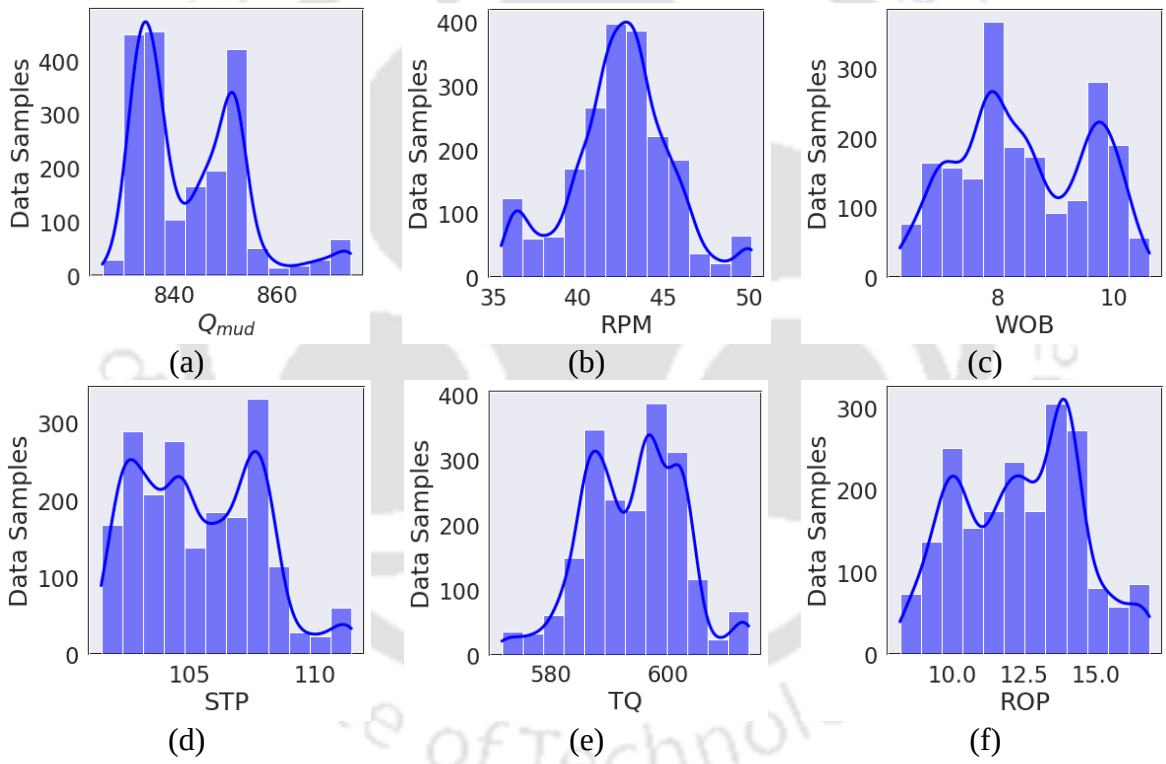

Figure 5.1. Data distribution for the training data of Well-E
(Electronic version is recommended to differentiate colour)

Table 5.1 Statistical analysis report for Well-E data

	WOB (ton(US))	**RPM** (rpm)	**Q_{mud}** (gpm)	**TQ** (kgf.m)	**STP** (kgf/cm^2)	**ROP** (m/h)
Mean	8.47	42.49	843.34	594.08	105.41	12.38
Standard deviation	1.10	3.00	10.45	8.29	2.40	2.08
Minimum	6.34	35.48	826.12	571.67	101.49	8.19
Maximum	10.61	50.14	874.21	613.89	111.45	16.86

As it was discussed WOB, RPM and Q_{mud} are three primary drilling parameters that can be manipulated in real-time by driller to maximize ROP. In addition to the above parameters, the STP and TQ are also expected to affect ROP that are function of primary parameters and the downhole conditions.

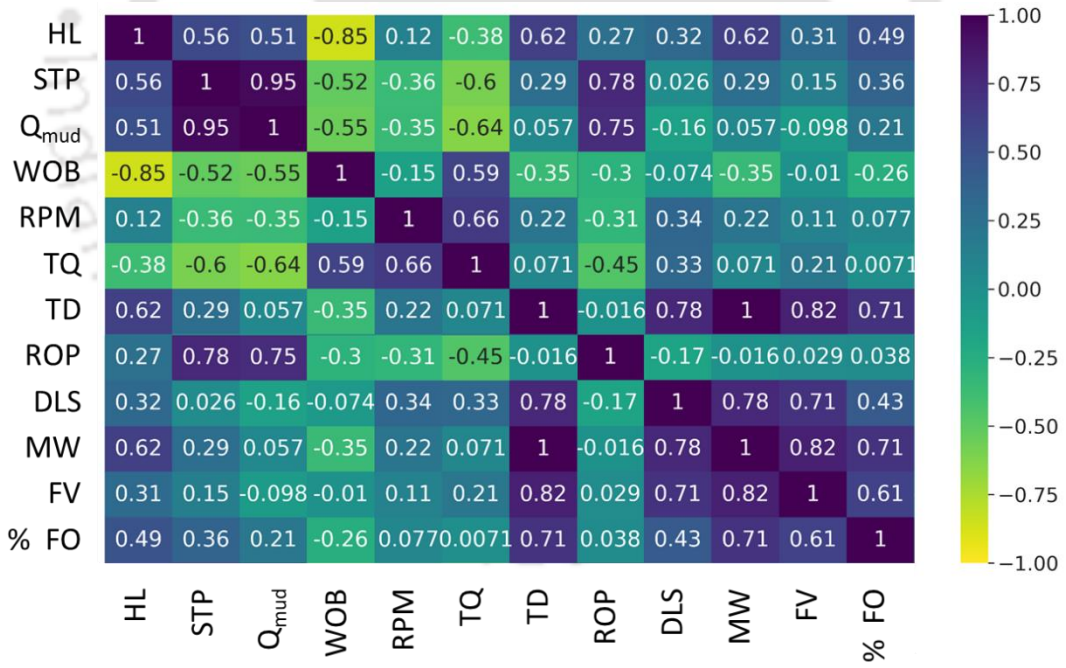

Figure 5.2. Correlation heat map of drilling parameters and variables
(Electronic version is recommended to differentiate colour)

The correlation heat-map analysis was performed and presented on a scale of -1 to +1, where the '-' sign signifies negatively correlated and vice versa (Figure 5.2).

As evident from the above Figure 5.2, ROP has a higher correlation with STP (0.78) and Q_{mud} (0.75), and is negatively correlated with TQ, RPM and WOB. When the annulus is not clean, the cutting concentration would vastly affect the torque required to maintain the desired RPM. As STP is a function of cutting concentration, it negatively correlates with torque. The influence of WOB on TQ is also evident from the above correlation heat map (0.59).

5.2.2. AI model layers I and II

The literature survey has shown that the ROP is immensely dependent on WOB, RPM, Q_{mud}, TQ, and STP. The same was confirmed by the correlation heat map (Figure 5.2). Out of them, only WOB, RPM, and Q_{mud} are the variables that can be controlled in real-time. TQ and STP are dependent on primary variables (WOB, RPM, and Q_{mud}) and factors such as mud properties, formation properties, bit depth, and wellbore uncertainties.

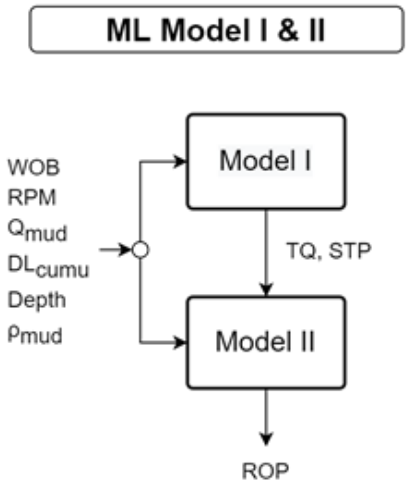

Figure 5.3. Two-layers of ML model for prediction of ROP

To include TQ and STP as predictors of ROP, there is a need to compute them in real-time to improve the prediction accuracy and reduce dependency on sensor information for TQ and STP. Therefore, an intermediate model for TQ and STP prediction was built (Model-I). As discussed in the chapter-1, the formation properties cannot be accessed in real-time. Hence, the

input to the intermediate model was limited to the primary variable (WOB, RPM and Q_{mud}) and certain secondary variables such as DLS, depth, and mud density. The above inputs were concatenated with the output of Model-I (TQ and STP) and fed to Model-II (ROP prediction). The implementation of this two-layer model is shown in Figure 5.3.

5.3. Model Training

As the formation properties change along with the wellbore depth, most of the literature reported models to become inaccurate over time. The researchers tried to calibrate the models for every new borewell. However, model predictions continued to deviate over time due to changes in unpredictable wellbore conditions. Frequent calibration of the model is required to isolate the above-said parameters on ROP prediction. Therefore, this work proposes calibration of the developed two-layer model once every hour with the data from the last four hours.

The time-series prediction problem is transformed into a supervised learning problem utilizing this technique. The training batch size (4 hours of data) was decided based on the required accuracy and computational demand, which may vary with formation. The moving window technique described above is depicted in Figure 5.4

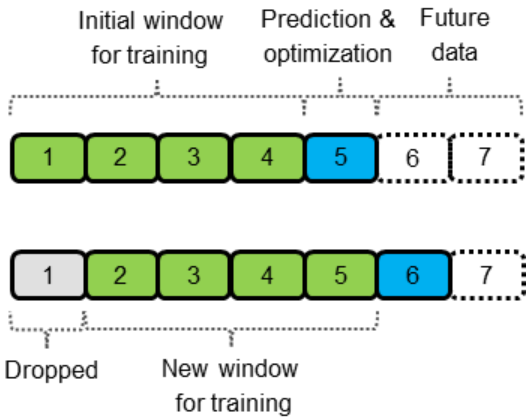

Figure 5.4. Moving window for ML model training
(Electronic version is recommended to differentiate colour)

Hyper-parameter tuning is searching for an optimal set of hyper-parameters for the learning algorithm (i.e AI/ML) to achieve high precision and accuracy. Hyper-parameters are model arguments which are chosen before training the model. Selecting an optimal hyper-parameter improves the model performance significantly. Searching hyper-parameters manually by hit-and-trial can be tedious. Therefore, the inbuilt function 'GridSearchCV' from the 'scikit-learn' python library was used with 5-fold cross-validation.

In this work, Linear regression and many other data driven AI/ML models are developed. Their efficiency was tested with real drilling data. List of those models and their respective hyper-parameter search spaces are given in Table 5.2

Table 5.2. Hyper-parameter search space for selected algorithms

Model	Model Parameters	Search Range
KRR	Alpha	[50, 75, 100]
	Kernal type	[liner, rbf, poly]
	Gamma	[1e-2, 1e-1, 1]
	Degree	[2, 3]
PLS	No. of components	[2,3,4]
SVR	Penalty (C)	[0.1,1,3,5]
	Kernal type	[liner, rbf, poly]
	Epsilon	[0.1, 0.5, 1]
	Gamma	[1e-3, 1e-4]
	C	[0.1, 1, 10]
	Degree	[2,3]
LGBM	No. of estimators	[5, 10, 15]
	Boosting algorithm	[dart, gbdt, goss]
	Learning Rate	[0.01, 0.05, 0.1, 0.5]

	Max. depth of the tree	[5,12,15,17,20]
	No. of leaves node	[2, 5, 10]
	Maximum depth	[2, 5, 10]
GB	No. of estimators	[3, 5, 7]
	Learning rate	[0.01, 0.05, 0.8,0.1,0.5]
	Max. depth of the tree	[3, 5, 10]
	Min. samples to split an internal node	[2, 5, 10, 15]
RF	No. of estimators	[3, 5, 7]
	Max. depth of the tree	[3, 5, 10]
	Min. samples to split an internal node	[2, 5, 10, 15]

The training and testing were performed before using the Model-I and II for real-time prediction. The best-fit algorithm and its optimal hyper-parameters are given in Table 5.3. The performance of other algorithms mentioned in Table 5.2 are provided in Table D.1 and Table D.2.

Table 5.3. Details of best performing ML models for TQ, STP and ROP prediction

Description	**Model-I**		**Model-II**
Output	TQ	STP	ROP
Algorithm	SVR	SVR	SVR
Kernel	Linear	Linear	Linear
C	0.5	0.1	1

C - Regularization parameter.
The strength of the regularization is inversely proportional to C.

The support vector regressor (SVR) model is built on the concept of a support vector machine (SVM). The main objective of the SVM algorithm is to find an optimal hyperplane in an n-dimensional space that separates the data points [21]. It reduces the error by determining the

hyperplane and minimizing the difference between the predicted and the actual values. The error of model predictions was analyzed statistically by evaluating the metrics, such as mean squared error (MSE) and coefficient of determination (R^2 score).

From the Table D.1 and Table D.2, it can be understood that linear kernel algorithms were performing better than other algorithms. It could be due to lesser volume of training data (4 hours) and the linear correlation ROP with critical variables which does not require complicated algorithms such as LGBM, GB and RF. However, the best performing algorithm may change with respect to drilling rig, formation and range of process variables.

5.4. Formation of the objective function

The objectives of the optimization problem are

i. Minimization of energy consumption during drilling operation
ii. Maximization of ROP
iii. Enhancing the cutting transport

All these objectives are combined into a single objective and presented as mathematical expression as given in equation (5.1)

$$F_{obj} = DSE_{\text{mod}} = \frac{WOB}{A_B} + \frac{120 \times \pi \times RPM \times TQ}{A_B \times ROP} - \frac{1,98,000 \times \lambda \times HHP_{SPP}}{A_B \times ROP} \tag{5.1}$$

$$HHP_{SPP} = \frac{SPP \times Q_{mud}}{1714} \tag{5.2}$$

$$A_B = \frac{\pi}{4} D_{bit}^2 \tag{5.3}$$

The presented objective function is a modified version of the drilling specific energy (DSE) formula proposed by Armenta et al. [112]. The drill bit hydraulic horsepower (HHP_{bit}) has been replaced by total hydraulic horsepower consumption (HHP_{spp}). The HHP_{spp} can be calculated from the standpipe pressure as shown in equation (5.2).

The first two terms of the objective function represent the mechanical energy consumption, and the last term represents hydraulic energy consumption during the drilling operation. By introducing the HHP_{spp} into the objective function, the maximum hydraulic power limit of the mud pump can be made available for utilization to ensure adequate hole-cleaning. However, the Q_{mud} will be constrained by the critical velocity of the open-hole section of the wellbore (equation (3.37)). The objective is to minimize energy and maximize ROP. For the second term, the objective functions are not conflicting. However, they are conflicting with the third term as it is with a negative sign. Thus, increase in ROP increases the value of third term which cause the objective function to become higher.

The primary variables (WOB, RPM and Q_{mud}) that can be manipulated by the driller in real-time were considered as decision variables (DVs) to optimize an objective function. The trained two-layer AI model will be utilized to predict TQ, STP, and ROP required to feed the objective function. The area of the drill bit can be estimated by equation (5.3). The values of drill bit diameter (D_{bit}) and hydraulic factor (λ) are given in Table 5.4.

Table 5.4. Drill bit size and hydraulic factor details

Phase	Bit diameter (Db)(inch)	Bit hydraulic factor (λ)
I	26	0.00275
II	17.5	0.0045
III	12.25	0.0085
IV	8.5	0.0175
V	6	0.035

The DVs are estimated by minimizing the objective function in real-time. As the mechanical terms of DSE_{mod} is positive, it will be minimized while the hydraulic term is maximized due to its negative sign. The mechanical term of the DSE_{mod} will be much higher than the hydraulic

term [67]. Hence, at the optimum condition, it is expected to maximize ROP and reduce the overall energy consumption of the drilling operation. At the same time, it enhances the cutting transport to achieve adequate hole-cleaning.

The bounds of decision variables (DVs) were decided by the data set range (DSR) used for model training. The criteria for determining the bound of DVs are given in equations (5.4) and (5.5), where EP is the percentage of extending the search range.

$$\text{Lower bound of DVs} = \text{Lowest value of dataset} - DSR \times \frac{EP}{100} \tag{5.4}$$

$$\text{Upper bound of DVs} = \text{Highest value of dataset} + DSR \times \frac{EP}{100} \tag{5.5}$$

5.5. Results and discussion

5.5.1. Sensitivity analysis

The sensitivity analysis on the two-layer SVR model was performed to understand the influence of DVs on the model prediction. The simulation range of DVs was decided based on their distribution in the training data set Table 5.1.

The sensitivity analysis of Model-I (TQ and STP) is given in Figure 5.6. The blue points correspond to the actual values of STP, and TQ with respective changes in DVs, while the orange points provide an estimate of the general trend of the complete response. The predicted TQ and STP were plotted against WOB, RPM and Q_{mud}. The trend of TQ was found to be linearly increasing with respect to WOB and RPM, while STP did not show any correlation. The pressure drop is highly dependent on the mudflow rate (Q_{mud}) rather than WOB and RPM (Figure 5.6 (e)). The increase in mudflow rate is expected to reduce the cutting concentration of the wellbore. Hence, the torque requirement was also reduced with an increase in Q_{mud} (Figure 5.6 (f)).

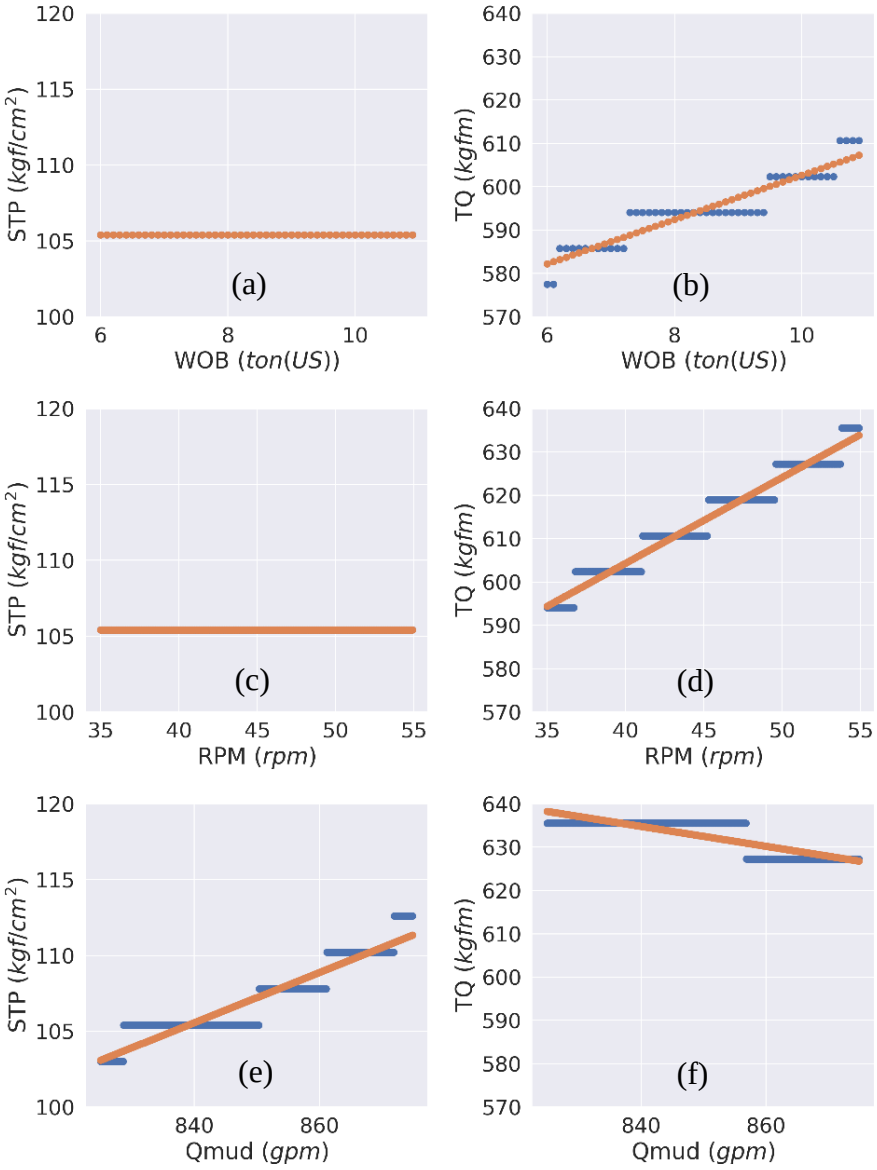

Figure 5.6. Sensitivity analysis of Model – I
(Electronic version is recommended to differentiate colour)

The sensitivity analysis of Model-II and the objective function are given in Figure 5.7. The trend of ROP was linearly decreasing as the WOB increased (Figure 5.7 (a)). The value of WOB applied might be above the founder point during the period of the training data set [113]. The effect of RPM on the trend ROP was predicted to be insignificant (Figure 5.7 (c)). Like WOB, Qmud also negatively impacted ROP (Figure 5.7 (e)). This can be due to the bit

bouncing at a higher flow rate. The trend of an objective function expressed a positive correlation to all the three DVs (Figure 5.7 (f)).

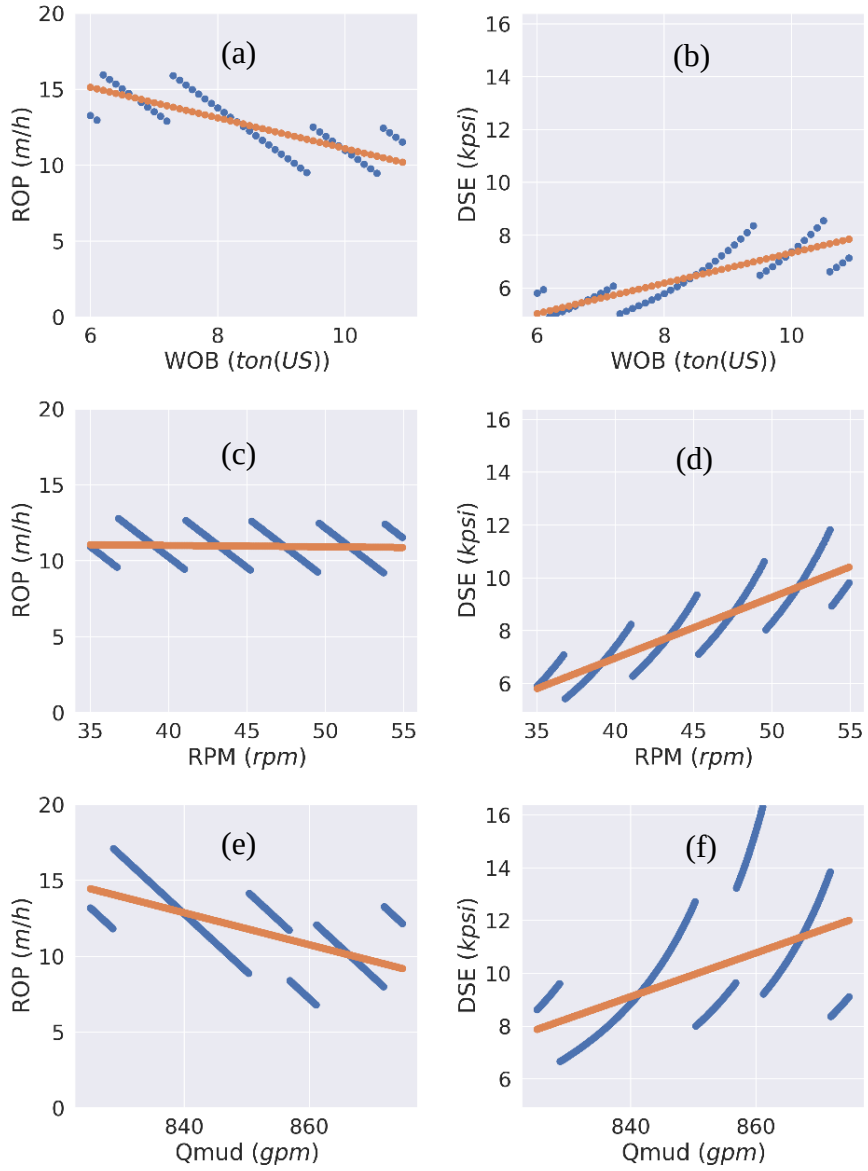

Figure 5.7. Sensitivity analysis of Model – II and objective function
(Electronic version is recommended to differentiate colour)

5.3.2. Prediction performance of two-layer AI model

The two-layer SVR model developed in this work was tested with field data (Well-E). First, the model was trained with four hours of drilling data. The trained model was used to predict

the ROP in real-time for the next one hour of the drilling operation. The prediction results for both training and testing are presented in this section.

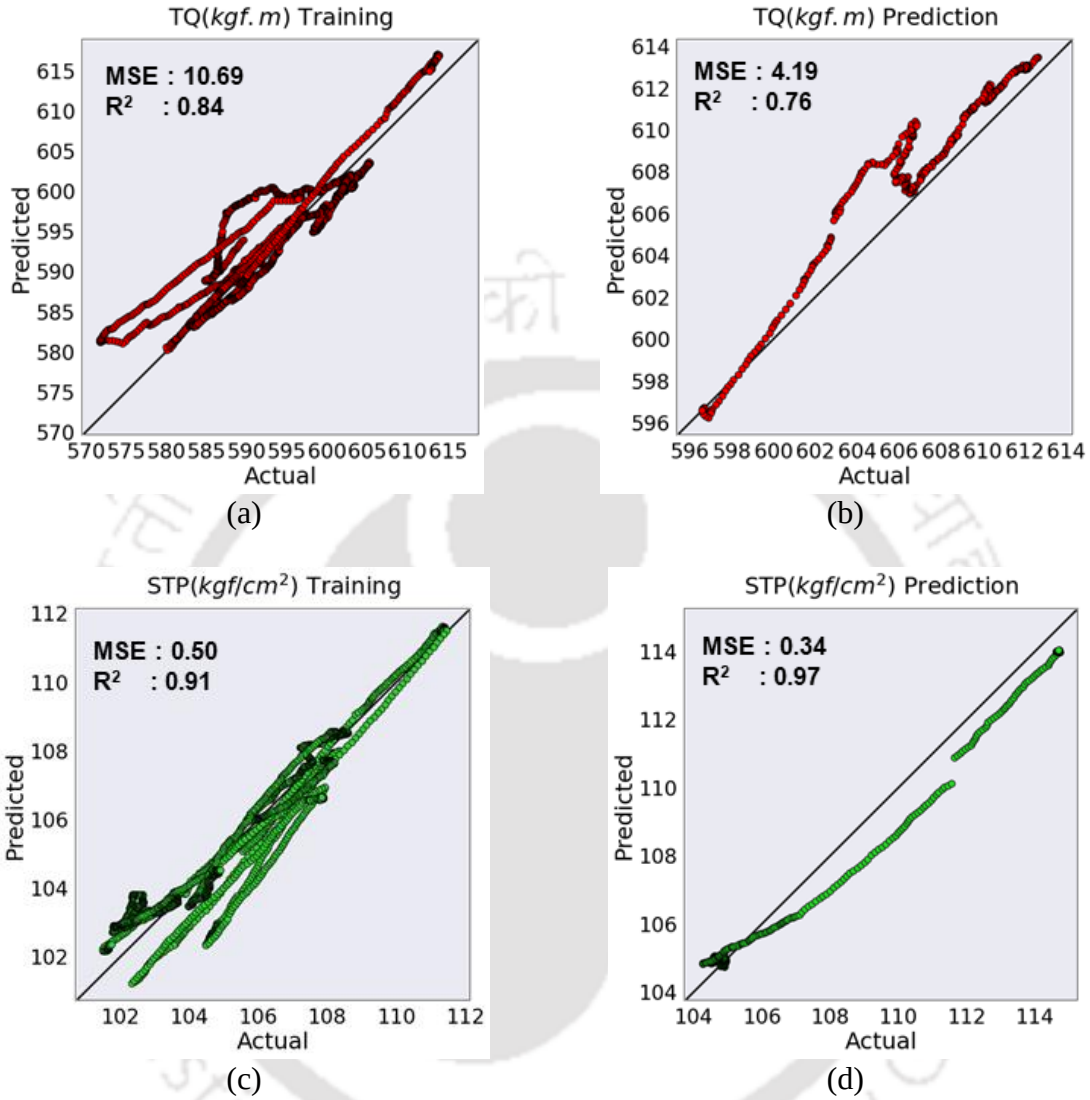

Figure 5.8. The performance of first layer of ML Model

The predicted values of TQ and STP are plotted against their actual values, as shown in Figure 5.8. Any data point falling on those plots' diagonal lines signifies zero deviation between prediction and actual. In a highly complex process like drilling, where many influencing parameters cannot be accessed for real-time prediction, the minor deviation is very well expected. However, the prediction results show a good correlation with the actual data.

Figure 5.8 shows that Model-I could predict STP with exceptional accuracy (MSE<1 and R^2>0.9) for both training and testing data set. This can be attributed to the fact that STP is a strong function of one of the DVs (Q_{mud}). On the other hand, TQ prediction was also in good agreement with the actual values. The minor over prediction of TQ and underprediction of STP could be due to fluctuations in annulus cutting concentration and effective mud density.

The results from Model-II, as shown in Figure 5.9, indicate that the two-layer approach could predict ROP with MSE<1 and R^2>0.7. The above accuracy was achieved with the minimum possible model parameters available in real-time (without formation properties).

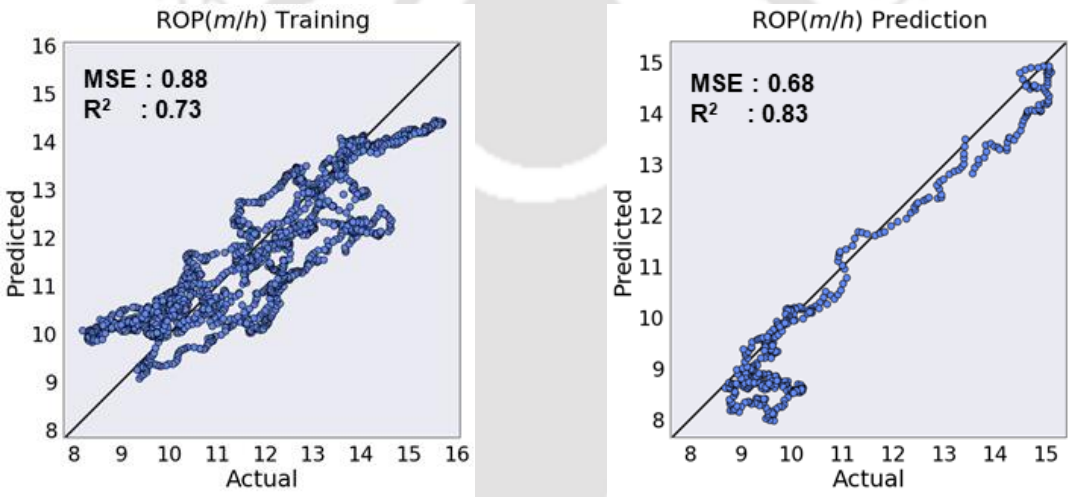

(a) (b)

Figure 5.9. The performance of second layer of ML Model

The actual and predicted values of TQ, STP and ROP with respect to time for both training and testing is visualized in Figure 5.10. The model predictions are found to be in good agreement with actual values which reiterates the capability of using the developed two-layer AI model for the optimization of drilling operation.

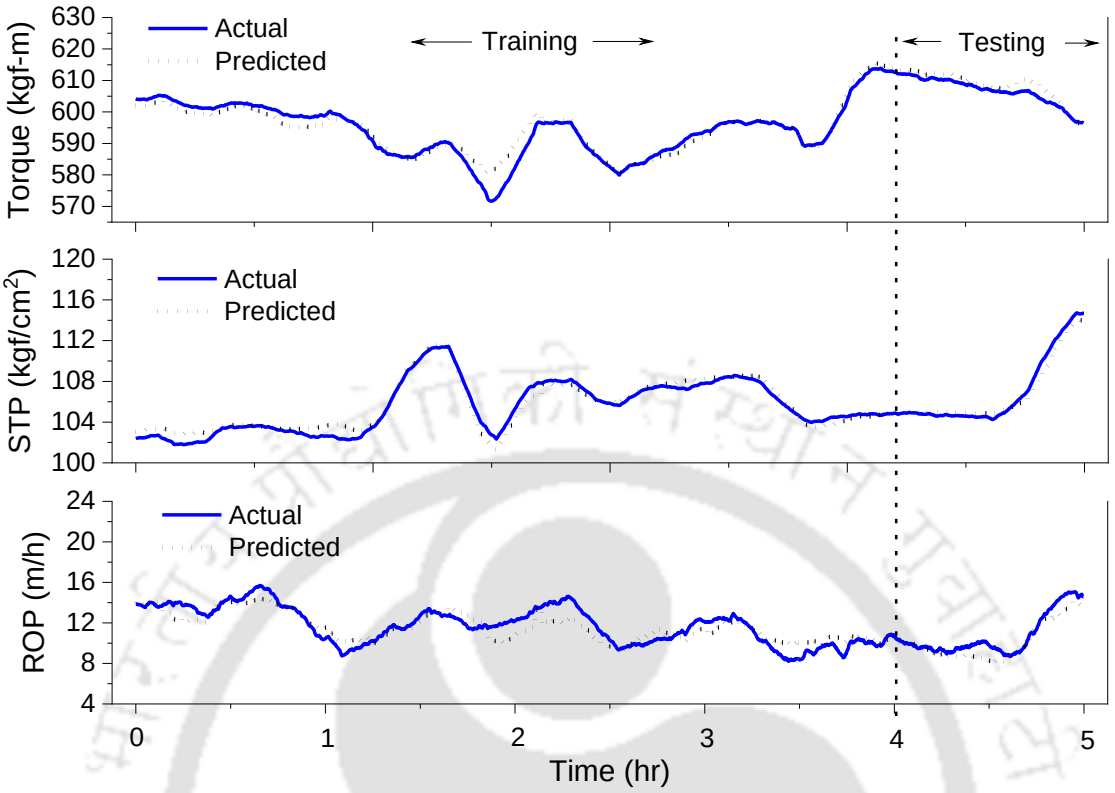

Figure 5.10. Training and testing results of two-layer model for the prediction of TQ, STP and ROP

5.3.3. Optimization results

The developed two-layer model can predict TQ, STP and ROP in real-time for a given set of DVs and other model variables. The optimization problem formulated in section 5.4 was solved in real-time using an inbuild python optimizer. In this work SLSQP optimization algorithm available in the python library 'scipy.optimize' was used. SLSQP optimization technique is one of the most efficient deterministic methods to solve optimization problems in real-time. As the developed two-layer AI model (SVR) uses a linear kernel (Table 5.3) in both the prediction layers, SLSQP is expected to perform well for real-time applications.

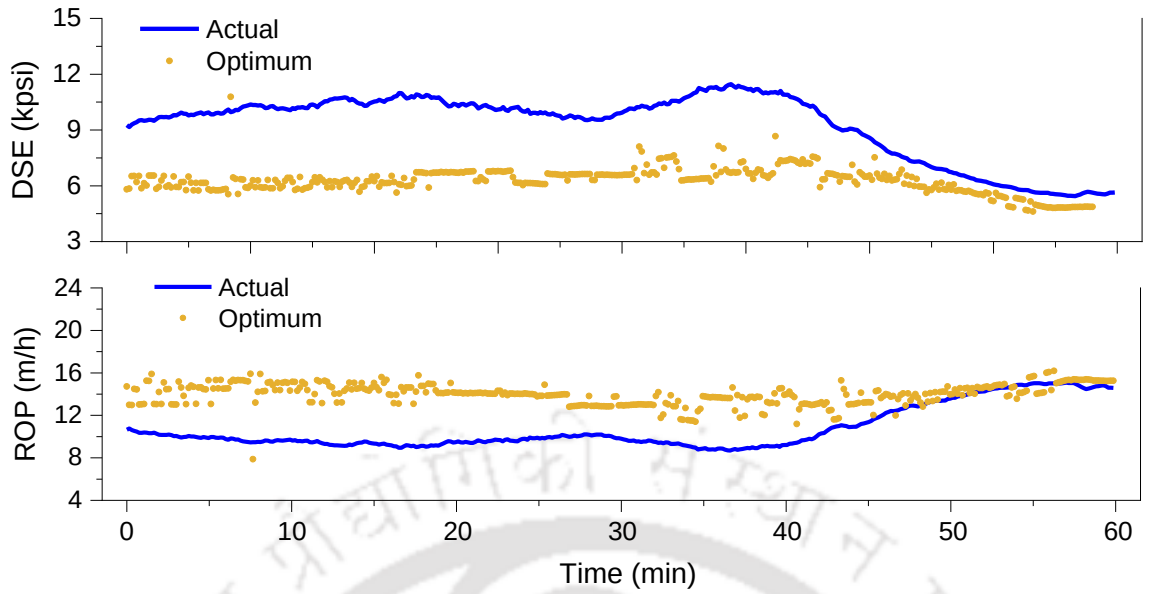

Figure 5.11. Performance of real-time optimization module for maximizing ROP and minimizing DSE_{mod}

Figure 5.11 shows the real-time optimized values of DSE_{mod} (i.e., objective function) computed from the optimal values of DVs. The last 10 min plot shows that when the actual objective function value is brought down to the lowest possible value (i.e., optimum point), the ROP can be maximized.

Since the optimization was done for every data point, the resultant optimum values appear noisy. However, the same can be improved by using a real-time data smoothing technique to avoid fluctuation in optimal DV's. This will also improve the efficiency and the controller's life if the optimizer is integrated with the auto drilling controller to implement the results in real-time. The performance comparison of two-layer model with literature is presented in Table 5.5.

Table 5.5. Comparative assessment of model performance with literature

S.N	Method followed	Advantages	Drawbacks	Improvement	Reference
1	Real-time ROP optimization using data-driven models	1. Real-time 2. Proved the possibility of increasing ROP through real-time optimization	1. Optimization of ROP, torque on bit and MSE are done separately 2. Formation property (UCS) was used as one of the inputs, which is not available in many of the drilling sites for real-time usage	1. Optimization improved ROP by 28% and reduced MSE by 4%	Hegde et al. 2018 [114]
2	Real-time ROP optimization with ML model	1. Real-time 2. Isolation of formation effect by continuous training	1. Energy minimization was not considered an objective of optimization	1. The minimum RMSE = 4.88 of ROP prediction (training interval 10ft of drilling)	Soares et al. 2019 [81]
3	Real-time prediction of ROP with ML and ANN	1. Could be used for complex lithology	1. Gamma ray data used to train AI model for ROP prediction which will be available in most of the drilling site for real-time application	1. The RMSE for ROP prediction was observed to < 0.66.	Salaheldin 2021 [89]
4	Real-time optimization to maximize ROP, reduce energy consumption and enhance cutting transport by using a ML based ROP	1. Only WOB, RPM and Q_{mud} are the critical parameters required to train ROP model 2. The effect of formation on ROP has been isolated by doing moving window to train	1. The optimization range is highly depending on the training data set distribution	1. Possibility of increasing ROP by 31% and reducing DSE by 32% is explored by real-time optimization 2. The RMSE for ROP prediction was observed to < 1.	This work

prediction and modified DSE models	the ROP model and optimization 3. Three objectives are combined in a single objective function such as minimization DSE, maximization of ROP and enhancing hole-cleaning. 4. The intermediate variables required for optimization; TQ and STP were predicted by ML model in real-time	3. No formation details required for ROP prediction

5.6. Summary

Typically, the drilling plan is based on a geological survey and historical data of the previously drilled well (i.e., from the exact geological location). However, each well's formation properties and wellbore condition can be different, which can be minor to major. This chapter presents a new methodology for real-time optimization of process parameters concerning the dynamic wellbore condition and formation change. A method for two-layer AI model development and training with historical drilling data has been proposed to predict TQ, STP and ROP. The predicted values of the above variables, critical process and design variables were utilized to optimize the drilling operation. The optimization function was formulated to minimize the overall energy consumption and maximize ROP. The best process parameter for every one hour of the drilling operation can be updated in real-time with the help of an optimizer. The optimization results were found to be in line with actual drilling services. As the optimization time required is lesser than a second, the proposed approach has vast implication in drilling automation.

Chapter 6

Conclusion and Future Work

6. Conclusion and Future Work

This chapter outlines the thesis's significant contributions to develop dynamic models to prevent downhole complications and optimize drilling process parameters in real-time. In addition, the drilling rig's performance evaluation was also performed through energy analysis. The critical observations made from the field case study conducted in North-Eastern parts of India are presented.

6.1 Downhole problem prevention by enhanced cutting transport

The drilling problems associated with inadequate hole-cleaning and mud hydraulics were addressed in this section. The wellbore is assumed as multiple small sections connected in series and configured in an object-oriented programing tool called Dymola.

1) An unsteady state and one-dimensional model was used to define each sub-section of the wellbore and integrated to form a flowchart model.
2) In addition to the drilling operation's slipping and cutting transport mechanisms, the settling effect of no circulation condition was also captured by the model. Therefore, the model predicted the cutting concentration around BHA, open hole, and closed-hole sections even when there is no drilling and mud circulation.
3) The developed model was tuned and tested with field data to predict the critical downhole problems such as drill sting washout and cutting accumulation. The surface problems related to mud pump failure were also predicted in real-time.
4) The mud pump problem was predicted 8 hours before the pump failed to discharge due to choking in the strainer in both case studies 1 & 2. Also, The drill string mud leakage was predicted in its early stage (i.e., mud cut) so that complete drill string washout avoided.

5) The hole-cleaning model also predicted the concentration of cutting in the annulus and its accumulation during down-time. The cutting accumulating around BHA is observed to increase more than 5% if the mud circulation was interrupted for more than 1.5 h for case 1 and 5 h for case 2.

6) The model was an efficient platform for resolving problems and uncertainties associated with oil-well drilling operations. The model-based platforms have the maturity and edge to resolve critical issues related to the drilling process. Hence, it could instill confidence in the team to efficiently resolve challenges associated with real-time oil-well drilling operations.

6.2 Improving oil well drilling rig performance through energy consumption studies

The above analysis affirmed that the drilling rig performance could be improved significantly through the operation-wise energy consumption evaluation and analysis. The optimal range of drilling parameters (WOB = 2-4 ton (US), RPM = 75-85 rpm, and Q_{mud} = 530 gpm) that had been found from the analysis of Well-A data was set as a benchmark during the drilling of Well-B (270 m, 3559-3829 m depth, phase IV) to deliver a significant reduction in energy consumption and time. Despite the effect of lithology on the drilling rate, it was observed to be less critical than depth, dogleg severity, and the primary drilling parameters such as WOB, RPM, and Q_{mud} for a given well and drilling rig towards drilling energy consumption.

The proposed methodology assured the following improvement in the drilling process:

1) Due to improved ROP, the time spent in drilling activity was reduced by 27.1 % in the offset well (Well-B). Similarly, the energy consumption of drilling activity was reduced by 55.7 % (i.e., 26.8 MWh to 12.05 MWh).

2) At times, excess circulation was allowed in due course of drilling stoppage or a downhole or surface problem. The DS pull-out (until the last casing shoe) is recommended for such scenarios immediately after adequate circulation. Thereby, a vast amount of energy could be saved (In Well-A, 6623 kWh of energy got wasted for 11.7 h of excessive mud circulation).

3) The reduction of energy consumption in moving from one phase to the next was apparent in the trend of energy consumption for drilling operations but not in the MSE's trend.

4) For the chosen case study, the total CO_2 emission reduction was estimated to be 12291 kg for the drilling operation alone and 21666 kg for all the other operations along with drilling.

In summary, the methodology outlined in this article is a potential repository for the assurance of energy consumption reduction in all major drilling rig activities. Thereby, the production cost of crude oil could be minimized for a surcharged global economy.

6.3 Real-time optimization using artificial intelligence model

A two-layer AI model was developed to predict ROP, TQ and STP in real-time. The developed model were tested on the data of Well-E that was drilled in the northeast part of India.

1) The first layer model (Model-I) was performing exceptionally well for STP prediction (R^2 >0.85). The same can be utilized to monitor pump-related drilling problems in real-time.

2) The simulation results guaranteed that the two-layer AI model could predict the trend of ROP with good accuracy (R^2 > 0.7) by taking few inputs that are available in real-time.

3) The optimization results are in line with the actual drilling scenario. The maximum ROP that was attained during drilling was in good agreement with the model prediction when the process parameters changed to the optimum values

6.4 Recommendation for future research

The presented thesis work proposes an integrated decision support system to guide drillers in real-time. The developed DSS architecture predicts downhole problems related to inadequate hole-cleaning and wellbore instability in real-time. It also performs the evaluation of drilling rig performance across various drilling operations and benchmarking. In addition, prediction and optimization of ROP in real-time were achieved with minimum input from the drilling rig. However, from the research work conducted and reported in this thesis, it is recognized that further research and development can be done to improve the reliability of the developed DSS such as

- The developed hole-cleaning model uses SCADA data to train the one-dimensional unsteady-state model. The model prediction accuracy can be improved by employing flow and particle count sensors at the mud return.
- The reliability of DSS can be improved by introducing a measuring while drilling (MWD) tool to measure the downhole parameters such as WOB and torque on bit (TOB). Considering the possibility of significant drilling cost reduction due to real-time monitoring and optimization, investing in MWD tools is highly recommended.
- The data-driven models have been widely recognized as a better option for simulating a complex system like wellbore. Therefore, sensor calibration, data acquisition, transmission and storage have to be prioritized to ensure data quality.

- Integration of mechanical and electrical efficiency curves of equipment like mud pumps and top drive systems into energy audit and real-time optimization modules can improve the reliability of KPI benchmarking and optimization results.
- Incorporation of stick-slip (i.e., torsional vibration) and bit bouncing (i.e., lateral vibration) phenomenon into the ROP prediction and optimization module shall lead to trouble-free (i.e., reduction of downtime) and efficient drilling (energy minimization and ROP maximization).
- Including redundancy in sensors, soft sensors and MWD tools in the drilling rig could improve the reliability of the model outputs. Hence, developing and successfully implementing a closed-loop predictive control system will be possible.
- Validation of the developed DSS using various types of well data for the improvement of the system's reliability.

References

[1] H. Rabia, *Well Engineering & Construction*. London: Entrac Consulting Limited, 2002.

[2] Dtedrilling, "Components of a Land-Based Rotary Drilling Platform." [Online]. Available: https://dtetechnology.wordpress.com/2014/05/04/components-of-a-land-based-rotary-drilling-platform/.

[3] S. Robert and Pindyck, "The Optimal Exploration and Production of Nonrenewable Resources," *J. Polit. Econ.*, vol. 86, no. 5, pp. 841–861, 1978.

[4] S. Kangogo, "Rig Selection and Comparison of Top Drive and Rotary Table Drive Systems for Cost Effective Drilling Projects in Kenya," Orkustofnun, Iceland, 2009.

[5] D. K. Tuli and R. Gupta, "Production and consumption of petroleum and compressed natural gas in India, oil and gas import, development of alternative energy sources, price escalation pattern, and its effect on Indian economy," in *Sustainable Biofuels Development in India*, 2017, pp. 3–20.

[6] H. Qu, H. Huang, H. Cui, J. Liu, and L. Zhao, "Methods and Countermeasures of Controlling Drilling Cost under New Normal," *Energy Power Eng.*, vol. 07, no. 13, pp. 584–590, 2015.

[7] M. J. Kaiser, "Modeling the time and cost to drill an offshore well," *Energy*, vol. 34, no. 9, pp. 1097–1112, 2009.

[8] E. M. Ozbayoglu, S. Z. Miska, N. Takach, and T. Reed, "Sensitivity Analysis of Major Drilling Parameters on Cuttings Transport during Drilling Highly-inclined Wells," *Pet. Sci. Technol.*, vol. 27, no. June 2015, pp. 122–133, 2009.

[9] L. Zhou, "Hole Cleaning During UBD in Horizontal and Inclined Wellbore ,"

IADC/SPE Drill. Conf., no. December 2005, p. 9, 2006.

[10] J. T. Ford, J. M. Peden, M. B. Oyeneyin, E. Gao, and R. Zarrough, "Experimental Investigation of Drilled Cuttings Transport in Inclined Boreholes," *SPE Annu. Tech. Conf. Exhib.*, pp. 197–206, 1990.

[11] S. Talabani, G. Chukwu, and D. Hatzignatiou, "Drilling Successfully Through Deforming Shale Formations: Case Histories," *Low Permeability Reservoirs Symposium*. 26-Apr-1993.

[12] M. K. Al-Arfaj, A. Abdulraheem, A. Sultan, M. Amanullah, and I. Hussein, "Mitigating Shale Drilling Problems through Comprehensive Understanding of Shale Formations," *International Petroleum Technology Conference*. 06-Dec-2015.

[13] M. Keshavarz Moraveji and M. Naderi, "Drilling rate of penetration prediction and optimization using response surface methodology and bat algorithm," *J. Nat. Gas Sci. Eng.*, vol. 31, pp. 829–841, Apr. 2016.

[14] M. E. Hossain, "Drilling Costs Estimation for Hydrocarbon Wells," *J. Sustain. Energy Eng.*, vol. 3, no. 1, pp. 3–32, 2015.

[15] P. Skalle and A. Aamodt, "Knowledge-based decision support in oil well drilling: Combining general and case-specific knowledge for problem solving," *IFIP Adv. Inf. Commun. Technol.*, vol. 163, no. October 2004, pp. 443–455, 2004.

[16] O. E. Gundersen, F. S{\o}rmo, A. Aamodt, and P. Skalle, "A Real-Time Decision Support System for High Cost Oil Well Drilling Operations," *AI Mag.*, vol. Spring, pp. 21–32, 2013.

[17] S. Alyaev, E. Suter, R. B. Bratvold, A. Hong, X. Luo, and K. Fossum, "A decision support system for multi-target geosteering," *J. Pet. Sci. Eng.*, vol. 183, no. March, p.

106381, 2019.

[18] S. V. Shokouhi, A. Aamodt, P. Skalle, and F. Sørmo, "Comparing two types of knowledge-intensive CBR for optimized oil well drilling," in *4th Indian International Conference on Artificial Intelligence*, 2009, pp. 722–737.

[19] A. Moazzeni, M. Nabaei, and S. G. Jegarluei, "Decision making for reduction of nonproductive time through an integrated lost circulation prediction," *Pet. Sci. Technol.*, vol. 30, no. 20, pp. 2097–2107, 2012.

[20] C. . Williams, G. . Bruce, and G. H. B. C.E. Williams Jr, "Carrying Capacity of Drilling Muds," *Trans AIME*, vol. 192, pp. 11–120, 1951.

[21] E. a. Hopkin, "Factors Affecting Cuttings Removal During Rotary Drilling," *J. Pet. Technol.*, vol. 19, no. 6, 1967.

[22] J. Lummus, "Drilling Optimization," *J. Pet. Technol.*, vol. 22, no. 11, pp. 2–4, 1970.

[23] T. R. Sifferman, G. M. Myers, E. L. Haden, and H. A. Wahl, "Drill Cutting Transport in Full Scale Vertical Annuli," *J. Pet. Technol.*, pp. 1295–1302, 1974.

[24] J. M. Peden, J. T. Ford, and M. B. Oyeneyin, "Comprehensive Experimental Investigation of Drilled Cuttings Transport in Inclined Wells Including the Effects of Rotation and Eccentricity," *Eur. Pet. Conf.*, vol. 192, 1990.

[25] R. B. Adari, S. Miska, E. Kuru, P. Bern, and A. Saasen, "Selecting Drilling Fluid Properties and Flow Rates For Effective Hole Cleaning in High-Angle and Horizontal Wells," *SPE Annu. Tech. Conf. Exhib.*, pp. 1–9, 2000.

[26] R. Nybø, J. Frøyen, A. D. Lauvsnes, T. Korsvold, and M. Choate, "The overlooked drilling hazard: Decision making from bad data," in *Society of Petroleum Engineers - SPE Intelligent Energy International 2012*, 2012, vol. 2, pp. 873–880.

[27] A. T. Tunkiel, D. Sui, and T. Wiktorski, "Impact of data pre-processing techniques on recurrent neural network performance in context of real-time drilling logs in an automated prediction framework," *J. Pet. Sci. Eng.*, vol. 208, no. July 2021, 2022.

[28] A. Kyllingstad, J. Horpestad, S. Klakegg, A. Kristiansen, and B. Aadnoy, "Factors Limiting the Quantitative Use of Mud-Logging Data," in *SPE Asia Pacific Oil and Gas Conference held in Singapore*, 1993.

[29] S. J. Sciwciryn, N. Whiteley, A. Deady, A. Borresen, and N. Gibson, "The influence of data quality on workflows and decision making in well delivery," *SPE Drill. Complet.*, vol. 26, no. 1, pp. 32–40, 2011.

[30] E. Cayeux, T. Mesagan, S. Tanripada, M. Zidan, and K. K. Fjelde, "Real-Time Evaluation of Hole Cleaning Conditions Using a Transient Cuttings Transport Model," *SPE/IADC Drill. Conf.*, 2013.

[31] C. Moore *et al.*, "Realtime Monitoring , Using All Available Data , Plays A Vital Role In Successful Drilling Operations," 2016.

[32] P. A. Dosunmu, C. Orun, C. Anyanwu, E. Ekeinde, and P. Harcourt, "Optimization of Hole Cleaning Using Dynamic Real-Time Cuttings Monitoring Tools," *SPE Annu. Conf. Exhib.*, no. 1970, 2015.

[33] C. . Williams and G. . Bruce, "Carrying Capacity Of Drilling Muds," *J. Pet. Technol.*, vol. 192, 1951.

[34] P. H. Tomren, A. W. Iyoho, and J. Azar, "Experimental Study of Cuttings Transport in Directional Wells," *SPE Drill. Eng.*, no. February, pp. 43–56, 1986.

[35] Slavomir Siavomir Okrajni and J. J. Azar, "The Effects of Mud Rheology on Annular Hole Cleaning in Directional Wells," *SPE Drill. Eng.*, vol. 1, no. 04, pp. 297–308,

1986.

[36] R. A. S. J.J.Azar, “Important Issues in Cuttings Transport for Drilling Directional Wells,” *SPE Lat. Am. Pet. Eng. Conf.*

[37] P. Kenny, E. Sunde, T. Hemphill, and B. D. Fluids, “Hole Cleaning Modelling: What’s ‘n’ Got To Do With It?,” *IADC/SPE Drill. Conf.*, 1996.

[38] J. R. B. Roland R. Sorelle, Ricardo A. Jardiolin, Peter Buckley, “Mathematical Field Model Predicts Downhole Density Changes In Static Drilling Fluids,” *SPE Annu. Tech. Conf. Exhib.*, 1982.

[39] N. Moroni, K. Ravi, T. Hemphill, and P. Sairam, “Pipe Rotation Improves Hole Cleaning and Cement-Slurry Placement: Mathematical Modeling and Field Validation,” *Offshore Eur. 8-11 Sept.*, no. 1996, 2009.

[40] D. Nguyen and S. S. Rahman, “A Three-Layer Hydraulic Program for Effective Cuttings Transport and Hole Cleaning in Highly Deviated and Horizontal Wells,” *SPE Drill. Complet.*, vol. 13, no. 03, pp. 182–189, 1998.

[41] O. O. Akinsete and S. O. Isehunwa, “An Analysis of Formation Damage During the Drilling of Deviated Wells,” *Pet. Sci. Technol.*, vol. 31, no. 21, pp. 2202–2210, 2013.

[42] A. M. Qahtani, E. Arc, and S. Aramco, “Prediction of Hole Cleaning Efficiency Using a Simple , User Friendly and Better Performing Simulation Model,” 2010.

[43] T. Hemphill, K. Ravi, P. Bern, J. C. Rojas, and B. P. Exploration, “A Simplified Method for Prediction of ECD Increase with Drillpipe Rotation,” *SPE Annu. Tech. Conf. Exhib.*, no. September, pp. 21–24, 2008.

[44] C. Wu, M. Chen, and Y. Jin, “Real-time prediction method of borehole stability,” *Pet. Explor. Dev.*, vol. 35, no. 1, pp. 80–84, 2008.

[45] A. Saasen, "Hole Cleaning During Deviated Drilling - The Effects of Pump Rate and Rheology," *SPE Eur. Pet. Conf.*, 1998.

[46] H. I. Bilgesu, N. Mishra, and S. Ameri, "Understanding the effect of drilling parameters on hole cleaning in horizontal and deviated wellbores using computational fluid dynamics," *East. Reg. Meet.*, pp. 2–8, 2007.

[47] M. S. Bizanti and S. F. Alkafeef, "A Simplified Hole Cleaning Solution to Deviated and Horizontal Wells," *Middle East Oil Show*, no. 1, pp. 1–11, 2003.

[48] M. Mohammadsalehi, N. Malekzadeh, I. Central, and O. Company, "Optimization of Hole Cleaning and Cutting Removal in Vertical , Deviated and Horizontal Wells," *SPE Asia Pacific Oil Gas Conf. Exhib.*, p. 8, 2011.

[49] A. Merlo, R. Maglione, and C. Piatti, "Innovative model for drilling fluid hydraulics," in *SPE - Asia Pacific Oil & Gas Conference*, 1995, pp. 77–93.

[50] N. Malekzadeh, M. Mohammadsalehi, and I. C. Oilfields, "SPE 143676 Hole Cleaning Optimization in Horizontal Wells , a New Method to Compensate Negative Hole Inclination Effects," 2011.

[51] A. A. Gavignet and I. J. Sobey, "Model Aids Cuttings Transport Prediction," *J. Pet. Technol.*, vol. 41, no. 09, pp. 916–921, 1989.

[52] S. Gasbarri and V. Wills, "A Simplified Computer Model for Determination of Cuttings Concentration and Wellbore Cleaning dx x," no. 1, pp. 1–18, 2014.

[53] R. Rooki, F. Doulati Ardejani, and A. Moradzadeh, "Hole Cleaning Prediction in Foam Drilling Using Artificial Neural Network and Multiple Linear Regression," *Geomaterials*, vol. 04, no. 01, pp. 47–53, 2014.

[54] B. Busahmin, N. H. Saeid, U. H. B. H. Hasan, and G. Alusta, "Analysis of Hole

Cleaning for a Vertical Well," *OALib*, vol. 04, no. 05, pp. 1–10, 2017.

[55] F. J. Adewale, A. P. A. Lucky, A. Fadairo, and A. A. Adedeji, "Modification of Bingham plastic rheological model for better rheological characterization of synthetic based drilling mud," *J. Eng. Appl. Sci.*, vol. 13, no. 10, pp. 3573–3581, 2018.

[56] *Baroid Fluids Handbook*, 3rd ed. Houston: Baroid Drilling Fluids, Inc, 1997.

[57] I. . Ben A. Eaton (Eaton Industries of Houston, "The Equation for Geopressure Prediction from Well Logs," *Soc. Pet. Eng. J.*, 1975.

[58] G. Bowers, "Pore Pressure Estimation From Velocity Data : Accounting for Overpressure Mechanisms Besides Undercompaction," no. June 1995, 2018.

[59] J. B. Foster, H. E. Whalen, and T. O. Co, "Estimation of Formation Pressures From Electrical Surveys-Offshore Louisiana," 1966.

[60] A. Alqahtani, R. Selmi, and O. Hongbing, "The financial impacts of jump processes in the crude oil price: Evidence from G20 countries in the pre- and post-COVID-19," *Resour. Policy*, vol. 72, no. June 2020, p. 102075, 2021.

[61] X. Gao, W. Fang, F. An, and Y. Wang, "Detecting method for crude oil price fluctuation mechanism under different periodic time series," *Appl. Energy*, vol. 192, pp. 201–212, 2017.

[62] C. G. Jie Zhou, Mei Sun, Dun Han, "Analysis of oil price fluctuation under the influence of crude oil stocks and US dollar index — Based on time series network model," *Physica A*, p. 109231, 2021.

[63] P. Li and Z. Dong, "Time-varying network analysis of fluctuations between crude oil and Chinese and U.S. gold prices in different periods," *Resour. Policy*, vol. 68, no. July, p. 101749, 2020.

[64] R. Teale, "The concept of specific energy in rock drilling," *Int. J. Rock Mech. Min. Sci.*, vol. 2, no. 1, pp. 57–73, 1965.

[65] F. Dupriest and W. Koederitz, "Maximizing Drill Rates with Real-Time Surveillance of Mechanical Specific Energy," *SPE/IADC Drill. Conf.*, 2005.

[66] M. Armenta, "Identifying inefficient drilling conditions using drilling-specific energy," *Proc. - SPE Annu. Tech. Conf. Exhib.*, vol. 7, no. September, pp. 4409–4424, 2008.

[67] V. Ramba, S. Selvaraju, S. Subbiah, M. Palanisamy, and A. Srivastava, "Optimization of drilling parameters using improved play-back methodology," *J. Pet. Sci. Eng.*, vol. 206, no. May, p. 108991, 2021.

[68] K. Mohan, F. Adil, and R. Samuel, "Tracking drilling efficiency using hydro-mechanical specific energy," *SPE/IADC Drill. Conf. Proc.*, vol. 1, no. March, pp. 493–504, 2009.

[69] C. Hammoutene, "FEA modelled MSE/UCS values optimise PDC design for entire hole section," *Soc. Pet. Eng. - North Africa Tech. Conf. Exhib. 2012, NATC 2012 Manag. Hydrocarb. Resour. a Chang. Environ.*, vol. 1, no. February, pp. 66–76, 2012.

[70] X. Chen, J. Yang, and D. Gao, "Drilling Performance Optimization Based on Mechanical Specific Energy Technologies," *Drilling*, 2018.

[71] L. Amado, *Chapter 12 - Field Case Evaluations*, vol. i. Gulf Professional Publishing, 2013.

[72] J. W. Graham and N. L. Muench, "Analytical determination of optimum bit weight and rotary speed combinations," *Soc. Pet. Eng. - Fall Meet. Soc. Pet. Eng. AIME, FM 1959*, 1959.

[73] E. M. Galle and H. B. Woods, “Best Constant Weight and Rotary Speed for rotary Rock Bits,” 1963.

[74] B. A. Legarth and A. Saadat, “Energy Consumption for Geothermal Wells,” in *proceedings world geothermal congress 2005*, 2005, no. April.

[75] L. F. F. M. Barbosa, A. Nascimento, M. H. Mathias, and J. A. de Carvalho, “Machine learning methods applied to drilling rate of penetration prediction and optimization - A review,” *J. Pet. Sci. Eng.*, vol. 183, no. March, p. 106332, 2019.

[76] C. Hegde, H. Daigle, and K. E. Gray, “Performance comparison of algorithms for real-time rate-of-penetration optimization in drilling using data-driven models,” *SPE J.*, vol. 23, no. 5, pp. 1706–1722, 2018.

[77] W. C. Maurer, “The ‘Perfect - Cleaning’ Theory of Rotary Drilling,” *J. Pet. Technol.*, vol. 14, no. 11, pp. 1270–1274, 1962.

[78] M. G. Bingham, *A New Approach to Interpreting Rock Drillability*. Petroleum Pub. Co., 1965.

[79] A. T. Bourgoyne and F. S. Young, “A multiple regression approach to optimal drilling and abnormal pressure detection,” *SPE Repr. Ser.*, vol. 4, no. 49, pp. 27–36, 1974.

[80] R. E. Osgouei, “Rate of Penetration Estimation Model for Directional and Horizontal Wells,” no. September, p. 83, 2007.

[81] C. Soares and K. Gray, “Real-time predictive capabilities of analytical and machine learning rate of penetration (ROP) models,” *J. Pet. Sci. Eng.*, vol. 172, no. September 2018, pp. 934–959, 2019.

[82] K. Amar and A. Ibrahim, “Rate of penetration prediction and optimization using advances in artificial neural networks, a comparative study,” *IJCCI 2012 - Proc. 4th*

Int. Jt. Conf. Comput. Intell., pp. 647–652, 2012.

[83] R. A. Arehart, "Drill bit diagnosis using neural networks," *Soc. Pet. Eng. AIME, SPE*, vol. DELTA, no. August, pp. 24–28, 1989.

[84] H. I. Bilgesu, L. T. Tetrick, U. Altmis, S. Mohaghegh, and S. Ameri, "New approach for the prediction of rate of penetration (ROP) values," *Proceedings - SPE Eastern Regional Conference and Exhibition*. pp. 175–179, 1997.

[85] B. Mantha and R. Samuel, "ROP optimization using artificial intelligence techniques with statistical regression coupling," *Proc. - SPE Annu. Tech. Conf. Exhib.*, vol. 2016-Janua, 2016.

[86] S. Abdulmalek Ahmed, S. Elkatatny, A. Abdulraheem, M. Mahmoud, and A. Z. Ali, "Prediction of rate of penetration of deep and tight formation using support vector machine," *Soc. Pet. Eng. - SPE Kingdom Saudi Arab. Annu. Tech. Symp. Exhib. 2018, SATS 2018*, 2018.

[87] C. Hegde, H. Daigle, H. Millwater, and K. Gray, "Analysis of rate of penetration (ROP) prediction in drilling using physics-based and data-driven models," *J. Pet. Sci. Eng.*, vol. 159, pp. 295–306, 2017.

[88] X. Ren *et al.*, "Lithology identification using well logs: A method by integrating artificial neural networks and sedimentary patterns," *J. Pet. Sci. Eng.*, vol. 182, no. December 2018, 2019.

[89] S. Elkatatny, "Real-time prediction of rate of penetration while drilling complex lithologies using artificial intelligence techniques," *Ain Shams Eng. J.*, vol. 12, no. 1, pp. 917–926, 2021.

[90] S. Alyaev, E. Suter, R. B. Bratvold, A. Hong, X. Luo, and K. Fossum, "A decision

support system for multi-target geosteering," *J. Pet. Sci. Eng.*, vol. 183, no. March, p. 106381, 2019.

[91] D. C. Braga, "Field Drilling Data Cleaning and Preparation for Data Analytics Applications," Louisiana State University, 2019.

[92] C. Chebiyyam, "Reconciliation — An Inevitable Challenge in Upstream Oil Industry," *SPE Annu. Conf. Exhib.*, no. January, pp. 20–22, 2010.

[93] S. F. Chien, "Settling velocity of irregularly shaped particles," *Proc. - SPE Annu. Tech. Conf. Exhib.*, vol. Delta, no. December, pp. 9–22, 1994.

[94] M. Johan, "Potential of Real-Time Use of Dynamic Drilling Models," Norwegian University of Science and Technology (NTNU), 2011.

[95] D. Moeller and D. Murphy, "Net Energy Analysis of Gas Production from the Marcellus Shale," *Biophys. Econ. Resour. Qual.*, vol. 1, no. 1, pp. 1–13, 2016.

[96] A. R. Brandt, T. Yeskoo, and K. Vafi, "Net energy analysis of Bakken crude oil production using a well-level engineering-based model," *Energy*, vol. 93, pp. 2191–2198, 2015.

[97] A. R. Brandt, "Oil depletion and the energy efficiency of oil production: The case of California," *Sustainability*, vol. 3, no. 10, pp. 1833–1854, 2011.

[98] J. H. K. Phandi, "Minimizing Energy Consumption and Downtime in Oil and Gas," Texas A&M University, 2018.

[99] C. Soares, H. Daigle, and K. Gray, "Evaluation of PDC bit ROP models and the effect of rock strength on model coefficients," *J. Nat. Gas Sci. Eng.*, vol. 34, pp. 1225–1236, 2016.

[100] O. E. Agwu, J. U. Akpabio, S. B. Alabi, and A. Dosunmu, "Artificial intelligence techniques and their applications in drilling fluid engineering: A review," *J. Pet. Sci. Eng.*, vol. 167, no. February, pp. 300–315, 2018.

[101] K. Nagy and E. Hajrizi, "Beyond the Age of Oil and Gas – How artificial intelligence is transforming the energy portfolio of the societies," *IFAC-PapersOnLine*, vol. 51, no. 30, pp. 308–310, 2018.

[102] N. R. Deeks and T. Halland, "SPE 112016 WITSML Changing the Face of Real-Time," no. February, pp. 25–27, 2008.

[103] A. M. Tripathi, R. DuttaBaruah, and S. Subbiah, "Oil well drilling activities recognition using a hierarchical classifier," *J. Pet. Sci. Eng.*, vol. 196, no. September 2020, p. 107883, 2021.

[104] Y. Jiang, Z. Deng, K. S. Choi, F. L. Chung, and S. Wang, "A novel multi-task TSK fuzzy classifier and its enhanced version for labeling-risk-aware multi-task classification," *Inf. Sci. (Ny).*, vol. 357, pp. 39–60, 2016.

[105] API RP 13D, *API Recommended Practice 13D – Rheology and hydraulics of oil-well drilling fluids*. Washington, DC: American Petroleum Institute, 2009.

[106] W. C. Lyons, G. J. Plisga, and M. D. Lorenz, *Standard Handbook of Petroleum and Natural Gas Engineering*, Third Edit. Gulf Professional Publishing, 2016.

[107] G. G. Müller, "Development of an Energy Consumption Model Based on Standard Drilling Parameters," Montan Universitat, 2015.

[108] L. Robinson, "Drill Bit Nozzle Pressure Loss," in *AADE Fluids Conference and Exhibition*, 2010.

[109] M. J. Kaiser, "A Review of Exploration, Development, and Production Cost Offshore

Newfoundland," *Nat. Resour. Res.*, vol. 30, no. 2, pp. 1253–1290, 2021.

[110] S. Selvaraju, V. Ramba, S. Subbiha, R. Uppaluri, P. K. Dubey, and A. Musale, "An innovative system architecture for real-time monitoring and alarming for cutting transport in oil well drilling," *Soc. Pet. Eng. - Abu Dhabi Int. Pet. Exhib. Conf. 2019, ADIP 2019*, 2019.

[111] A. Q. Jakhrani, A. R. H. Rigit, A. K. Othman, S. R. Samo, and S. A. Kamboh, "Estimation of carbon footprints from diesel generator emissions," *Proc. 2012 Int. Conf. Green Ubiquitous Technol. GUT 2012*, pp. 78–81, 2012.

[112] M. Armenta, "Identifying Inefficient Drilling Conditions Using Drilling-Specific Energy," *Soc. Pet. Eng.*, 2008.

[113] B. Daireaux, A. Ambrus, L. A. Carlsen, R. Mihai, K. Gjerstad, and M. Balov, "Development, Testing and Validation of an Adaptive Drilling Optimization System," in *SPE/IADC International Drilling Conference and Exhibition*, 2021.

[114] C. Hegde and K. Gray, "Evaluation of coupled machine learning models for drilling optimization," *J. Nat. Gas Sci. Eng.*, vol. 56, no. December 2017, pp. 397–407, 2018.

Appendix A: Definitions

Different types of drilling rig operations

Drilling: The drill bit, aided by the weight of thick-walled pipes called "drill collars" above it, cuts into the rock. This cutting is aided by the rotation of the drill bits at particular revolutions per minute (rpm) set by the driller. Followed by the cuttings are carried to the surface through the annulus with the help of drilling fluid.

Tripping: An act of pulling the drill string out of the borehole by disconnecting the standpipes for many purposes and running back in by joining the standpipes to resume the drilling.

Reaming: It is an operation to enlarge the size of a previously formed under-gauged hole by a small amount with the desired accuracy for removing burrs and leaving smooth sides with the help of specially designed reamers or a new drill bit.

Circulation: In normal drilling operations, mud is circulated through the borehole to regulate temperature, carry the cuttings from the bottom of the hole to the surface and lubricate the process.

Reciprocation: Changing the bit position up and down for a few meters of amplitude to ensure the drill string is free from being stuck frequently.

Casing/Tubing and Cementing: After completing each phase of drilling, steel pipes will be placed inside the wellbore and cemented with the formation wall to protect the wellbore from caving and collapsing. In addition, it prevents mud loss and contamination also.

Downhole problems and definitions

Pipe stuck

i. Mechanical pipe sticking

It is the condition where drill string will be stuck inside the wellbore due to reasons such as cutting accumulation, dogleg severity (i.e, abrupt hole-deviation), borehole instability and key seating.

ii. Differential-pressure pipe sticking

It is the condition where drill string will be stuck inside the wellbore by embedding into the mud cake due the high-pressure difference between the wellbore and the formation.

Loss of circulation

The mud that has been pumped into the wellbore may be lost through the high permeable or cavernous formation zones. Sometime it may be caused due to natural or induced formation fractures.

Hole-ballooning

It is a formation anomaly where the formation takes drilling fluid due to circulating pressure without fracturing the formation. Once the circulating pressure is off (i.e., pump is switched off), the trapped mud fluid will be released back inside the wellbore.

Hole-deviation

The drill bit sometime may get deviated from the pre-planned wellbore trajectory due to reasons like loose formation, non-uniform rock density. This shall lead to mechanical stuck and restrict the weight transfer to bit.

Drill pipe failures

Due to the excessive torque applied on the drill string then it may go through any of the following failure modes

i. Twist-off
ii. Parting
iii. Collapse and Burst
iv. Fatigue

Kick and blowout

When a formation fluid enters into the wellbore due to higher formation pressure, it is called as kick. If the formation fluid or gas entry is uncontrollable, then it may lead to blowout. Blowout can be so severe it can entirely destroy the rig and risk human life

Borehole instability

It is a condition where the wellbore is not able to maintain its gauge size, shape or structural integrity.

Mud contamination

Any foreign material enters into mud system and brings undesirable changes to the mud properties like

- Mud Density
- Viscosity

Major contaminants are solids, calcium-ions, bicarbonate and carbonate, hydrogen sulfide and salt/saltwater

Appendix B: Model Equations of Hole-Cleaning Module

Table B.1. Rheological property calculation

Variable Name	Equations	Eqn No.
Flow behavior Index	$n = (3.32)\ log\left(\frac{(\theta_{600} - \tau_o)}{(\theta_{300} - \tau_o)}\right)$	(B.1)
Flow consistency index	$k = \frac{\theta_{300}}{511^n}$	(B.2)
Yield point (cp)	$\tau_o = \theta_3$	(B.3)

Table B.2. Drill bit and surface equipment model equations

Variable Name	Equations	Eqn No.
Pressure drop at surface equipment	$\Delta P_{SC} = (C_{SC})(\rho_{mud})\left[\frac{Q_{in}}{100}\right]^{1.86}$	(B.4)
Pressure drop at drill bit	$\Delta P_{bit} = \frac{156.5 \times Q_{in}^2 \rho_{mud}}{32 \times \left(\sum_{i=1}^{i=nn} D_i^2\right)^2}$ nn - number of nozzles	(B.5)

Table B.3. Drill string side model equations

Variable Name	Equations	Eqn No.
Velocity	$v_p = \frac{4Q_{in}}{3.14D_{pi}^2}$	(B.6)
Correction coefficient	$C_p = 1 - \frac{1}{2n+1}\left(\frac{\tau_0}{\tau_0 + k\left(\frac{8(3n+1)Q_{in}}{n\pi D_{P_I}^3}\right)^n}\right)$	(B.7)
Effective viscosity	$\mu_{ep} = \frac{\tau_o + k\left[\left(\frac{3n+1}{nC_p}\right)\left(\frac{8Q_{in}}{\pi D_{P_I}^3}\right)\right]^n}{\left(\frac{3n+1}{nC_p}\right)\left(\frac{8Q_{in}}{\pi D_{P_I}^3}\right)}$	(B.8)
Pipe side Reynolds number	$\mathrm{Re}_p = \left(2\frac{3n+1}{n}\right)\frac{\rho_{mud} v_p^{(2-n)}\left(\frac{D_{P_I}}{2}\right)^n}{\tau_0\left(\frac{D_{P_I}}{2v_p}\right)^n + k\left(2\frac{3n+1}{nC_p}\right)^n}$	(B.9)
Critical Reynolds number	$\mathrm{Re}_{cp} = \left(\frac{4(3n+1)}{ny}\right)^{\frac{1}{1-z}}$	(B.10)
	$y = \frac{(\log n + C_{pt})}{C_{pt2}}, C_{pt} = 3.93, C_{pt2} = 50$	(B.11)
	$z = \frac{(1.75 - \log n)}{7}$	(B.12)
Friction factor	**Laminar Flow if ($\mathrm{Re_a} < \mathrm{Re_c}$)** $f_p = \frac{C_{pl}}{\mathrm{Re}_p}\left(\frac{3n+1}{n}\right), C_{pl} = 4$.	(B.13)
	Turbulent Flow if ($\mathrm{Re_c} < \mathrm{Re_a}$) $f_p = y(C_p \mathrm{Re}_p)^{-z}$	(B.14)
Pressure drop inside the drill string	$\Delta P_p = f_p \rho_{mud} L \frac{32Q_{in}^2}{\pi^2 D_{P_I}^5}$	(B.15)
Total pressure drop in drill string	$\Delta P_{pT} = \sum \Delta P_p$	(B.16)

Table B.4. Annulus side model equations

Variable Name	Equations	Eqn No.
Overall volume balance equation	$Q_{out} + Q_{set\_out} = Q_{in} + Q_{cut} + Q_{set\_in}$	(B.17)
	$Q_{cut} = \left(\frac{\pi D_h^2}{4}\right) ROP$	(B.18)
	$Q_{set\_out} = v_{slip}\left(\frac{\pi(D_h^2 - D_{po}^2)}{4}\right)\left(\frac{C_{out}}{100}\right)$	(B.19)
Cutting balance equation	$Q_{in}C_{in} + Q_{cut}C_{gen} + Q_{set\_in}C_{set} - (Q_{out}C_{out} + Q_{set\_out}C_{set}) = V_{ann}\frac{dC_{out}}{dt}$	(B.20)
	$V_{ann} = \left(\frac{\pi D_h^2}{4}\right) L$	(B.21)
	$C_{gen} = 100\%$ and $C_{set} = 100\%$	(B.22)
Effective density	$\rho_{eff} = \frac{V_{cut\_ann}\,\rho_{cut} + (V_{ann} - V_{cut\_ann})\,\rho_{mud}}{V_{ann}}$	(B.23)
	$V_{cut\_ann} = V_{ann}\left(\frac{C_{out}}{100}\right)$	(B.24)
Annulus velocity	$v_a = \frac{4Q_{in}}{3.14(D_h^2 - D_{po}^2)}$	(B.25)
Slip velocity [56]	$v_{slip} = 12\frac{\pi_{eff}}{D_c\rho_{eff}}\left(\sqrt{1 + 7.27D_c\left(\frac{\rho_{cut} - \rho_{mud}}{\rho_{mud}}\right)\left(\frac{D_c\rho_{eff}}{\pi_{eff}}\right)^2} - 1\right)$	(B.26)
Cutting transport efficiency	$E_t = \left(1 - \frac{v_{slip}}{v_a}\right) \times 100$	(B.27)
Net particle transport velocity	$NTV = V_A - V_S$	(B.28)
Interval's transport time	$ITT = \frac{L}{NTV}$	(B.29)

Annular transport time

$$ATT = \sum ITT \text{ values} \tag{B.30}$$

Correction coefficient

$$C_a = 1 - \frac{1}{n+1}\left(\frac{\tau_0}{\tau_0 + k\left(\frac{16(2n+1)Q_{in}}{n(D_h - D_{P_O})\pi(D_h^2 - D_{P_O}^2)}\right)^n}\right) \tag{B.31}$$

Effective viscosity

$$\mu_{ea} = \frac{\tau_o + k\left[\left(\frac{4(2n+1)}{n(D_h - D_{P_O})}\right)\left(\frac{4Q_{in}}{\pi C_a (D_h^2 - D_{P_O}^2)}\right)\right]^n}{\left(\frac{4(2n+1)}{n(D_h - D_{P_O})}\right)\left(\frac{4Q_{in}}{\pi C_a (D_h^2 - D_{P_O}^2)}\right)} \tag{B.32}$$

Annulus reynolds number

$$\mathrm{Re}_{eq,a} = \left(4\frac{2n+1}{n}\right)\frac{\rho_{mud} v_a^{(2-n)}\left(\frac{D_h - D_{P_O}}{2}\right)^n}{\tau_0\left(\frac{D_h - D_{P_O}}{2v_a}\right)^n + k\left(2\frac{2n+1}{nC_a}\right)^n} \tag{B.33}$$

Critical reynolds number

$$\mathrm{Re}_{eqcr,a} = \left(\frac{8(2n+1)}{ny}\right)^{\frac{1}{1-z}} \tag{B.34}$$

$$y = \frac{(\log n + C_{at})}{C_{at2}}, C_{at} = 3.93, C_{at2} = 50 \tag{B.35}$$

$$z = \frac{(1.75 - \log n)}{7} \tag{B.36}$$

Critical velocity

$$V_c = \frac{\mathrm{Re}_{eqcr,a}}{\rho_{mud}(D_h - D_{Po})}\left(\frac{\tau_o + k\left[\left(\frac{4(2n+1)}{n_a(D_h - D_{P_O})}\right)\left(\frac{4Q_{in}}{\pi C_a (D_h^2 - D_{P_O}^2)}\right)\right]^n}{\left(\frac{4(2n+1)}{n_a(D_h - D_{P_O})}\right)\left(\frac{Q_{in}}{\pi C_a (D_h^2 - D_{P_O}^2)}\right)}\right) \tag{B.37}$$

Friction factor

Laminar Flow if ($Re_a < Re_c$)

$$f_a = \frac{C_{al}}{\mathrm{Re}_{eq,a}}\left(\frac{2n+1}{n}\right) \quad \text{(B.38)}$$

$$C_{al} = 8$$

Turbulent Flow if ($Re_c < Re_a$)

$$f_a = y(C_a \mathrm{Re}_a)^{-z} \quad \text{(B.39)}$$

Pressure drop in annulus

$$\Delta P_a = f_a \rho_{mud} L \frac{32 Q_{in}^2}{\pi^2 (D_h - D_{P_O})(D_h^2 - D_{P_O}^2)^2} \quad \text{(B.40)}$$

Total pressure Drop in the annulus

$$\Delta P_{aT} = \sum \Delta P_a \quad \text{(B.41)}$$

Equivalent circulation density

$$ECD = \frac{P_{aT}}{(0.052)(TVD)} + \rho \quad \text{(B.42)}$$

SI metric unit conversion

bar	× 1.0*	E+05	= N/m^2 (Pa)
cP	× 1.0*	E-03	= Pa.s
ft	× 3.048*	E-01	= m
g/100sqcm	× 9.576	E-01	= N/m^2 (Pa)
in	× 2.54*	E+00	= cm
lb_f/in^2 (psi)	× 6.894757	E+00	= kPa
lb_f/100sqft	× 4.788026	E-01	= N/m^2 (Pa)
lb_f s^n/100sqft	× 4.788026	E-01	= $Pa.s^n$

Appendix C: Formation Details

Table C.1. (a, b). Formation details of oil Well-C

Phase	Measured Depth	Lithology	Formation length
I (26″ hole)	10	Sandy Clay	140
	150	Clay	56
II (17.5″ hole)	206	Clay	44
	250	Sandy Clay	155
	405	Clay	125
	530	Sandy Clay	145
	675	Clay	30
	705	Sandy Clay	40
	745	Sandstone	35
	780	Clay	35
	815	Sandstone	30
	845	Sandy Clay	30
	875	Clay	20
	895	Sandy Clay	40
	935	Clay	105
	1040	Slitstone	15
	1055	Claystone	45
	1100	Slitstone	15
	1115	Claystone	30
	1145	Slitstone	20
	1165	Claystone	35
	1200	Slitstone	10
	1210	Claystone	30
	1240	Sandstone	30
	1270	Clay	20
	1290	Slitstone Sandy	20
III (12.25″ hole)	1310	Shale	30
	1340	Sandstone	20
	1360	Clay	35
	1395	Sandstone	35
	1430	Clay	20
	1450	Slity shale	55
	1505	Clay	25
	1530	Slitstone Sandy	30
	1560	Claystone	60
	1620	Sandstone	20

(a)

Phase	Measured Depth	Lithology	Formation length
III (12.25″ hole)	1640	**Shale**	30
	1670	**Slitstone**	10
	1680	**Slity shale**	40
	1720	**Shale**	20
	1740	**Slity shale**	80
	1820	**Shale**	70
	1890	**Slity shale**	20
	1910	**Shale**	35
	1945	**Slity shale**	27
	1972	**Shale**	40
	2012	**Sandstone**	18
	2030	**Slity shale**	12
	2042	**Slity shale**	43
	2085	**Shale**	35
	2120	**Sandstone**	25
	2145	**Slity shale**	25
	2170	**Slitstone Sandy**	35
	2205	**Shale**	17
	2222	**Sandstone**	18
	2240	**Shale**	30
	2270	**Sandstone**	35
	2305	**Slitstone Sandy**	25
	2330	**Shale**	20
	2350	**Slitstone**	22
	2372	**Shale**	43
IV (8.5″ hole)	2415	**Slitstone**	65
	2480	**Slity shale**	50
	2530	**Slitstone**	35
	2565	**Shale**	45
	2610	**Slitstone**	15
	2625	**Shale**	45
	2670	**Slitstone**	35
	2705	**Shale**	45
	2750	**Sandstone**	65
	2815	**Slitstone**	25
	2840	**Shale**	30

(b)

Table C.2. (a, b). Formation details of oil Well-D

Phase	Measured Depth	Lithology	Formation length
I (26″ hole)	0	KB	15
	15	Alluvium	210
	225	Sandstone	155
	380	Claystone	120
	500	Sandstone	125
II (17.5″ hole)	625	Sandstone	75
	700	Claystone	12
	712	Claystone	88
	800	Sandstone	150
	950	Claystone	50
	1000	Sandstone	150
	1150	Claystone	50
	1200	Sandstone	100
	1300	Claystone	65
	1365	Sandstone	15
	1380	Claystone	17
	1397	Claystone	84
	1481	Claystone	19
	1500	Limestone	15
	1515	Claystone	14
	1529	Claystone	51
	1580	Limestone	11
	1591	Limestone	9
	1600	Claystone	70
	1670	Limestone	20
	1690	Claystone	10
	1700	Claystone	65
	1765	Sandstone	20
	1785	Claystone	65
	1850	Limestone	15
	1865	Claystone	35
	1900	Limestone	15
	1915	Claystone	8

(a)

Phase	Measured Depth	Lithology	Formation length
III (12.25″ hole)	1923	Claystone	19.2
	1942.2	Claystone	22.8
	1965	Sandstone	20
	1985	Limestone	23
	2008	Sandstone	15
	2023	Limestone	5
	2028	Claystone	42
	2070	Limestone	20
	2090	Claystone	55
	2145	Sandstone	15
	2160	Claystone	155
	2315	Sandstone	40
	2355	Shale	215
	2570	Sandstone	15
	2585	Shale	58
IV (8.5″ hole)	2643	Shale	19
	2662	Shale	33
	2695	Sandstone	20
	2715	Shale	203
	2918	Shale	22
	2940	Sandstone	30
	2970	Shale	10
V (6″ hole)	2980	Shale	60
	3040	Sandstone	15
	3055	Shale	10
	3065	Sandstone	20
	3085	Shale	35
	3120	Sandstone	40
	3160	Shale	27
	3187	Shale	58
	3245	Sandstone	20
	3265	Shale	90
	3355	Sandstone	4
	3359	Shale	11
	3370	Shale	50

(b)

Appendix D: Different Types of Drilling Operations

Table D.1. Performance of AI and ML models for TQ and STP prediction (layer 1)

S.N	Algorithm Name	Best hyper- parameter (for both TQ and STP prediction)	Model 1A (TQ prediction)				Model 1B (STP prediction)			
			Training		Testing		Training		Testing	
			R^2	MSE	R^2	MSE	R^2	MSE	R^2	MSE
1	LR	NA	0.87	8.75	-0.166	20.37	0.91	0.47	0.94	0.69
2	KRR	kernel: linear, alpha: 100	0.71	9.33	0.55	7.85	0.88	1.09	0.90	0.50
3	PLS	n_components: 4	0.869	8.97	0.021	17.088	0.915	0.486	0.93	0.82
4	SVR	C = 0.1 kernel: Linear	0.84	10.9	0.82	3.06	0.91	0.49	0.97	0.34
5	LGBM	learning_rate: 0.5, max_depth: 10, n_estimators: 15, num_leaves: 10, boosting_type: gbdt	0.99	0.27	-1.15	37.64	0.99	0.02	0.81	2.16
6	GB	learning_rate: 0.5, max_depth: 10, n_estimators: 7, min_samples_split: 2,	0.99	0.005	-0.34	23.88	0.99	0.0005	0.66	3.98
7	RF	max_depth: 10, min_samples_split: 2, n_estimators: 7	0.99	0.038	-1.2	38.52	0.99	0.003	0.72	3.29

Table D.2. Performance of AI and ML models for ROP prediction (layer 2)

S.N	Algorithm Name	Model 2 (ROP prediction)				
		Best hyper-parameter	Training		Testing	
			R^2	MSE	R^2	MSE
1	LR	NA	0.71	0.92	0.92	0.29
2	KRR	kernel: linear, alpha: 100	0.60	1.28	0.746	1.01
3	PLS	n_components: 4	0.59	1.32	0.83	0.68
4	SVR	kernel: linear, C: 1	0.727	0.88	0.879	0.479
5	LGBM	learning_rate: 0.5, max_depth: 10, n_estimators: 15, boosting_type: gbdt, num_leaves: 10	0.99	0.027	0.59	1.59
6	GB	learning_rate: 0.5, max_depth: 10, min_samples_split: 10, n_estimators: 7	0.99	0.0006	0.39	2.43
7	RF	max_depth: 10, min_samples_split: 5, n_estimators: 7	0.99	0.003	0.45	2.18

Patent and Publications

Patent

1. **S Senthil**, S Senthilmurugan, D.B Rashmi, R Viswanth, M.T Achyut, V.M Balakumara, M Amol, S.K Gauba, **"A System and Method for Activity Identification and Problem Prediction During Oil and Gas Well Drill"**; Indian Provisional Patent Application No. 201911040595

Journal Publications

1. **Senthil Selvaraju**, R Viswanth, S Senthilmurugan, R Uppaluri **"Improving Oil Well Drilling Rig Performance through Energy Consumption Studies"**, Energy (Communicated)
2. **Senthil Selvaraju**, Viswanth R, Suman Kumari, Balakumar Vignesh M, Senthilmurugan S, Uppaluri R **"Real-Time Prediction and Optimization of ROP using Artificial Intelligence in Oil Well drilling"** (Under preparation)

Conference Publications

1. **S Senthil**, R Viswanth, S Senthilmurugan, R Uppaluri. P K Dubey, M Amol. **"An Innovative System Architecture for Real-Time Monitoring and Alarming for Cutting Transport in Oil Well Drilling"**; Abu Dhabi International Petroleum Exhibition & Conference (ADIPEC 2019), Abu Dhabi, UAE. https://doi.org/10.2118/197870-ms
2. **S Senthil**, R Viswanth, S Senthilmurugan, R Uppaluri.**"Prediction and Alarming for Complications during Oil Well Drilling: Case Study with Field Data"** NCUPE 2019, IIT Guwahati